DERIVATION OF HYDROGRAPHS FOR SMALL WATERSHEDS FROM MEASURABLE PHYSICAL CHARACTERISTICS

by

Donald Maurice Gray

A Dissertation Submitted to the

Graduate Faculty in Partial Fulfillment of

The Requirements for the Degree of

DOCTOR OF PHILOSOPHY

Major Subjects: Agricultural Engineering
Civil Engineering

Approved:

Signature was redacted for privacy.

Signature was redacted for privacy.

In Charge of Major Work

Signature was redacted for privacy.

Signature was redacted for privacy.

Heads of Major Departments

Signature was redacted for privacy.

Dean of Graduate College

Iowa State University
Of Science and Technology
Ames, Iowa

1960

TABLE OF CONTENTS

INTRODUCTION	1
REVIEW OF LITERATURE	4
Surface Runoff Phenomena	4
The Hydrograph	5
Topographic Factors and the Hydrograph	9
Unit Hydrograph	15
Distribution Graph	20
Synthetic Unit Hydrographs	21
INVESTIGATIONS, RESULTS AND DISCUSSION	29
Basic Data	30
Topographic Characteristics	30
Preliminary Hydrograph Analysis	42
Fitting the Two-Parameter Gamma Distribution to the Dimensionless Graph	51
Selection of the Time Parameter	61
Relation between Parameters, q and γ'	67
Estimation of the Storage Factor, P_R/γ', from Basin Characteristics	75
Relation of Period of Rise, P_R, and Parameter, γ'	89
Application of Results	100
SUMMARY AND CONCLUSIONS	101
Topographic Characteristics	101
Hydrologic Characteristics	102
SELECTED BIBLIOGRAPHY	104
ACKNOWLEDGMENTS	109
APPENDIX A: GLOSSARY OF TERMS AND SYMBOLS	110
APPENDIX B: EQUATIONAL FORMS OF THE UNIT HYDROGRAPH	113
APPENDIX C: TOPOGRAPHIC AND HYDROLOGIC DATA	118
APPENDIX D: DISTRIBUTION GRAPHS AND EMPIRICAL GRAPHS	131
APPENDIX E: DIMENSIONLESS GRAPHS	176
APPENDIX F: APPLICATION OF RESULTS	203

LIST OF TABLES

Table 1.	Relationship between basin characteristics, L_{ca} and A, for three simple geometric forms (30, p. 135)	38
Table 2.	Approximate maximum watershed size for which the prediction equations are applicable	100
Table 3.	Watershed name and corresponding number designation	118
Table 4.	Collection agencies for raw topographic and hydrologic data	120
Table 5.	Summary of topographic characteristics	121
Table 6.	Summary of storm characteristics and hydrograph properties	123
Table 7.	Discharge readings for storm of April 23-24, 1953, on watershed 19	142
Table 8.	Discharge readings for storm of June 10, 1954, on watershed 19	143
Table 9.	Discharge readings for storm of May 25, 1957, on watershed 19	144
Table 10.	Distribution graph for watershed 19 from storm of April 23-24, 1953	151
Table 11.	Distribution graph for watershed 19 from storm of June 10, 1954	152
Table 12.	Distribution graph for watershed 19 from storm of May 25, 1957	153
Table 13.	Coordinates of the synthesized unit hydrograph	205

LIST OF FIGURES

Figure 1.	Surface runoff phenomena	7
Figure 2.	Component parts of a hydrograph	7
Figure 3.	Relation of length of main stream, L, and watershed area, A	33
Figure 4.	Relation of length to center of area, L_{ca}, and length of main stream, L	36
Figure 5.	Relation of mean land slope, S_L, with the average slope of a representative sample of first-order streams, S_1, from the same watershed	41
Figure 6.	Empirical graph for watershed 19 plotted as a frequency histogram	48
Figure 7.	Influence of modifications of the input data on the fit of the two-parameter gamma distribution to the dimensionless graph for watershed 11	60
Figure 8.	Relation of lag, t_L, and period of rise, P_R, for 94 selected storms	66
Figure 9.	Theoretical and experimental relationships of parameters q and γ' for dimensionless graphs	70
Figure 10.	Variation in the geometry of the dimensionless graph resulting from selection of parameters $\hat{q}$ and $\hat{\gamma}$, in accordance with the regression equation $\hat{q} = 1.445 + 0.873\,\hat{\gamma}$	72
Figure 11.	Inconsistencies in the positioning of the peaks of the dimensionless graphs described by the fitted gamma distributions	74
Figure 12.	Relation of the storage factor, $P_R/\hat{\gamma}$, and watershed factor $L/\sqrt{S_c}$, for 33 selected watersheds	80
Figure 13.	Relation of slope of the main stream, S_c, and length of the main stream, L	83
Figure 14.	Relation of slope of the main stream, S_c, and length of the main stream, L, for watersheds in the two regions: Nebraska--Western Iowa, and Ohio	83

LIST OF FIGURES (continued)

Figure 15a.	Relation of storage factor, $P_R/\hat{\gamma}$, and watershed parameter, $L/\sqrt{S_c}$, for watersheds in Nebraska-Western Iowa	86
Figure 15b.	Relation of storage factor, $P_R/\hat{\gamma}$, and watershed parameter, $L/\sqrt{S_c}$, for watersheds in Central Illinois-Missouri-Illinois-Wisconsin	86
Figure 15c.	Relation of storage factor, $P_R/\hat{\gamma}$, and watershed parameter, $L/\sqrt{S_c}$, for watersheds in Ohio	86
Figure 16.	Relation of parameter, $P_R/\hat{\gamma}$, and period of rise, P_R, for 33 selected watersheds	92
Figure 17.	Relation of storage factor, $P_R/\hat{\gamma}$, and period of rise, P_R	96
Figure 18.	Relation of storage factor, $P_R/\hat{\gamma}$, and watershed parameter, $L/\sqrt{S_c}$, on rectangular coordinate paper	98
Figure 19a.	Station description for watershed 19	133
Figure 19b.	Rating tables for watershed 19	135
Figure 20a.	Stage graph for storm of April 23-24, 1953 on watershed 19	137
Figure 20b.	Stage graph for storm of June 10, 1954 on watershed 19	139
Figure 20c.	Stage graph for storm of May 25, 1957 on watershed 19	141
Figure 21a.	Discharge hydrograph for storm of April 23-24, 1953 on watershed 19	146
Figure 21b.	Discharge hydrograph for storm of June 10, 1954 on watershed 19	146
Figure 21c.	Discharge hydrograph for storm of May 25, 1957 on watershed 19	146
Figure 22.	Recession curve for watershed 19	150
Figure 23.	Distribution graphs for selected storms and empirical graphs for watersheds 1, 2, 3, and 4	155

LIST OF FIGURES (continued)

Figure 24.	Distribution graphs for selected storms and empirical graphs for watersheds 5, 6, 7, and 8	157
Figure 25.	Distribution graphs for selected storms and empirical graphs for watersheds 9, 10, 11, and 12	159
Figure 26.	Distribution graphs for selected storms and empirical graphs for watersheds 13, 14, 15, and 16	161
Figure 27.	Distribution graphs for selected storms and empirical graphs for watersheds 17, 18, 19, and 20	163
Figure 28.	Distribution graphs for selected storms and empirical graphs for watersheds 21, 22, 23, and 24	165
Figure 29.	Distribution graphs for selected storms and empirical graphs for watersheds 25, 26, 27, and 28	167
Figure 30.	Distribution graphs for selected storms and empirical graphs for watersheds 29, 30, 31, and 32	169
Figure 31.	Distribution graphs for selected storms and empirical graphs for watersheds 33, 34, 35, and 36	171
Figure 32.	Distribution graphs for selected storms and empirical graphs for watersheds 37, 38, 39, and 40	173
Figure 33.	Distribution graphs for selected storms and empirical graphs for watersheds 41 and 42	175
Figure 34.	Dimensionless graph of watershed 19 as a histogram	178
Figure 35.	Dimensionless graphs and fitted two-parameter gamma distributions for watersheds 1, 2, 3, and 4	182
Figure 36.	Dimensionless graphs and fitted two-parameter gamma distributions for watersheds 5, 6, 7, and 8	184
Figure 37.	Dimensionless graphs and fitted two-parameter gamma distributions for watersheds 9, 10, 11, and 12	186

LIST OF FIGURES (continued)

Figure 38.	Dimensionless graphs and fitted two-parameter gamma distributions for watersheds 13, 14, 15 and 16	188
Figure 39.	Dimensionless graphs and fitted two-parameter gamma distributions for watersheds 17, 18, 19, and 20	190
Figure 40.	Dimensionless graphs and fitted two-parameter gamma distributions for watersheds 21, 22, 23, and 24	192
Figure 41.	Dimensionless graphs and fitted two-parameter gamma distributions for watersheds 25, 26, 27, and 28	194
Figure 42.	Dimensionless graphs and fitted two-parameter gamma distributions for watersheds 29, 30, 31, and 32	196
Figure 43.	Dimensionless graphs and fitted two-parameter gamma distributions for watersheds 33, 34, 35, and 36	198
Figure 44.	Dimensionless graphs and fitted two-parameter gamma distributions for watersheds 37, 38, 39, and 40	200
Figure 45.	Dimensionless graphs and fitted two-parameter gamma distributions for watersheds 41 and 42	202
Figure 46.	Synthetic unit hydrograph for five-square-mile watershed used in illustrative problem	208

INTRODUCTION

Wisler and Brater (59, p. 3) define hydrology as "The science that deals with the processes governing the depletion and replenishment of the waters of the land areas of the earth." It is concerned with the transportation of the water through the air, over the ground surface and through the strata of the earth.

The manner in which water passes to a stream channel governs its terminology. The accepted components of stream-flow are interflow, ground water, channel precipitation and surface runoff. Of primary importance in this study is surface runoff or water which passes to a stream channel by traveling over the soil surface. It has as its origin, water arising from melting snow or ice, or rainfall which falls at rates in excess of the soil infiltration capacity.

The majority of work completed concerning the phenomena of surface runoff has been directed in two distinct area groups; those hydrologic studies conducted by engineers and applied to large basins varying in size from a hundred to several thousand square miles, and those conducted by agricultural engineers and applied to small areas of a hundredth-acre to a few acres. Work on the larger areas has been initiated largely by the United States Corps of Engineers and the Bureau of Reclamation for construction of large hydraulic structures. In contrast, agricultural research has investigated erosion, water yield and rates of surface runoff from small-sized plots having varied physical and cultural treatments. The number of hydrologic investigations on watersheds of intermediate size is relatively very small.

Engineers require for design purposes a knowledge of the time-rate distribution of surface-runoff volumes. This distribution is depicted graphically by the hydrograph as a continuous plot of the instantaneous discharge rate with time. The design of small hydraulic structures as road culverts and chutes, water-conveyance channels, detention structures, weirs, spillways, drop inlets and others, as recommended for use for either conveyance, control or conservation of surface runoff by the Bureau of Public Roads and the Soil Conservation Service, depend largely on the discharge-time relationships resulting from intense rains occurring on basins of only a few square miles area.

In many areas of the country for which rainfall records are available there is a definite lack of stream-gaging stations in operation. For these ungaged areas, the surface-runoff hydrograph for a given storm may be approximated by two techniques:

1. Use of a recorded hydrograph from a like storm obtained from a physically similar area, or
2. Use of a synthetic hydrograph.

The success of method one is limited by the degree of similarity between the significant runoff-producing characteristics of the watersheds involved. If they are not closely alike, an erroneous approximation of the true hydrograph may result. The latter method is limited by the reliability of the synthetic technique applied, which in many cases will have been developed from empirical data collected from large areas located in a different region.

Further hydrologic investigations on watersheds of intermediate size

can be easily justified in view of the high expenditures of state and federal funds annually invested for the control and conservation of surface runoff, and the relative inadequacy of the data on which the designs of the facilities are based. The application of economic principles at the watershed level requires that damages and benefits arising from structural and conservation programs be associated with individual sub-units or sub-basins within a large area. For example, the relative proportion of offsite damages attributable to a given area due to flooding downstream should be prorated according to the contribution of this area to the flooding process. Obviously, such an estimate can be made properly only after the runoff characteristics of the area are known.

The following dissertation describes a procedure whereby the unit hydrograph of surface runoff for small watershed areas may be synthesized. It presents the methodology and necessary relationships to perform this approximation once the pertinent physical characteristics of the watershed are determined.

REVIEW OF LITERATURE

Surface Runoff Phenomena

Depending upon the rate at which rain falls, the water may either infiltrate into the soil or accumulate and flow from the area as surface runoff. If the rainfall intensity, neglecting interception and evaporation losses, is less than the infiltration capacity, all the water will enter the soil profile. In the other case, when the rainfall intensity is in excess of the soil infiltration capacity, a sequence of events occurs which ultimately produces surface runoff.

Excess water produced by a high intensity rain must first satisfy soil and vegetal storage, detention and interception requirements. When the surface depressions are filled, the surface water then begins to move down the slopes in thin films and tiny streams. At this stage, the overland flow is influenced greatly by surface tension and friction forces. As described by Horton (21) in Figure 1; as precipitation continues, the depth of surface detention increases and is distributed according to the distance from the outlet. With the increase in depth or volume of supply, there is a corresponding increase in the rate of discharge. Therefore, the rate of outflow is a function of the depth of water detained over the area.

The paths of the small streams are tortuous in nature and every small obstruction causes a delay until sufficient head is built up to overcome this resistance (23). Upon its release, the stream is suddenly speeded on its way again. Each time there is a merging of two or more

streams the water is accelerated further in its downhill path. It is the culmination of all these small contributions which produces the ultimate hydrograph of surface runoff. After the excess rain ends, the water remaining on the area as surface detention disappears progressively from the watershed as a result of the combined action of surface runoff and infiltration.

The Hydrograph

A hydrograph of a stream is the graphical representation of the instantaneous rate of discharge with time. It includes the integrated contributions from ground-water, interflow, surface-runoff, and channel-precipitation sources. For any stream, the nature of the hydrograph produced by a single, short-duration, excessive storm occurring over the drainage area follows a general pattern. This pattern shows a period of rise or a period of increasing discharge which culminates in a peak or crest followed by a recession of flow which may or may not recede to zero depending on the amount of ground-water flow. A typical hydrograph divided into its three principal parts is shown in Figure 3. For small watershed areas, the total contribution to the runoff hydrograph by ground-water flow, channel precipitation and interflow is usually small in comparison to the amount received from surface runoff. For this reason, the ensuing discussions will be directed toward hydrographs resulting mainly from surface runoff with small amounts of channel precipitation.

Figure 1. Surface runoff phenomena

Figure 2. Component parts of a hydrograph

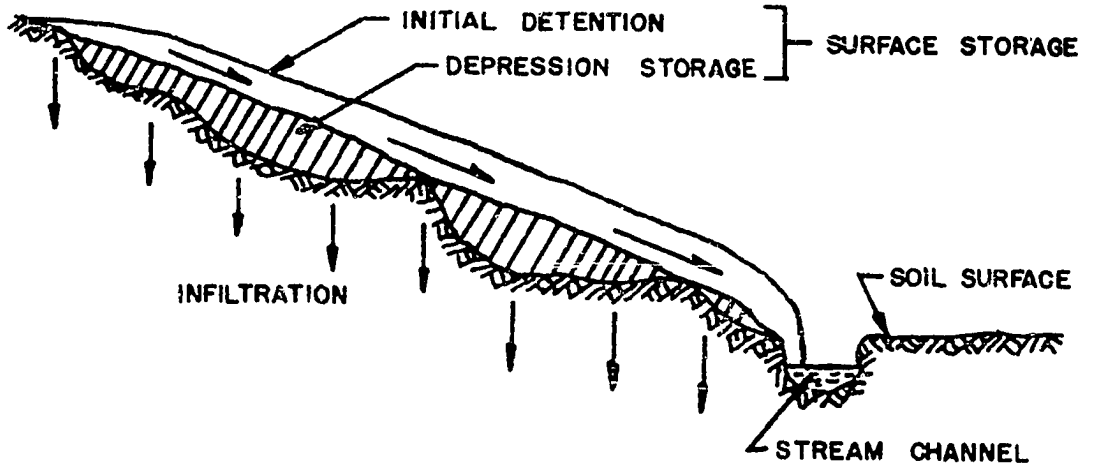
INITIAL DETENTION
DEPRESSION STORAGE
SURFACE STORAGE
INFILTRATION
SOIL SURFACE
STREAM CHANNEL

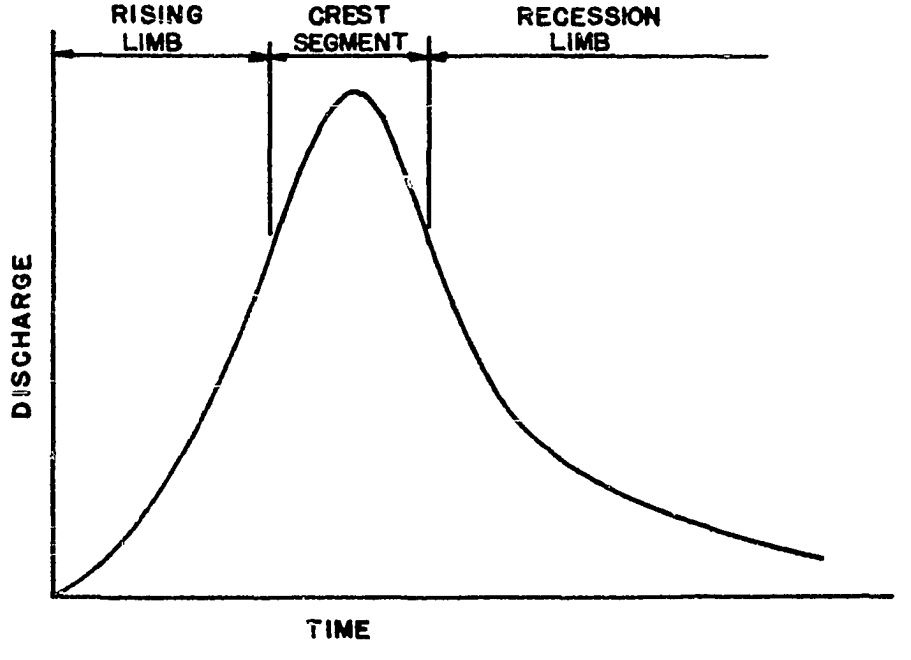
RISING LIMB
CREST SEGMENT
RECESSION LIMB
DISCHARGE
TIME

Rising limb or concentration curve

The rising limb extends from the time of beginning of surface runoff to the first inflection point and represents the increase in discharge produced by an increase in storage or detention on the watershed. Its geometry is characterized by the distribution of the time-area histogram of the basin and the duration, intensity, and uniformity of the rain. The initial portion is concave upwards as a result of two factors; the greater concentration of area between adjacent isochrones within the middle and upper reaches of the basin and the greater opportunity for infiltration, evaporation, surface detention, and interception during the initial periods of the storm (32, p. 390).

Crest segment

The crest segment includes that part of the hydrograph from the inflection point on the rising limb to a corresponding point on the recession limb. The peak of the hydrograph or the maximum instantaneous discharge rate occurs within this time interval. The peak represents the arrival of flow from that portion of the basin receiving the highest concentration of area-inches of runoff. Ramser (41, p. 799) states,

> The maximum rate of runoff from any watershed area for a given intensity rainfall occurs when all parts of the area are contributing to flow. That part of the watershed nearest the outlet must still be contributing to the flow when the water from the most remote point on the watershed reaches the outlet.

That is, the duration of rain must be equal to or exceed the time of concentration.

Recession limb

The recession limb includes the remaining part of the hydrograph. It represents the withdrawal of water from storage after all the excess rainfall has ceased. Consequently, it may be considered as the natural decrease in the rate of discharge due to the draining-off process. The shape of the curve is independent of time variations in rainfall or infiltration and is dependent essentially upon the physical features of the channel alone. Horner and Flynt (19) and Barnes (4) have listed mathematical expressions describing the recession limb. The general equation is of the form

$$q_t = q_o k^{\Delta t} \qquad (1)$$

where q_t = instantaneous discharge at time, t,

q_o = instantaneous discharge at time, t_o,

k = recession constant, and

Δt = elapsed time interval, $t - t_o$.

This equation produces a straight line when plotted on semi-logarithmic paper. The value of the recession constant, k, is generally not constant throughout all discharge rates. Frequently, the recession curve is broken to a series of line segments to obtain several values of k with each value applicable within a given range of flows.

Topographic Factors and the Hydrograph

The surface-runoff hydrograph for a watershed represents the integrated effect of all the basin physical characteristics and their

modifying influence on the translation and storage of a rainfall-excess volume. The factors which are involved are numerous, some having a major bearing on the phenomena whereas others are of negligible consequence. Sherman (44) suggests the dominant factors are:

1. Drainage-area size and shape,
2. Distribution of the watercourses,
3. Slope of the valley sides or general land slope,
4. Slope of the main stream, and
5. Pondage due to surface or channel obstructions forming natural detention reservoirs.

Drainage-area size and shape

The major influence of increasing drainage-area size on the geometry of the surface-runoff hydrograph is the lengthening of the time-base of the hydrograph (59, p. 42). It follows therefrom that for a given rainfall excess, the peak ordinate when expressed in units of cfs per square mile will likewise decrease with area.

Drainage-area shape is instrumental in governing the rate at which water is supplied to the main stream as it proceeds to the outlet (59, p. 44). It is, therefore, a significant feature which influences the period of rise. For example, a semi-circular basin in which the flow converges from all points to the outlet will define a hydrograph with a shorter time to peak than one produced on a long narrow basin of equal area. Langbein and others (30, p. 133) summarize the effect as follows,

> A drainage basin whose drainage tributaries are compactly organized so that water from all parts of the basin has a

> comparatively short distance to travel will discharge its runoff more quickly and reach greater flood crests than one in which the larger part of the basin is remote from the outlet.

Although drainage areas can adopt a multiplicity of shapes, they are generally ovoid- or pear-shaped. Dooge (12, p. 57) found that unless the shape of a watershed deviated appreciably from generally-ovoid, the geometry of the hydrograph remained relatively constant.

Distribution of water courses

The pattern and arrangement of the natural stream channels determine the efficiency of the drainage system. Other factors being constant, the time required for water to flow a given distance is directly proportional to the length. Since a well-defined system reduces the distance water must move in overland flow, the corresponding reduction in time involved is reflected by an outflow hydrograph having a short, pronounced concentration of runoff.

Slope of main stream

After reaching the main drainageway, the time necessary for a flood wave to pass the outlet is directly related to the length of traverse and the slope of the waterway. The velocity of flow of water, v, in an open-channel may be expressed in the general form

$$v = AR^m \ S_c{}^n \qquad (2)$$

where A = constant depending on the roughness of the channel,

R = hydraulic radius,

S_c = channel slope, and

m, n = exponents.

It follows from Equation 2 that the time, t, required for a particle of water to move a given distance, l, is inversely related to some power of the slope value. According to Manning, the values of the exponents are respectively, m = 2/3 and n = 1/2. Dooge (12, p. 95) shows that in loose boundary hydraulics, however, roughness and slope are not independent and the velocity relationship depends on the size of the bed material. He indicates for a channel in equilibrium the travel time varies inversely with the cube root of the channel slope.

The influence of channel slope is reflected in the time elements of the hydrograph. Since the recession limb represents the withdrawal of water from channel storage, the effect of channel slope should be influential in that portion of the hydrograph. Correspondingly, with increased channel slope, the slope of the recession limb increases and the base time of the hydrograph decreases.

Slope of valley sides or general land slope

The general land slope has a complex relationship to the surface runoff phenomena arising from its influence on infiltration, soil moisture content, and vegetative growth. The influence of land slope on hydrograph shape is manifested in the time of concentration of the runoff volumes to defined stream channels. On large watershed areas, the time involved in overland flow is small in comparison with the time of flow in the stream channel. Conversely, on smaller areas the overland flow

regime exerts a dominating effect on the time relationships and the peak of the hydrograph (11).

The velocity of overland flow is not readily computed because of the variations in types of flow that may exist along the paths of transit. Overland flow may range from purely laminar for slight detention depths to purely turbulent over smooth slopes. Horton (22, 23) describes an additional type of flow, subdivided flow, in which flow is subdivided by grass or vegetal matter as to produce a condition where the velocity is practically uniform over the depth of flow and resistance is very great.

Theoretical and empirical considerations of the overland flow regime were expressed by Butler (8, p. 316) in the following relationship

$$q = ay^b S_L^c \qquad (3)$$

where q = rate of outflow per unit width,

y = average depth of surface storage,

S_L = land slope, and

a,b,c = coefficient and exponents which vary with Reynold's number, raindrop impact and roughness.

Equation 3 indicates that the effect of land slope is similar to that of channel slope. With increasing land slope the time elements of the hydrograph decrease.

Pondage or storage

Since storage must first be filled, then emptied, its delaying and modifying effect on the excess precipitation volumes is instrumental in

determining hydrograph shape. Much of the variation caused by differences in sub-intensity patterns and areal distribution of a rain, and by differences in travel-times of the sub-basins as a result of their positioning from the outlet is evened out.

Storage effects exist in both overland and channel flow. Sherman (45) summarizes the effect on the unit graph of storage arising from differences in topography as follows,

> Topography with steep slopes and few pondage pockets gives a unit graph with a high sharp peak and short time period. A flat country with large pondage pockets gives a graph with a flat rounded peak and a long time period.

During its passage through a watercourse, a flood wave may be considered to undergo a simple translation (uniformly progressive flow) and reservoir or pondage action (29, p. 562). The extent of modification of the flood wave can be ascertained by employing flood routing procedures if the flow characteristics and the geometrical properties of the stream channel are known. In general, storage causes a decrease in the peak discharge and a lengthening of the time base of the hydrograph.

The foregoing discussion considers only the generalized influences of topographic factors on hydrograph shape. It is impossible within the bounds of this study to cover the influence of each individual factor in detail. Each effect may be obscured by another. The final hydrograph will depend on the cumulative effect of all the factors as they act alone or in combination with others.

Unit Hydrograph

In 1932, L. K. Sherman (45) advanced the theory of the unit hydrograph or unit graph, now recognized as one of the most important contributions to hydrology related to the surface runoff phenomena. A unit hydrograph is a discharge hydrograph resulting from "one-inch" of direct runoff generated uniformly over the tributary area at a uniform rate during a specified period of time.

The theory is based in principle on the criteria (26, p. 137):

1. For a given watershed, runoff-producing storms of equal duration will produce surface runoff hydrographs with equivalent time bases, regardless of the intensity of the rain,
2. For a given watershed, the magnitude of the ordinates representing the instantaneous discharge from an area will be proportional to the volumes of surface runoff produced by storms of equal duration, and
3. For a given watershed, the time distribution of runoff from a given storm period is independent of precipitation from antecedent or subsequent storm periods.

Obviously, criterion one cannot be exactly correct because the effect of channel storage will vary with stage. However, since recessions approach zero asymptotically, a practical compromise is possible without excessive error (32, p. 445). In addition, the effective gradient and the resistance to flow change with the magnitude of the flood wave. Thus, hydrographs resulting from excessive rains of equal duration but of different intensities would be expected to show minor variations

in their time elements.

Sherman (43) confirmed the hypothesis regarding the proportionality of ordinates provided that the selected time unit is less than the minimum concentration period. This was accomplished by reducing the quantitative phenomena of rainfall, loss, pondage, and runoff to a purely hydraulics problem that could be solved by well-known and accepted hydraulic formulae.

With respect to criterion three, antecedent precipitation is important to the runoff phenomena primarily because of its effect on the soil infiltration capacity and the resultant total volume of runoff occurring from a given storm.

The unit-graph theory has been accepted generally by most hydrologists. Its use as a hydrologic tool is perhaps best summarized by Mitchell (34, p. 14),

> There has been developed no rigorous theory by which the unit-hydrograph relationships may be proven. However, the results which have been obtained by a judicious application of the relationship have been so predominately satisfactory that there can be no doubt that it is indeed, a tool of considerable value for resolving to some extent the complex relations of rainfall and runoff and for advancing the science of hydrology.

Unit-storm and unit-hydrograph duration

Theoretically, an infinite number of unit hydrographs are possible for a given basin because of the effects of rainfall duration and distribution. It is necessary for practical considerations, however, to know the tolerance or range of unit-storm periods within which a given unit graph is applicable. This information is required for the synthesis of a

hydrograph for a storm of long duration and the development of a representative unit graph for an area.

Several investigators have expressed different opinions, based on experience, regarding the critical rainfall duration for a given basin. Wisler and Brater (59, p. 38) employ a unit storm defined as, "A storm of such duration that the period of surface runoff is not appreciably less for any storm of shorter duration." The authors found that an appropriate duration of the unit storm varies with characteristics of the basin. For small watersheds (areas less than ten square miles), unit hydrographs result from short, isolated storms whose durations are less than the period of rise. For larger watersheds, however, the unit-storm duration may be less than the period of rise, possibly no more than half as long (59, p. 309). They recommend that in applying the distribution graph (see footnote p. 44) to a given storm sequence on small watersheds,

> The volume of rainfall excess may be converted to runoff by means of a single application of the distribution graph, if its duration is no longer than the period of rise. The graph resulting from a longer rain must be derived by successive applications of the distribution graph to unit durations of rainfall excess.

For the larger areas they conclude,

> The distribution graph is not a sufficiently precise tool to be sensitive to differences in duration of rainfall excess that are small compared with the period of rise . . . . It will require further research before enough experimental evidence is available to establish the nature of the variation for small changes in duration.

The more common principle is to associate the unit graph with the storm from which it was produced. For example, for a given area there may be a two-hour unit graph or a six-hour unit graph depending on

whether the unit-storm duration was either two hours or six hours, respectively, provided that the time of concentration of the basin had not been exceeded. Unit graphs for various storm durations can be developed from one of known duration using the S-curve technique as outlined by Linsley, et al. (32, p. 451 ff.).

The selection of a proper time period for unit hydrographs is important. Sherman (46, p. 524) suggests the following criteria to be used in its selection,

> For areas over 1000 square miles use 12-hour units in preference to 24 hours. For areas between 100 and 1000 square miles use units of 6, 8 or 12 hours. For areas of 20 square miles use 2 hours. For smaller areas use a time unit of about one-third or one-fourth of the approximate concentration time of the basin.

Mitchell (34, p. 30) recommends that the storm duration or unit-hydrograph duration which is most convenient for use on any basin is about 20 percent of the time between the occurrence of a short storm of high intensity and the occurrence of peak discharge. He relates (34, p. 35),

> The effect upon the unit hydrograph becomes significant only when there is substantial variation between the unit-hydrograph duration and the storm duration . . . . It is usually permissible to allow the storm duration to vary between 50 per cent and 200 per cent of the unit-hydrograph duration before any correction factor for this effect will become necessary.

Linsley, et al. (33, p. 195) cite that in practical applications, experience has shown that the time unit employed should approximate one-fourth the basin lag time (time from the center of mass of effective precipitation to the peak of the unit graph). They suggested that the effect of small differences in storm duration is not large and that a

tolerance of ±25 percent from the adopted unit-hydrograph duration is acceptable.

Yet another criterion is adopted by the Corps of Engineers (56, p. 8). They found that for drainage areas of less than 100 square miles, values of the unit-storm duration equal to about one-half the basin lag time appears to be satisfactory.

Mathematical interpretation of the unit hydrograph

Among the most recent contributions to the field of hydrology has been the development of theoretical expressions which define the geometry of the unit graph. Two such mathematical expressions have been proposed, one by Edson (13) and the other by Nash (38). Since these results occupy an important role in the current study, the complete derivation given by each author is listed in Appendix B. Although the resultant Equations 30h and 31f, Appendix B, were founded on different underlying assumptions, both may be reduced to the common form

$$Q_t = \frac{V(\alpha)^\beta}{\Gamma(\beta)} e^{-\alpha t} t^{\beta-1} \qquad (4)$$

where Q_t = instantaneous ordinate of the unit graph at time t,

V = volume,

α = parameter having the dimensions of time,

β = dimensionless parameter,

e = base of the natural logarithms, and

Γ = gamma function (see pp. 115, 116).

The result is especially applicable to the formulation of a synthetic

procedure. Foremost, for this purpose, it offers the investigator a useful tool whereby a solution can be obtained in logical sequence from reason to result. Edson explains that the general failure encountered in correlating physical characteristics of the basin and the hydrograph properties, peak discharge and period of rise may be attributed to the fact that the functional relationships between this latter set of factors and the parameters α and β are sufficiently complex to restrict a satisfactory tie-in.

In addition, the use of the two-parameter equation enables the description of the complete unit graph once the relationships between the physical characteristics and the parameters α and β have been established. Thus, the necessity for single point correlations, as used almost exclusively in the past, can be eliminated. The application of the continuous curve is advantageous to practically all hydrologic problems.

Distribution Graph

As an outgrowth of the unit-hydrograph principle, Bernard (5) conceived the concept of the distribution graph. A distribution graph is a unit hydrograph of surface runoff modified to show the proportional relation of its ordinates expressed as percentages of the total surface-runoff volume. In accordance with the unit-hydrograph principle, if the base time of the unit hydrograph is divided into any given number of equal-time increments, the percentage of the total volume of flow that occurs during a given time interval will be approximately the same, regardless of the magnitude of total runoff.

Since the area under each distribution graph is equal to 100 percent, differences in the runoff characteristics between watersheds are reflected in the respective shapes of their distribution graphs. The distribution graph is used in preference to the unit graph when hydrograph characteristics from areas of different size are compared.

Synthetic Unit Hydrographs

Numerous procedures have been derived whereby the unit hydrograph for an ungaged area can be constructed. Each procedure, however, differs somewhat from another either in the relationships established or the methodology employed. The ensuing discussions are confined to a brief summary of the more pertinent synthetic techniques published in the literature.

Snyder

Snyder (48), in 1938, was the first hydrologist to establish a set of formulas relating the physical geometry of the basin and properties of the resulting hydrograph. In a study of watersheds located mainly in the Appalachian highlands, which varied in size from 10-10,000 square miles, he found that three points of the unit hydrograph could be defined by the following expressions[1].

$$t_L = C_t \, (LL_{ca})^{0.3} \tag{5a}$$

---

[1]In order to be consistent, the symbols have been changed from those appearing in the original articles to conform to the designations employed throughout the thesis.

where t_L is the basin lag (time difference in hours between the centroid of rainfall and centroid of runoff), L is the length of the main stream in miles from the outlet to divide and L_{ca} is the distance in miles from the outlet to a point on the stream nearest the center of area of the watershed. For the watersheds studied, the coefficient C_t varied from 1.8-2.2.

$$Q_p = (640\ C_p\ A)/t_L \tag{5b}$$

where Q_p is the peak discharge of the unit hydrograph in cfs and A is the drainage area in square miles. The coefficient, C_p, ranged in magnitude from 0.56-0.69.

$$T_B = 3 + 3\ (t_L/24) \tag{5c}$$

where T_B is the length of the base of the unit hydrograph in days.

Equations 5a, 5b and 5c define points of the unit hydrograph resulting from a rain of duration, $t_r = t_L/5.5$. For storms of different rainfall durations, t_R, an adjusted form of lag, t_{LR}, determined by the equation

$$t_{LR} = t_L + (t_R - t_r)/4 \tag{5d}$$

must be substituted in Equation 5b and 5c.

Once the three quantities, t_L, Q_p and T_B are known, the unit hydrograph can be sketched. It is constructed so that the area under the curve represents a one-inch volume of direct runoff accruing from the watershed. As an aid to this sketching process, the Corps of Engineers (56) have developed a relation between the peak discharge and the width

of the unit hydrograph at values of 50 percent and 75 percent of the peak ordinate.

A study similar to that of Snyder's was conducted by Taylor and Schwarz (52) on 20 watersheds located in the Atlantic States, varying in size from 20-1,600 square miles. Probably the most significant difference in the relationships found for lag and peak discharge was the inclusion of a weighted slope term.

Commons

In 1942, Commons (10) suggested that a dimensionless hydrograph, the so-called basic hydrograph, would give a generally acceptable approximation of the flood hydrograph on any basin. This hydrograph was developed from flood hydrographs in Texas. It is divided so that the base time is expressed as 100 units, the peak discharge as 60 units, and the area as a constant 1,196.5 units.

The absolute values for a hydrograph are established once the volume of runoff and peak discharge are known. The volume in second-foot-days is divided by 1,196.5 to establish the value of each square unit. Dividing the peak flow by 60 gives the value of one unit of flow in cfs. The magnitude of one time unit is then computed by dividing the value of the square unit by that of the flow unit. Finally, the hydrograph is synthesized by converting the listed values of the basic graph to absolute time and discharge readings according to the calculated conversions.

Soil Conservation Service (SCS)

The method of hydrograph synthesis used by the SCS employs an average dimensionless hydrograph developed from an analysis of a large number of natural unit hydrographs for watersheds varying widely in size and geographical location (55, pp. 3.16-4ff). This dimensionless hydrograph has its ordinate values expressed as the dimensionless ratio, Q_t/Q_p, and its abscissa values as the dimensionless ratio, t/P_R. Q_t is the discharge at any time, t, and P_R is the period of rise. For a given watershed, once the values of Q_p and P_R are defined, the unit hydrograph can be constructed. The following expressions are given for this purpose.

$$Q_p = (484\ AV)/P_R \tag{6a}$$

where V is the volume of runoff in inches, which for a unit hydrograph is unity. With A expressed in square miles, V in inches and P_R in hours, the units of Q_p are cubic feet per second. P_R is determined from the expression

$$P_R = t_R/2 + t_L\ . \tag{6b}$$

The lag, t_L, can be estimated in two ways, either by the expression

$$t_L = \frac{\Sigma A_x\ V_x\ T_x}{\Sigma A_x\ V_x} \tag{6c}$$

where A_x and V_x are respectively the area and depth of runoff of subarea x, and T_x is the time required for water to travel from the centroid of the subarea to the basin outlet, or by the expression

$$t_L = 0.6T_c \tag{6d}$$

where T_c is the time of concentration. Approximations for T_c can be obtained from expressions given in the SCS handbook (55) or from data reported by Kirpich (27).

Hickok, Keppel and Rafferty

The approach to hydrograph synthesis given by Hickok, et al. (17) is very similar to that employed by the SCS. However, their investigations were confined entirely to small watershed areas. The runoff characteristics of 14 watersheds which vary in size from 11-790 acres, located in semi-arid regions, were investigated and an average dimensionless graph (Q_t/Q_p versus t/t_L') developed. In this study, lag, t_L', was taken as the time difference between the centroid of a limited block of intense rainfall and the resultant peak discharge. The authors presented two different methods for determining lag.

For reasonably homogeneous semi-arid rangelands up to about 1,000 acres in area

$$t_L' = K_1(A^{0.3}/S_L\sqrt{DD})^{0.61} \qquad (7a)$$

where S_L is the average land slope of the watershed and DD is the drainage density. With A in acres, S_L in percent and DD in feet per acre; lag is given in minutes and the value of the coefficient, K_1, is equal to 106.

For watersheds with widely different physiographic characteristics

$$t_L' = K_2\left(\frac{\sqrt{L_{csa} + W_{sa}}}{S_{La}\sqrt{DD}}\right)^{0.65} \qquad (7b)$$

where L_{csa} is the length from the outlet of the watershed to the center

of gravity of the source area, W_{sa} is the average width of the source area and S_{La} the average land slope of the source area. The source area was considered to be the half of the watershed with the highest average land slope. The coefficient, K_2, is equal to 23.

The authors suggested that Q_p could be obtained from the relation

$$\frac{Q_p}{V} = \frac{K_3}{t_L'} \tag{7c}$$

which gives Q_p in cfs when V is expressed in acre feet, t_L' in minutes, and K_3 taken equal to 545.

Clark

In 1943, Clark (9) suggested that the unit hydrograph for an area could be derived by routing the time-area concentration curve through an appropriate amount of reservoir storage. In the routing procedure, an instantaneous unit hydrograph (hydrograph resulting from an instantaneous rainfall of one-inch depth and duration equal to zero) is formed. The unit hydrograph for any rainfall duration, t_R, can be obtained from the instantaneous graph by averaging the ordinates of the instantaneous graph t_R-units of time apart and then plotting the average discharge at the end of the interval.

Clark used the Muskingham method of flood routing. The basic equations employed in this method are

$$I - O = dS/dt \tag{8a}$$

$$S = KQ \tag{8b}$$

$$Q = xI + (1-x)O \tag{8c}$$

where I = inflow rate,

O = outflow rate,

S = storage,

t = time,

K = storage constant,

Q = weighted discharge, and

x = dimensionless weight factor.

For storage routing through a reservoir, storage is directly related to outflow and the factor, x, taken equal to zero. Equations 8a, 8b and 8c thus can be combined to the simplified form

$$I - O = KdO/dt \tag{8d}$$

In order to apply this procedure to a given watershed, estimates of the storage constant, K, and lag through the basin must be obtained. Clark suggested that K is given by the relation

$$K = cL/\sqrt{S_c} \tag{8e}$$

where S_c is the mean channel slope. For L expressed in miles, c varies from about 0.8-2.2.

Linsley (31) in a discussion of Clark's paper conceived that the comparative magnitude of flood flows and storage in the tributaries would affect the relationship. He recommended the inclusion of the square root of area term in Equation 8e as a measure of these factors. The equation

formed is

$$K = \frac{bL\sqrt{A}}{\sqrt{S_c}} \qquad (8f)$$

where b is a coefficient.

Linsley, et al. (33, p. 241) suggest the value of t_L computed from a recognized formula can be used as an approximation of basin lag.

For further information on the use of routing techniques for hydrograph synthesis, the reader is referred to the works of Horton (24), Dooge (12), and Nash (38).

INVESTIGATIONS, RESULTS AND DISCUSSION

The basic format of this thesis has been designed to combine the individual sections of Investigations, Results, and Discussion for each phase of the problem.

The material is presented in a sequence similar to that in which the work was completed. The initial phase entailed the procurement, organization, and basic analyses of the topographic and hydrologic data. The important features of this part of the study included: the derivation of geometric properties of the watersheds, the listing of significant storm characteristics, the plotting of hydrographs and the development of a representative distribution graph for each basin, and a discussion of the salient relation between rainfall and runoff characteristics.

These results provided the basis upon which the synthetic technique was formulated. The theoretical work by Edson and Nash shows that the geometry of a unit hydrograph can be described by a two-parameter equation (see Equation 4). The necessity for point correlations is thus eliminated provided that the two constants can be evaluated and their relation with physical properties of the watersheds established.

These parameters were approximated by the best-fit estimators, q and γ', of the two-parameter gamma distribution, obtained by fitting this distribution to a dimensionless form of a representative distribution graph of each watershed. In the dimensionless form, the time relationships of the distribution graph were based on the period of rise, P_R.

Once the three variables, P_R, q and γ', for any watershed are known,

its dimensionless graph, distribution graph, and unit hydrograph can be constructed. The final step in the development of the synthetic method involved the determination of prediction equations from which values of the three parameters could be estimated from topographic characteristics.

Basic Data

A complete listing of the basic topographic and hydrologic data employed in the study is given in tabular form in Tables 3, 4, and 5, Appendix C. These records were obtained from the listed collection agencies either by on-site visits to the location or through personal communication. At present, a complete file of these data is maintained at the Agricultural Engineering Department, Iowa State University of Science and Technology, Ames, Iowa.

Topographic Characteristics

The unit graph or distribution graph represents the integrated effect of all the sensibly constant basin factors and their modifying influence on the translation and storage of runoff from a uniform excess rain occurring during a unit period. It follows, therefrom, that pertinent characteristics of these graphs should be related to significant features of the basin. Five physical characteristics of each watershed were measured in an attempt to determine these relations. They included: drainage-area size, A; length of the main stream, L; length to center of area, L_{ca}; slope of the main stream, S_c; and mean land slope, S_L. A complete definition of each term as applied to this thesis is given in

the glossary of terms (see Appendix A).

The initial approach used to establish relationships between hydrograph geometry and basin properties was to employ the principles of dimensional analysis (37) in order to reduce the number of variables involved. Some work regarding the application of these principles to the field of geomorphology has been reported by Strahler (50). Accordingly, in applying these principles the variables employed must be selected with great care such that a dependent variable can be functionally related to a system of independent variables and no others.

The use of dimensional analysis to obtain the desired relations proved relatively unsuccessful, however. A possible reason for this failure was the lack of independence of the variables used. As a consequence, a study was initiated to determine whether the various topographic factors were related.

Length of the main drainageway, L, and drainage-area size, A

Superficially, an investigator might presume that the variables L and A would be poorly related because of the diversity in shapes expected between watersheds. In an effort to test this assumption, the values of L and A were plotted on logarithmic paper as shown in Figure 3. These data were supplemented with similar results reported by Taylor and Schwarz (52) to increase range of the resultant plot. The regression line fitted to the points is defined by the equation

$$L = 1.40\ A^{0.568} . \qquad (9)$$

Figure 3. Relation of length of main stream, L, and watershed area, A

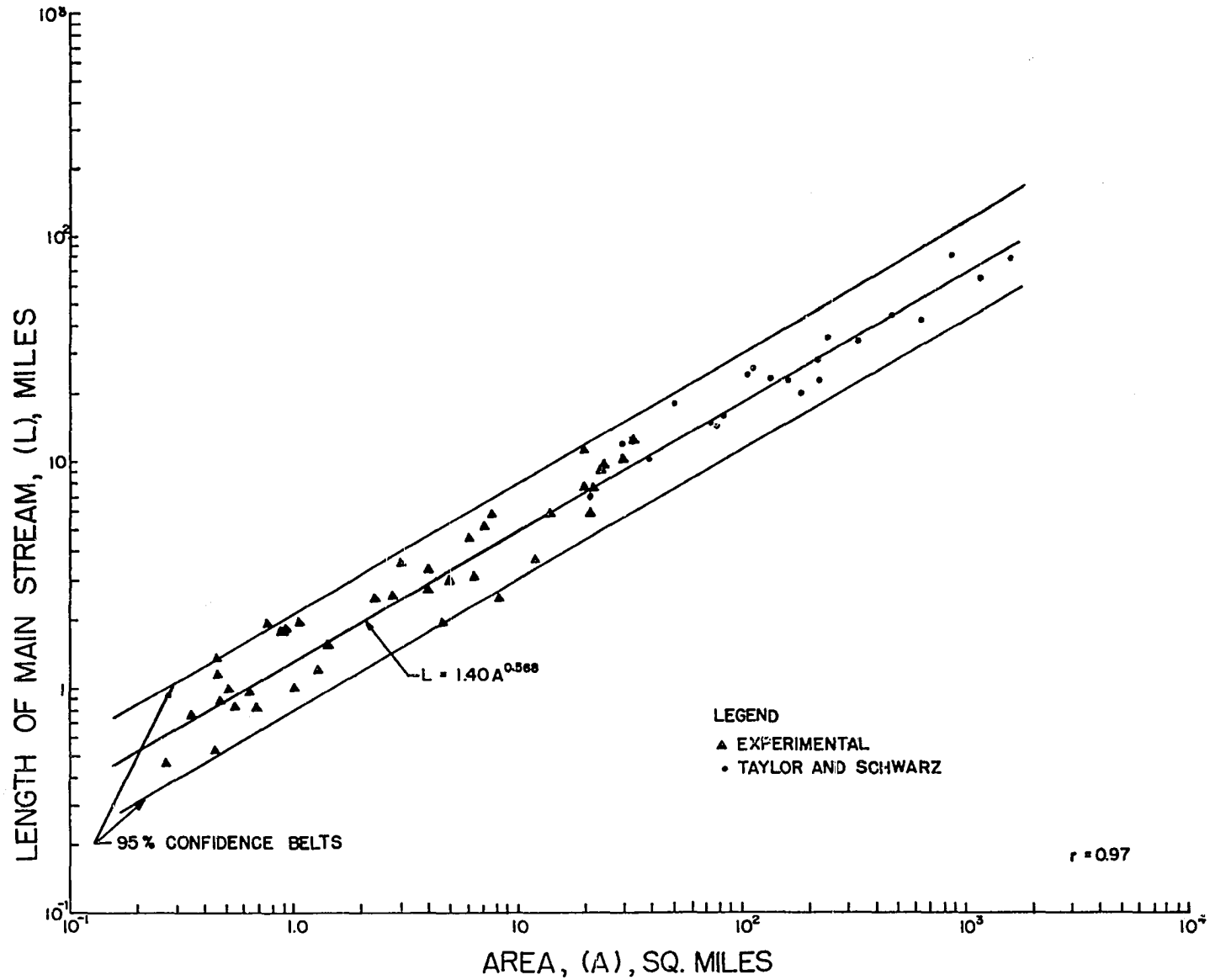
LENGTH OF MAIN STREAM, (L), MILES
AREA, (A), SQ. MILES
L = 1.40 A^0.568
95 % CONFIDENCE BELTS
LEGEND
▲ EXPERIMENTAL
• TAYLOR AND SCHWARZ
r = 0.97

An "F" test (40, p. 49), applied to the result indicated that for the experimental data the regression line significantly defines the relation between L and A. This result provides evidence that the two factors are not independent and therefore prohibits their use as independent terms in dimensional analysis techniques.

The length of the main stream corresponding to a given watershed area can be obtained with reasonable accuracy from Equation 9. The percent standard error of estimate for the regression was determined to be 24.8 percent (58).

Length to center of area, L_{ca}, and length of the main drainageway, L

Equation 9 suggests that the watersheds studied do not deviate appreciably in geometric form. If this characteristic persists, it follows that L_{ca}, the shape parameter, and L should be closely related. These data are presented graphically in Figure 4. As in the previous case, data reported by Taylor and Schwarz (52) were included.

A regression analysis applied to these values showed that the relationship between L_{ca} and L was significantly defined by the equation

$$L_{ca} = 0.54\ L^{0.96} \qquad (10a)$$

The percent standard error of estimate from regression was determined to be 14.8 percent.

Equation 10a suggests two important implications. First, the interdependence of the two parameters, L_{ca} and L, restricts their usage as independent terms in dimensional analysis and second, the use of the

Figure 4. Relation of length to center of area, L_{ca}, and length of main stream, L

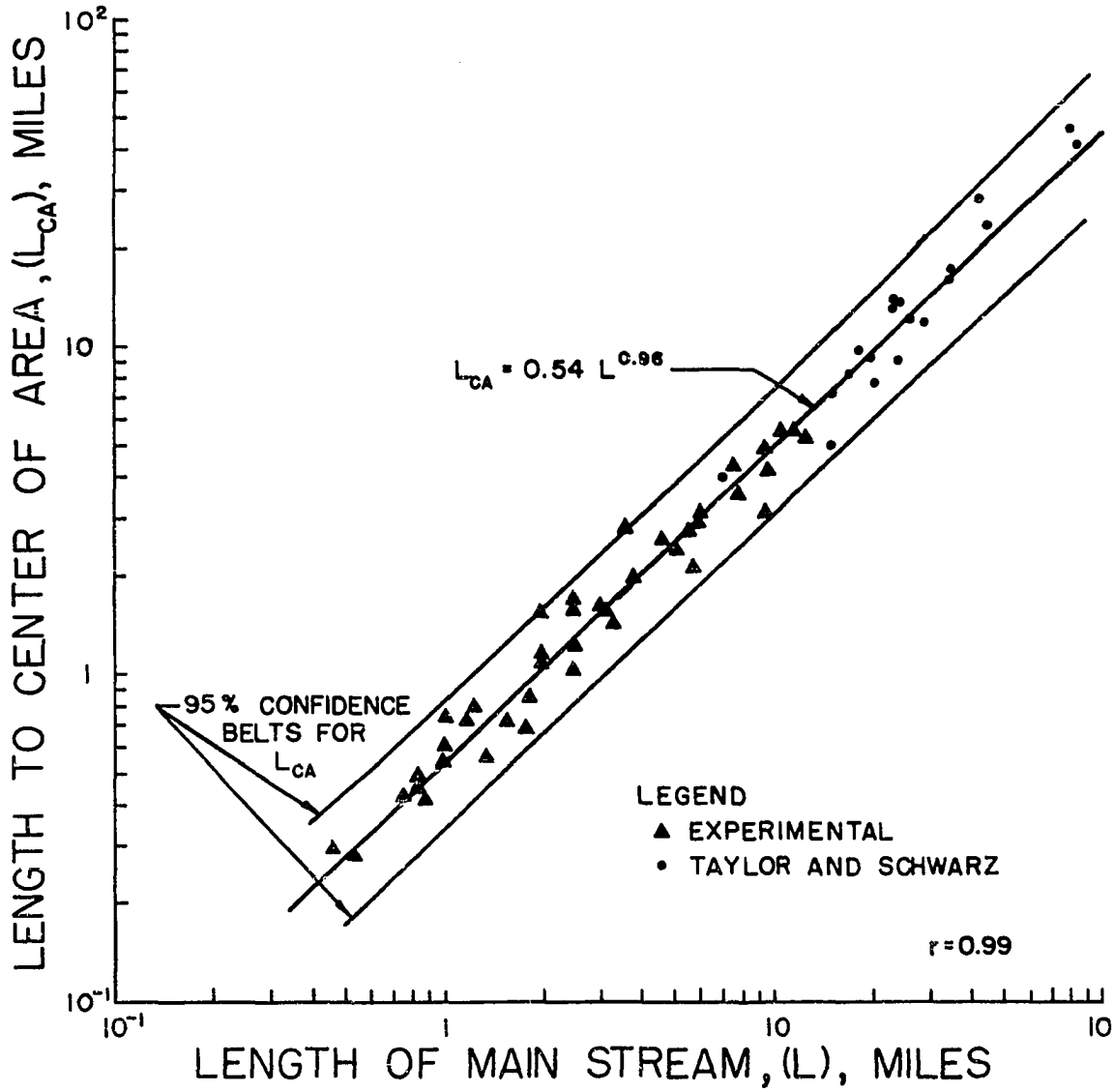
LENGTH TO CENTER OF AREA, (L_{CA}), MILES
10^2
10
1
10^{-1}
$L_{CA} = 0.54\ L^{0.96}$
95% CONFIDENCE BELTS FOR L_{CA}
LEGEND
▲ EXPERIMENTAL
• TAYLOR AND SCHWARZ
r = 0.99
10^{-1}
1
10
10^2
LENGTH OF MAIN STREAM, (L), MILES

product term, LL_{ca}, as used in many synthetic procedures, has little advantage over the use of either L or L_{ca} alone.

For practical purposes, Equation 10a may be reduced to the form

$$L_{ca} = 0.50\ L\ . \qquad (10b)$$

Discussion

The general compactness or shape characteristics of the watersheds listed were compared with those of 340 drainage basins from the Northeastern United States reported by Langbein and others (30). They evaluated the area-distance property for each of the watersheds by the factor, Σal, or the product of each partial area, a, by the channel distance from the midpoint of the main stream serving it downstream to the gaging station, 1. The regression of the factor, Σal, with drainage area, A, for the 340 drainage basins was determined to be

$$\Sigma al = 0.90\ A^{1.56}\ . \qquad (11a)$$

By definition, $L_{ca} = \Sigma al/A$, therefore Equation 11a may be written

$$L_{ca} = 0.90\ A^{0.56}\ . \qquad (11b)$$

The properties of the watersheds investigated in the current study can be expressed in a comparable form by combining Equations 9 and 10a to obtain

$$L_{ca} = 0.73\ A^{0.55}\ . \qquad (12)$$

Equations 11b and 12 define two lines which have practically the same

slope but differ in their intercept values. This indicates that the watersheds studied were generally more compact than those reported by Langbein and others.

For illustrative purposes, the equational forms of a few simple geometrical shapes were considered (see Table 1).

Table 1. Relationship between basin characteristics, L_{ca} and A, for three simple geometric forms (30, p. 135)

Geometric shape	Equational form between L_{ca} and A
Glory hole	$L_{ca} = 0.375\ A^{0.50}$
Equilateral triangle with outlet at one of the vertices	$L_{ca} = 0.94\ A^{0.50}$
Square with outlet at one of the corners	$L_{ca} = 0.76\ A^{0.50}$

The values of the exponent and coefficient of Equation 12 differ from those for any of the geometric forms listed. It appears that the general shape of the watersheds is probably intermediary between ovoid and pear-shape.

Channel slope, S_c, and length of the main stream, L

A complete discussion of the relation between the factors, S_c and L, is given on pp. 78ff. of this thesis.

Mean land slope, S_L, and slope of the first-order streams, S_1

In the study, the mean land slope, S_L, was taken as a quantitative measure of the general land slope of a watershed. Several methods are available whereby S_L can be determined for a given area. Two common methods are the intersection-line method and the grid-intersection method (20). Regardless of the method employed, however, the labor involved in computation is extensive and, in addition, the task requires topographic maps.

In an effort to minimize labor and to overcome difficulties arising from limited topographic information in the determination of S_L, an attempt was made to relate the variable with a more readily-measurable basin characteristic. It was hypothesized that the slopes of the first-order streams (21, p. 281) were related to their respective values of S_L. For a given area, the slopes of first-order streams can be determined either from topographic maps, or by field investigations with the aid of a barometric altimeter. When topographic maps are used, the delineation of the first-order streams should be accomplished by the contour method discussed by Morisawa (36).

The mean land slopes from 16 watersheds were compared with their respective mean-slope values, S_1, of a representative sample of first-order streams taken from each basin (see Figure 5). The regression equation computed by the method of least squares is

$$S_L = 0.86\ S_1^{\ 0.67} \qquad (13)$$

having a percent standard error of estimate of 28.6 percent.

Figure 5. Relation of mean land slope, S_L, with the average slope of a representative sample of first-order streams, S_1, from the same watershed

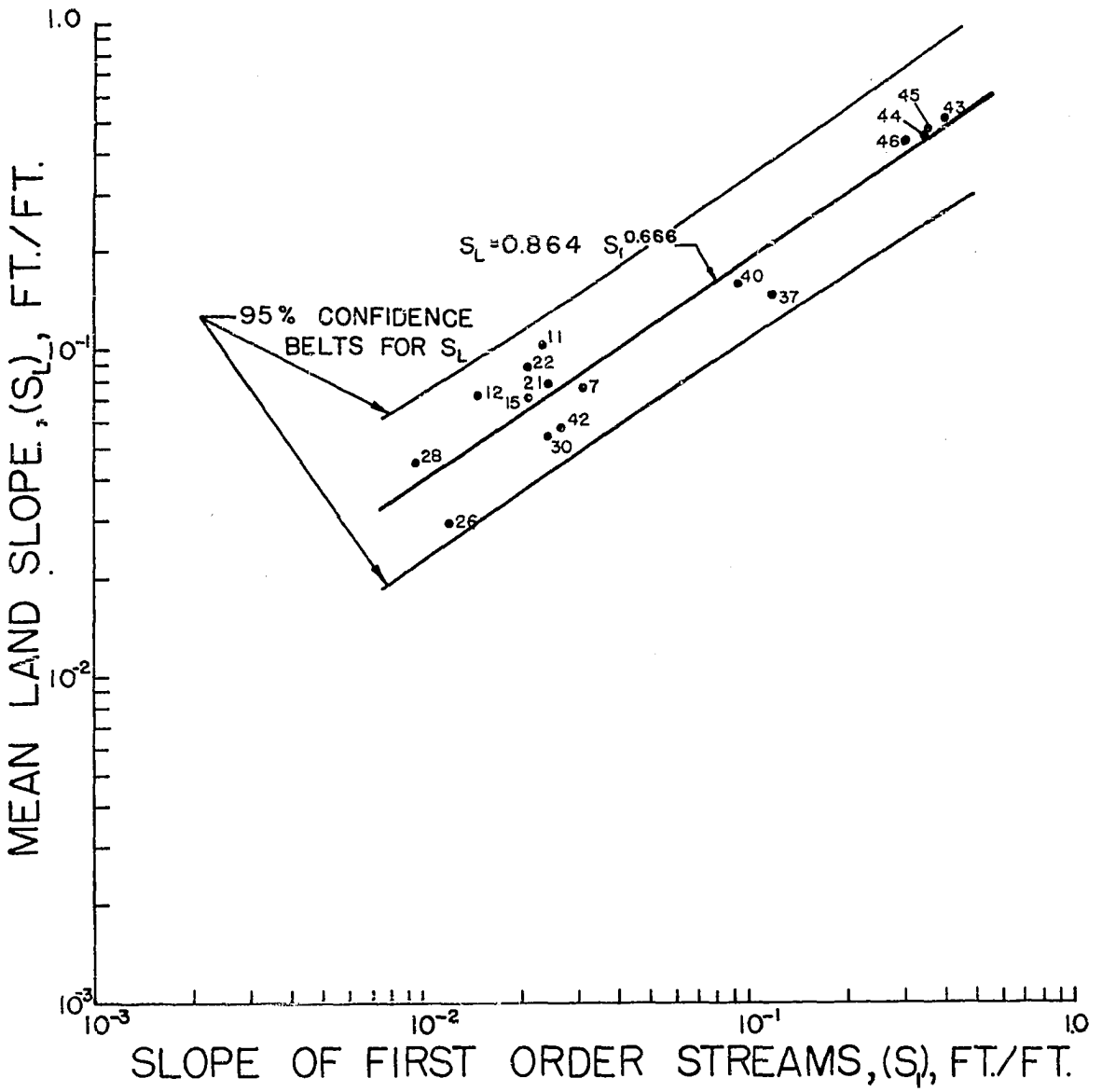
1.0
10^{-1}
10^{-2}
10^{-3}
MEAN LAND SLOPE, (S_L), FT./FT.
$S_L = 0.864\ S_l^{0.666}$
95% CONFIDENCE BELTS FOR S_L
45
44
46
43
40
37
11
22
21
12
15
7
42
30
28
26
10^{-3}
10^{-2}
10^{-1}
1.0
SLOPE OF FIRST ORDER STREAMS, (S_l), FT./FT.

Equation 13 furnishes a simple relationship whereby an estimate of the mean land slope can be obtained from the slopes of the first-order streams. The empirical results are valid only within the range of data included. Obviously, it is unrealistic for S_L to exceed S_1 as Equation 13 provides. However, because of the ease of measurement of S_1, additional work is warranted to establish the relation more concretely.

Land slope and channel slope

No attempt was made to relate the two variables, land slope and channel slope. Horton (21, p. 305) suggests that the ratio; channel slope: ground slope, is relatively constant for watersheds within a given region.

Preliminary Hydrograph Analysis

The selection of hydrologic data suitable for the development of a distribution graph tests the patience and judgment of the investigator.

The task is simplified when both rainfall and runoff records are available. Frequently, however, the difficulty encountered is that of selecting suitable records without the aid of adequate precipitation data. The influence of rainfall duration and distribution on the shape of the hydrograph and on the salient relationships between rainfall and runoff may cause considerable variation between distribution graphs and between the lag times of a given basin. In order to reduce the possibility of large errors in the results, consistent procedures were employed in the selection of data.

Bernard (5) and Brater (7, p. 1196) have suggested various criteria requisite for the selection of hydrologic data suitable for distribution-graph and/or unit-hydrograph development. These were summarized to formulate the basis of the following list of standards used in this study.

1. The rain must have fallen within the recording time interval or time unit and must not have extended beyond the period of rise of the hydrograph.
2. The storm must have been well-distributed over the watershed, all stations showing an appreciable amount.
3. The storm period must have occupied a place of comparative isolation in the record.
4. The runoff following a storm must have been uninterrupted by the effects of low temperatures and unaccompanied by melting snow or ice.
5. The stage graphs or hydrographs must have a sharp, defined, rising limb culminating to a single peak and followed by an uninterrupted recession.
6. All stage graphs or hydrographs for the same watershed must show approximately the same period of rise.

The degree of adherence to the above criteria in selecting data from a particular watershed was dictated by the accessibility and availability of these data. In some cases, due to an insufficient number of hydrographs, it was necessary to select those which were affected by small rains occurring either before or after the principle burst. In these cases, the "parasite" graphs were separated from the main graph by

accepted hydrologic procedures (32, p. 447, 49).

A listing of the storms selected for each watershed and pertinent information related to their characteristics appears in Table 6, Appendix C.

Development of an empirical distribution graph

The hydrographs and stage graphs selected were reduced to distribution graphs in a manner outlined in Appendix D.

A representative distribution graph for a given basin may be developed using one of several methods recommended by hydrologists. Linsley, et al. (33, p. 198) advise that the correct graph may be obtained by plotting the separate unit graphs[1] with a common time of beginning of excess precipitation, locating the average peak height and time and sketching a mean graph which conforms to the individual graphs as closely as possible.

Brater (7, p. 1,201) developed a composite distribution graph for each of the Coweeta watersheds by the following procedure. All the distribution graphs for each stream were first superimposed as nearly as possible on each other. The composite graph for the area was then developed either by selecting one of the individual graphs as representing an average or by drawing the average graph through the cluster and listing the percentages at selected time intervals.

---

[1]Since the distribution graph is simply a modified form of the unit hydrograph, all principles governing the selection, development, synthesis, and application of one graph also apply in the case of the other.

Another technique utilized by Mitchell (34, p. 34) recommends that the separate graphs be superimposed to a position of best fit and then the ordinates averaged to obtain the average distribution graph. In determining the position of best fit, the timing of the various elements are given weight in the following order of decreasing importance:

1. Maximum ordinate,
2. Time of occurrence of precipitation excess,
3. Ascending limb of the hydrograph, and
4. Descending limb of the hydrograph.

The major difference between the methods arises in positioning the separate graphs to the position of best fit. Care must be given to this aspect, otherwise an incorrect representative graph may result. If, for instance, positioning is disregarded and the concurrent ordinates simply averaged, the resultant graph will have a lower peak and broader time base.

In this study, the method of resolving a representative graph for an area was controlled by the discrepancy of the basic data. The times-of-occurrence and magnitudes of the peak discharges were considered the most significant factors. When the individual graphs plotted with a common time of beginning of surface runoff showed small time variations at the peak discharge, the average graph was obtained by the method described by Linsley, et al. (33). If, on the other hand, the composite plot indicated extreme horizontal scattering of the peaks, so as to restrict the graphic determination of an average peak, the graphs were positioned to a location of best fit in accordance with Mitchell. The average period of rise

and peak discharge were then obtained and an average distribution graph constructed by trial plottings.

A check on the final graph selected is executed easily since the sum of the ordinates of a distribution graph must total 100 percent. It is necessary in final results to complete adjustments of the initial trial graphs to satisfy this criterion.

The representative distribution graph of an area developed in this manner was designated as the empirical graph of the watershed. The terminology "empirical" was adopted to infer that the graph was developed from empirical data and to avoid the possibility of misinterpretation conveyed by the words mean or average.

The empirical graphs for the 42 watersheds are presented in Figures 23-33, Appendix D.

Relationship between empirical graph and statistical gamma distribution

The mathematical expressions proposed by Edson and Nash (see Appendix B) to describe the unit graph may be replaced by the generalized form given by Equation 4. Since the characteristic shape of a unit graph is retained by the distribution graph, this equation is also applicable in description of the latter. Only appropriate changes to the dimensions of the constants must be considered.

The shape of the unit graph or distribution graph appears to follow the form of a skew statistical frequency curve. This property is easily perceived when the distribution graph of a watershed is plotted as a discrete frequency histogram (see Figure 6). The analogy is further

Figure 6. Empirical graph for watershed 19 plotted as a frequency histogram

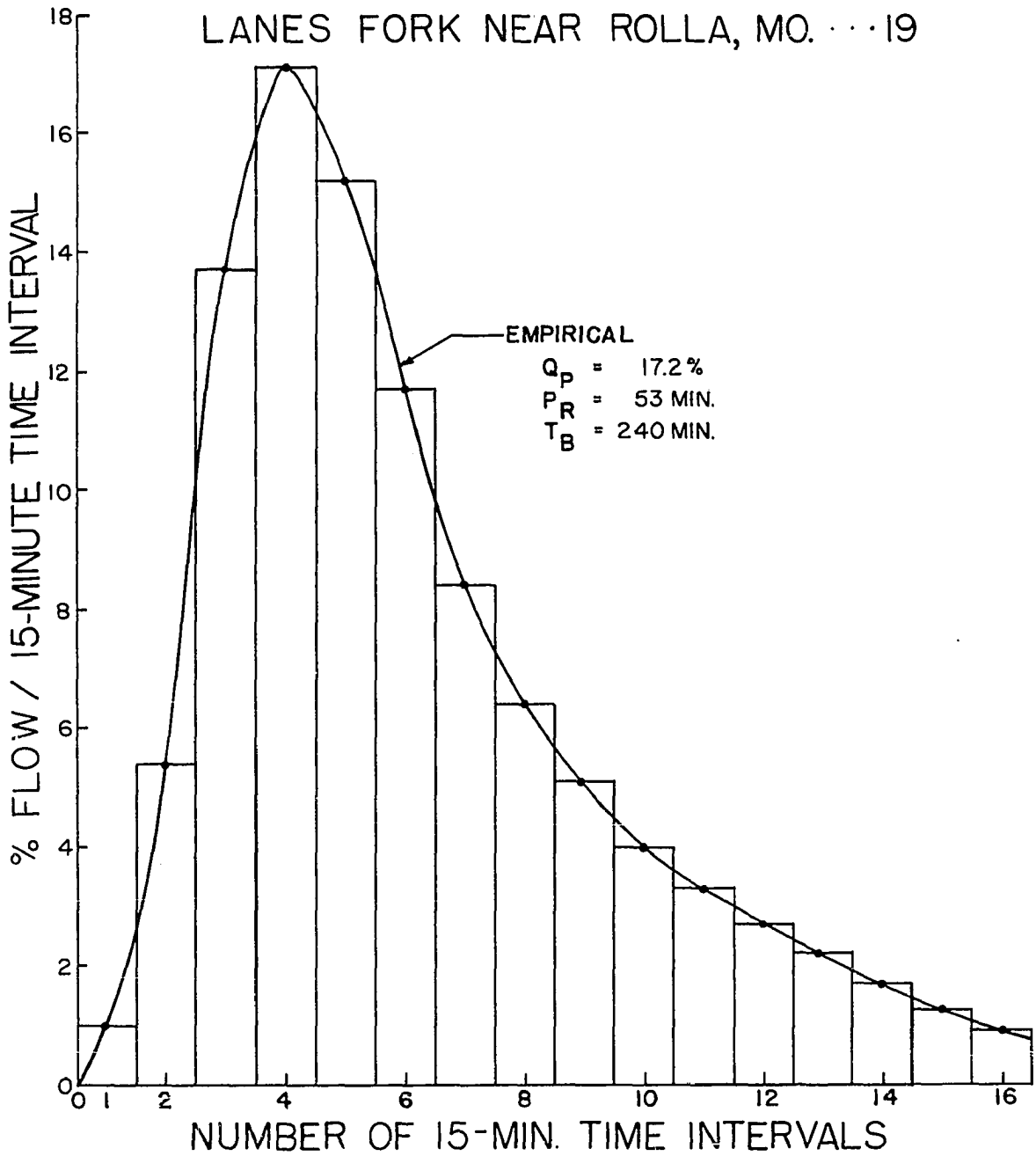
LANES FORK NEAR ROLLA, MO. · · · 19
% FLOW / 15-MINUTE TIME INTERVAL
NUMBER OF 15-MIN. TIME INTERVALS
EMPIRICAL
Q_P = 17.2%
P_R = 53 MIN.
T_B = 240 MIN.
0
2
4
6
8
10
12
14
16
18
0 1 2 4 6 8 10 12 14 16

supported by presenting the ordinate values as a percent flow based on a given time increment.

One of the most common and most flexible of the frequency curves, which has been used numerous times in the analysis of hydrologic data is Pearson's Type III curve. The equation for this distribution is given by Elderton (14) in the form

$$f(x) = y = (N/a)\frac{(p)^{p+1}}{e^{p}\,\Gamma(p+1)}\; e^{-cx}\,(1 + x/a)^{ca} \qquad (14a)$$

where the origin is at a, the mode. The origin can be transferred to zero by making the appropriate substitutions; x - a = x and p = ca, into Equation 14a to obtain

$$f(x) = y = \frac{N}{\Gamma(p+1)}\,(c)^{p+1}\, e^{-cx}\, x^{p} \; . \qquad (14b)$$

It follows, if q = p - 1 and γ = c, Equation 14b further reduces to

$$f(x) = y = \frac{N\,(\gamma)^{q}}{\Gamma(q)}\; e^{-\gamma x}\, x^{q-1} \qquad (14c)$$

where f(x) = y = any "y" value,

x = any "x" value,

N = total frequency or number of observations of x,

γ,q = scale and shape parameters respectively, estimated from observed x values,

Γ = gamma function, and

e = base of the natural logarithms.

Equation 14c defines a particular type of Pearson's Type III curve which commonly is referred to as the two-parameter or incomplete gamma

distribution.

It is easily recognizable that Equations 4 and 14c are identical when the following equalities exist:

$$f(x) = y = Q_t$$

$$N = V$$

$$x = t$$

$$\gamma, q = \alpha, \beta.$$

On the basis of this evidence it was assumed that the empirical graphs could be defined using the two-parameter gamma distribution as the model and by obtaining the estimators q and γ by statistical procedures.

Development of dimensionless graphs

The empirical graphs were reduced to a standardized form to avoid inconsistencies in the time increments used in their description. Each graph was adjusted with its ordinate values expressed in percent flow based on a time increment equal to one-quarter the period of rise (% flow/$0.25P_R$) and the abscissa as the ratio of any time, t, divided by the period of rise, P_R (see Figures 35 through 45, Appendix E). The empirical graphs described in this manner were referred to as dimensionless graphs. Although each ordinate value is expressed as % flow/$0.25P_R$, the connotation simply infers that it is the percentage of the total volume of flow based on a time-increment duration of $0.25P_R$; percent being dimensionless.

The time-increment duration of $0.25P_R$ was chosen on the following reasoning:

1. The initial increments used in subdividing the times bases of the hydrographs for a particular basin were of approximately equivalent duration and only small adjustments to the empirical graphs were necessitated,
2. The use of $0.25P_R$ enabled definition of the rising limb at four points,
3. The period of rise was ascertained to be a stable and important time characteristic for a given watershed, (see discussion pp. 63ff.) and
4. The distribution graph for a basin can be defined knowing three parameters.

The dimensionless graph represents a modified form of the unit hydrograph in which the basic shape has been retained. Its geometry can be described by modifying the constants of Equation 4. The general equation for the dimensionless graph can thus be expressed as:

$$Q_{t/P_R} = \frac{V'(\alpha')^{\beta}}{\Gamma(\beta)} e^{-\alpha' t/P_R} \, t/P_R^{\beta-1} \qquad (15a)$$

where Q_{t/P_R} is the % flow/$0.25P_R$ at any value of t/P_R, V' is the volume in percent and α' is a dimensionless parameter.

Fitting the Two-Parameter Gamma Distribution to the Dimensionless Graph

The evaluation of the parameters, α' and β, of Equation 15a from empirically-derived data by the usual curve-fitting procedures of the method of least squares or the method of moments is a cumbersome and

laborious task. Nash (38, 39) has given a procedure for evaluating the parameters, k and n, of Equation 31f (see Appendix B) from storm data by the method of moments. The application of this technique was prohibited, however, due to the limited rainfall data available.

The equality of the equational forms for the two-parameter gamma distribution and the unit hydrograph has been established. It can be assumed that each dimensionless graph represents a sample of t/P_R-values taken from the gamma population defined by the parameters q and γ', in which case γ', a dimensionless quantity, replaces the scale parameter, γ, of Equation 14c. Thom (53) found that efficient estimates of the parameters of the two-parameter gamma distribution could be obtained by the method of maximum likelihood. This method was used exclusively in the application of the distribution for the evaluation of the drought hazards in Iowa as reported by Barger and Thom (2).

The latter study is cited further because of an additional contribution made during its completion. This was the programming of the two-parameter gamma distribution to the IBM-650 computer (16). As a consequence, the maximum likelihood estimates, $\hat{q}$ and $\hat{\gamma}$, of q and γ', could be obtained from the dimensionless graphs by machine calculation. The use of this program resulted in a material reduction in time, labor, and cost in the current study.

The procedures involved in organizing and processing the dimensionless graphs to obtain $\hat{q}$ and $\hat{\gamma}$ by machine calculation are given in Appendix E. Each of the dimensionless graphs of the 42 watersheds included in the study were treated the same. In addition, in Appendix E,

it is shown that the equational form of the two-parameter gamma distribution describing the dimensionless graph (see Equation 14c) can be written

$$Q_{t/P_R} = \frac{25.0(\gamma')^q}{\Gamma(q)} \; e^{-\gamma' t/P_R} \; t/P_R{}^{q-1} \qquad (16)$$

Equation 16 can be solved for the experimental results by replacing q and γ' by their maximum likelihood estimates, $\hat{q}$ and $\hat{\gamma}$. The work involved in this solution is reduced by the use of appropriate mathematical tables (1, 18).

Goodness of fit of fitted distributions

Figures 35-45, Appendix E, show the best-fit gamma distributions plotted with their respective dimensionless graphs. It is evident from the figures, that the relative degree to which the fitted curve approximates the actual graph varies considerably. This is well-illustrated by comparing the curves for watershed 9, Figure 27, and those for watershed 25, Figure 41.

An attempt was made to minimize the effect of these differences to the precision of fit in further correlation studies involving the parameters, $\hat{q}$ and $\hat{\gamma}$, by choosing the values of the parameters from curves which exhibited good fit. Great difficulty was encountered, however, in selecting a suitable index of goodness of fit. The problem was manifested when considering both statistical and practical aspects.

The chi-square test may be employed to obtain a statistical measure of the goodness of fit (40, p. 65). Chi-square values, χ^2, are obtained by the formula

$$\chi^2 = \sum_{i=1}^{k} (O_i - E_i)^2/E_i \qquad (17)$$

where O_i = observed percent flow,

E_i = theoretical or expected percent flow, and

k = number of classes or increments, $t/P_R = 0.25$.

The probability level, P, of obtaining the calculated χ^2-value is obtained by comparing its magnitude with tabulated values at k-3 degrees of freedom (40, p. 445).

This test was completed for the two curves of each watershed. The probability levels of the calculated χ^2-values ranged from a minimum, P = 0.25, for watershed 13, Figure 38, Appendix E, to a maximum, P = >0.9995, for watersheds 4, 23 and 25, Figures 35, 40 and 41, Appendix E.

On the basis of this evidence, the hypothesis that the actual curve is of the same population as the fitted curve, cannot be rejected. By the same reasoning, the goodness of fit cannot be considered highly significant except in special cases, such as for the latter-mentioned watersheds. For these watersheds, the evidence is conclusive that the fit is good and the dimensionless graph can be represented by the two-parameter gamma distribution.

This discussion does not conclude the argument that the goodness of fit is adequate in all cases from a practical aspect. Hydrologists are concerned primarily with the agreement of the graphs within the portion bounded by the crest segment. Large discrepancies within this segment

invalidate the usefulness of the fitted curves for design purposes, especially for full-flow type structures. An example of wide variation is shown between the curves for watershed 11, Figure 37, Appendix E.

The major problem is one of defining quantitatively, hydrologic acceptance. Any measure employed must take into consideration:

1. The accuracy of the measuring instruments,
2. The scatter and deviations of the original data from the empirical graphs, and
3. The effect of the discrepancies on the agreement of actual and calculated hydrographs for a design storm of long duration.

At the time of this phase of work, additional consideration had to be given to the uncertainty of the expected relationships involving the parameters, q and γ', and basin characteristics. As a result, rather than attempting to determine an elaborate test for evaluating the precision of fit within the crest segment, an arbitrary "point" criterion was established. Hereafter, a satisfactory fit connotates that the fitted curves approximated the dimensionless graphs within ± 20 percent at the peak ordinate. The parameters, $\hat{q}$ and $\hat{\gamma}$, from the fitted curves which adhered to this criterion were used in further investigations.

Additional basic studies are needed concerning the application of statistics as measures of the variation of hydrologic data. For the particular problem indicated, a significant contribution could be made in developing a method to test the agreement of the curves within the crest segment. The association of the adopted measure and practical considerations will be resolved in the application of the synthetic

method presented herein to actual storm data.

Modified dimensionless graphs

Experience indicated that poor agreement between the fitted and dimensionless graphs generally occurs either:

1. When the dimensionless graph is of apparent different geometric shape than the gamma distribution (see watershed 12, Figure 27, Appendix E), or
2. When the dimensionless graph exhibited a prolonged recession (see watershed 11, Figure 37, Appendix E).

The obtainment of a dimensionless graph exhibiting a different shape than the gamma distribution is not unlikely considering the numerous factors affecting its geometry. For such cases, the agreement between the two curves would be poor since the comparison is essentially between empirically-derived data from one population and a theoretical model describing another population. Closer approximations would result by fitting these data to a more appropriate model, or possibly two different models; one describing the rising limb, the other the recession limb.

The prolonged, extended, recession limb of a dimensionless graph for a given area is probably the result of one of two causes:

1. Either the area in question has appreciable storage characteristics, or
2. An appreciable contribution of flow has occurred as interflow (35).

For these data, the fitted and the experimental curves deviate appreciably

within the crest segment. Since the method of maximum likelihood provides the "best-fit" line over the entire curve, the greater significance is given to the recession limb than to the crest segment. Thus, greater error is induced to the "best-fit" line near the center. Nash (38) encountered similar difficulties by using the method of moments as the fitting procedure.

The magnitude of this variation possibly may be reduced by employing the following procedures:

1. Increasing the number of points describing the dimensionless graph,
2. Applying different statistical fitting methods, or
3. Force-fitting.

Of the three alternatives suggested, the third offers the greatest potential with minimum labor. The versatility of the gamma distribution as demonstrated in Figure 10 suggests that by sacrificing accuracy within the relatively unimportant hydrologic portion of the curve as the recession limb, values of $\hat{q}$ and $\hat{\gamma}$ could be chosen to obtain a closer approximation of the dimensionless graph near the center. This technique is referred to herein as force-fitting. Its use was considered permissible because there is evidence that the dimensionless graph is of a gamma population.

Force-fitting

An arbitrary procedure was established to exemplify the results that could be obtained with simple manipulation of the original data. Alter-

nate values of t/P_R at increments of $t/P_R = 0.125$ were removed from the recession limb and the respective ordinate values summed. This total was then prorated over the crest segment in accordance with the ratio: % flow/$0.25P_R$ for the given ordinate value divided by the sum of the ordinates (% flow/$0.25P_R$) at increments of $t/P_R = 0.125$, within the crest segment. The respective additions were made to the dimensionless graph to form the pseudo-dimensionless graph (see Figure 7). The modified or "best-fit", two-parameter gamma distribution for the pseudo-dimensionless graph was then obtained by procedures outlined in Appendix E.

Figure 7 shows the dimensionless, fitted, pseudo-dimensionless and modified curves for watershed 11. As would be expected, the modified curve shows closer agreement with the dimensionless graph at the peak ordinate and greater deviation on the recession limb. Similar results were obtained for four other watersheds: watershed 15, Figure 38; watershed 17, Figure 39; watershed 24, Figure 40; and watershed 33, Figure 43 (see Appendix E). In all cases, the agreement between the curves has been improved within the crest segment although greater variation is noted in other portions of the curves. This observation is particularly evident for watershed 17. For this watershed, the rising limb appears to adopt different geometry than that described by the fitted distribution.

The results suggest that by minor adaptation of the input data, a two-parameter gamma distribution can be forced to fit dimensionless graphs with extended recession characteristics to give more practical results. Additional developmental work is required in the methodology

Figure 7. Influence of modifications of the input data on the fit of the two-parameter gamma distribution to the dimensionless graph for watershed 11

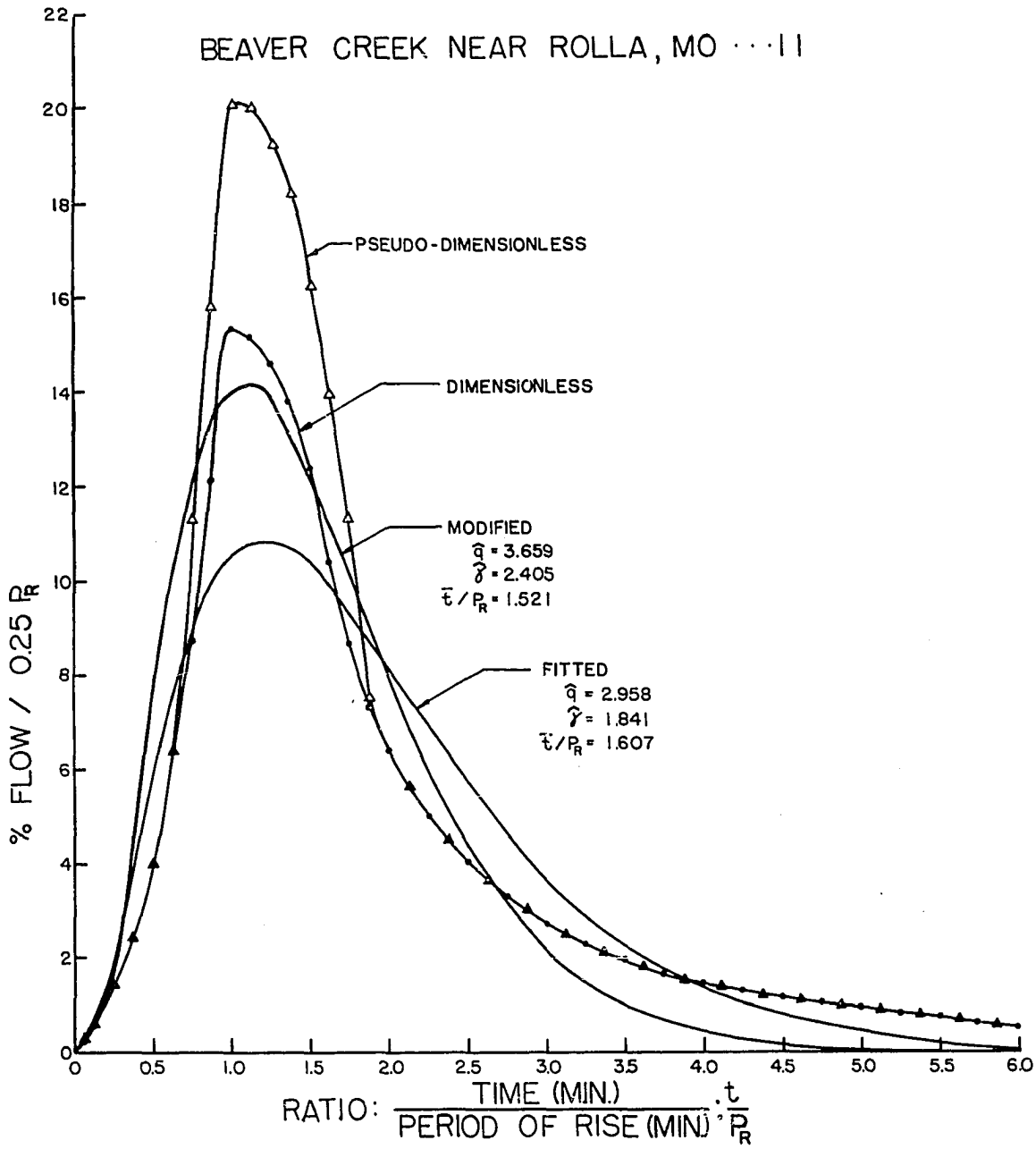
BEAVER CREEK NEAR ROLLA, MO ···11
PSEUDO-DIMENSIONLESS
DIMENSIONLESS
MODIFIED
$\hat{q}$ = 3.659
$\hat{\gamma}$ = 2.405
$\bar{t}/P_R$ = 1.521
FITTED
$\hat{q}$ = 2.958
$\hat{\gamma}$ = 1.841
$\bar{t}/P_R$ = 1.607
% FLOW / 0.25 P_R
RATIO: $\frac{\text{TIME (MIN.)}}{\text{PERIOD OF RISE (MIN)}} \cdot \frac{t}{P_R}$
0
2
4
6
8
10
12
14
16
18
20
22
0
0.5
1.0
1.5
2.0
2.5
3.0
3.5
4.0
4.5
5.0
5.5
6.0

of fitting to alleviate the successive trial procedures. Here, as before, the problem of evaluating the fit in terms of "hydrologic acceptance" remains.

Selection of the Time Parameter

Before synthetic techniques can be employed in synthesizing a hydrograph for a given area, it is necessary to have available a time parameter relating the salient features of rainfall and runoff for the area in question. Several forms of lag have been proposed for this purpose (3).

Two of the most widely used forms are those proposed by Horner and Flynt (19) and by Snyder (48). Horner and Flynt define lag as the time difference between the center of mass of precipitation excess and the center of mass of the resulting hydrograph. The authors found that for a given area lag was nearly constant and, therefore, independent of precipitation and topographic effects.

Snyder in 1938 introduced lag to define the time difference between the center of mass of a surface-runoff producing rain and the occurrence of peak discharge. In using this definition it was necessary to specify the storm type; otherwise, due to the unsymmetrical nature of the hydrograph, the magnitude of lag for a given area will vary with storm duration.

The constant property of lag is consistent with unit-graph theory. In addition, it is of major importance in synthetic studies since differences in lag values can be related to differences in physical conditions

of the watersheds such as size, shape, slope, and storage.

To avoid possible confusion in the balance of this thesis, the term lag, t_L, as used hereafter refers to the definition as proposed by Snyder. An attempt was made to determine the lag for each basin studied from an analysis of the available rainfall records. The results of this analysis are presented in Table 6, Appendix C.

Computing lag from available rainfall records

It is evident from Table 6, Appendix C, that the individual lag values within certain areas exhibit considerable scatter. These variations may be explained in part by the incomplete restriction of storm type. Moreover, the lack of agreement of the time properties reported on the rainfall and runoff charts was a major source of variation. In some cases this disagreement completely prohibited the calculation of lag.

These inconsistencies in time properties can be attributed to many variables, including:

1. Inadequate raingage placement and coverage,
2. Direction of storm movement,
3. Distribution of rainfall,
4. Inaccuracies arising from the malfunctioning of the recording instruments and difficulties encountered in prorating time errors over long periods,
5. Errors induced in the recording of data, and
6. Restrictions imposed by time-scale limitations on the original

data.

Item 6, above, is especially significant on data collected by the United States Geological Survey (USGS). On stage graphs obtained from this source, one hour of time is represented by 0.10-inch or 0.20-inch increments. As a result, the time of occurrence of the peak discharge could only be approximated with reasonable accuracy to the nearest 15-minute period on the former scale or to the nearest 7.5-minute period on the latter scale. This limitation is particularly critical in lag computations for small watershed areas.

Due to the difficulties encountered, lag was determined only for those storms in which there was reasonable agreement in the time properties of the precipitation and runoff data. In Table 6, Appendix C, the nonconformity between the recorded rainfall depths and peak discharges also can be discerned, particularly on the larger watersheds. This incongruity is not unexpected considering the interaction of inadequate raingage placement and storm characteristics. For such cases, the lag values were determined assuming that the time and shape of the recorded mass curve depicted the rainfall characteristics over the entire area.

Relation between lag and period of rise

In spite of the simplifications introduced, it was impossible to obtain lag for all the watersheds studied. In order to avoid these deletions from other investigations, an additional study was undertaken in an attempt to find a more suitable time parameter which may be measured for each basin.

Since the storms utilized in this study are of short duration and high intensity, it follows that lag, t_L, and period of rise, P_R, should be related. A plot of these two variables for 94 selected storms is shown in Figure 8. The regression line fitted by the method of least squares is defined by the equation

$$t_L = 0.996 P_R^{1.005} \quad . \qquad (18)$$

Since the values of the coefficient and exponent of Equation 18 are approximately unity, for all practical purposes t_L may be taken equal to P_R. A similar result was obtained by Hickok, et al. (17) in their studies of rainfall and runoff records from 14 experimental watersheds in Arizona, New Mexico, and Colorado. The authors reported (17, p. 615),

> Rise time varied from 74 per cent to 145 per cent of the lag time (time from the center of mass of a limited block of intense rainfall to the resulting peak of the hydrograph) for the individual watersheds in this study. The average for all watersheds was 102 per cent.

The association between the lag time used above and lag as used herein is assumed. For short-duration storms, as used in the development of unit graphs for small watersheds, the center of a limited block of intense rain and the mass center of the surface-runoff producing rain would be nearly coincident.

An analysis of variance of the regression of t_L on P_R produced a highly significant "F" value indicating the regression between the two variables is defined very well by Equation 18. Moreover, since it would be expected that a given change in P_R would be accompanied by a constant proportional change in t_L, there is strong evidence that Equation 18

Figure 8. Relation of lag, t_L, and period of rise, P_R, for 94 selected storms

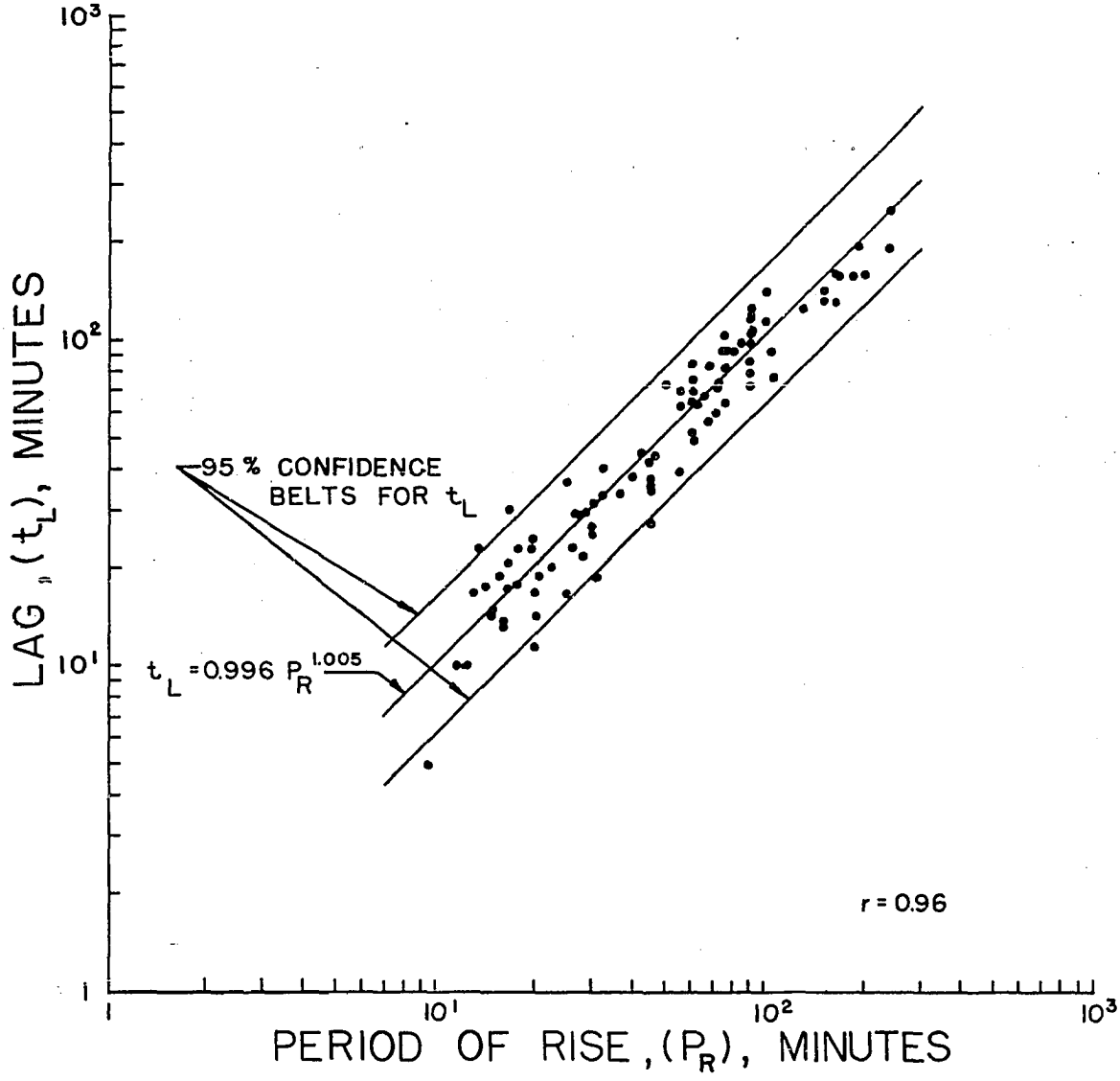
LAG , (t_L), MINUTES
PERIOD OF RISE, (P_R), MINUTES
95 % CONFIDENCE BELTS FOR t_L
$t_L = 0.996\ P_R^{1.005}$
r = 0.96
10^3
10^2
10^1
1
10^1
10^2
10^3

defines the functional relationship between the two variables (15, p. 106). The variances from regression for the t_L-values and P_R-values were approximately equal. The percent standard errors of estimate or coefficients of variation were calculated to be 27.1 percent and 25.7 percent, respectively.

On the basis of these results, the following conclusions were formulated:

1. Lag and period of rise are related functionally in a form defined by the regression equation, $t_L = 0.996P_R^{1.005}$, and
2. The period of rise of the hydrograph can be used to replace lag time as the time parameter for a given watershed.

The above conclusions are applicable generally for uniformly-distributed, short-duration, high-intensity storms occurring over small watershed areas.

Relation between Parameters, q and γ'

The use of the dimensionless graph leads to the development of a unique relation between the two parameters of the two-parameter gamma distribution. This property is brought about by the constant positioning of the mode or peak at a value, $t/P_R = 1$. By setting the first differential of Equation 16 equal to zero and substituting the value, $t/P_R = 1$, into the resultant expression, one obtains the relation

$$q - 1 = \gamma' \ . \qquad (19)$$

A study was conducted to test the agreement of the maximum likelihood

estimates $\hat{q}$ and $\hat{\gamma}$ obtained from the fitting process against the theoretical result (see Figure 9). The linear regression line fitted to the experimental data by the method of least squares is defined by the equation

$$\hat{q} = 1.445 + 0.873\,\hat{\gamma} \ . \qquad (20)$$

Figure 9 shows that for the experimental data, the values of q have been overestimated at the smaller values of γ' and underestimated at the larger γ'-values. The influence of this characteristic on the geometry of the dimensionless graph can be perceived from Figure 10. It is apparent that with increasing values of the peak percentage, Q_p, the values of t/P_R become less than unity. Similarly, at small values of Q_p, the values of t/P_R are greater than unity.

The failure of the experimental results to follow Equation 18b is a measure of the inability of the fitting procedure to achieve the proper positioning of the peak ordinates of the fitted graphs. In order to ascertain the magnitude of this discrepancy, the values of t/P_R of the fitted graphs at the peak were computed by the equation

$$t/P_R = (\hat{q}-1)/\hat{\gamma} \qquad (21)$$

and the respective values of Q_p found by substitution of the result in Equation 16. These values are plotted in Figure 11. The relation between t/P_R and Q_p for these data was found to be significantly described by the quadratic regression equation

$$t/P_R = 1.913 - 0.0808Q_p + 0.00165Q_p^{\,2} \ . \qquad (22)$$

Figure 9. Theoretical and experimental relationships of parameters q and γ' for dimensionless graphs

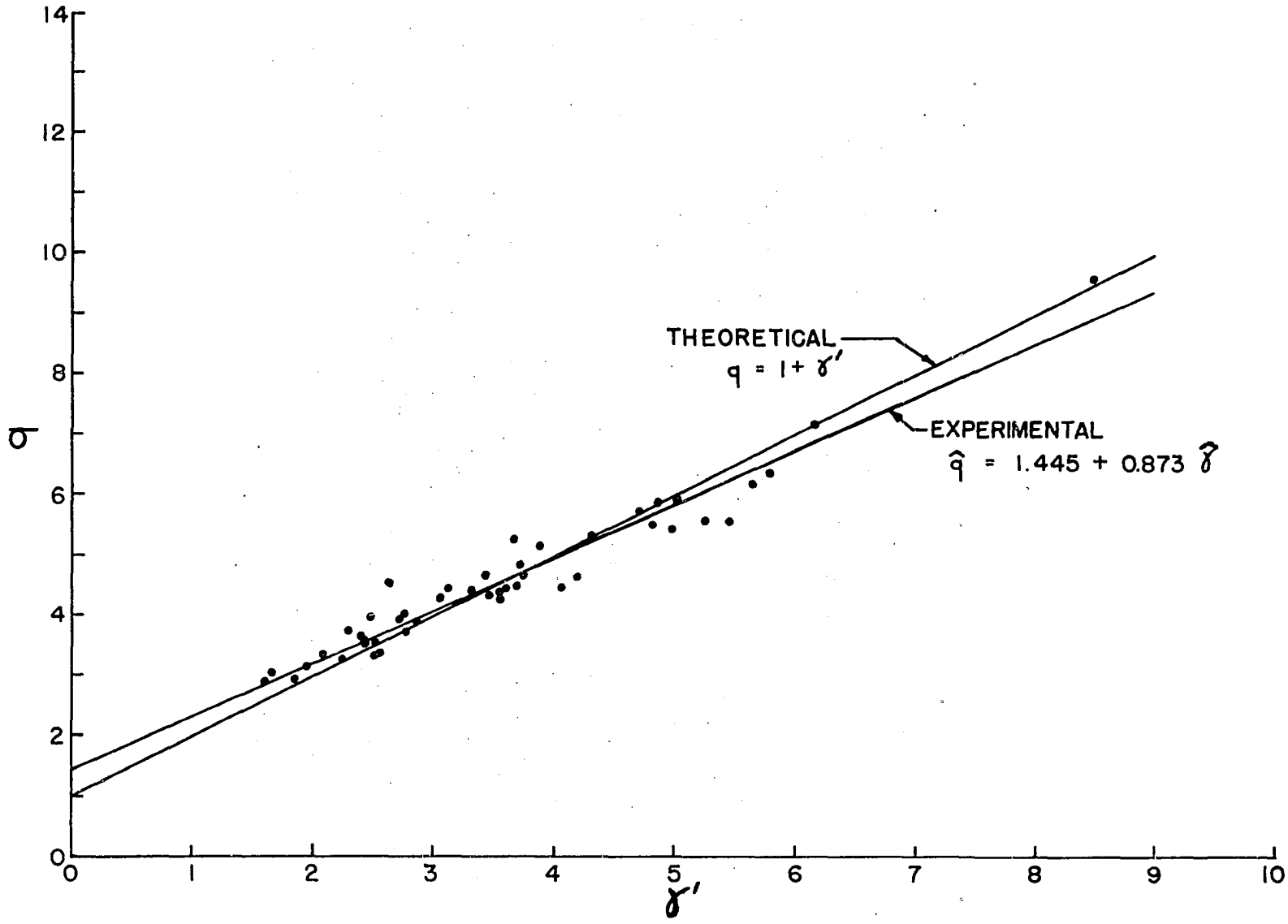
14
12
10
8
6
4
2
0
0
1
2
3
4
5
6
7
8
9
10
q
γ'
THEORETICAL
q = 1 + γ'
EXPERIMENTAL
q̂ = 1.445 + 0.873 γ̂

Figure 10. Variation in the geometry of the dimensionless graph resulting from selection of parameters $\hat{q}$ and $\hat{\gamma}$, in accordance with the regression equation $\hat{q} = 1.445 + 0.873\,\hat{\gamma}$

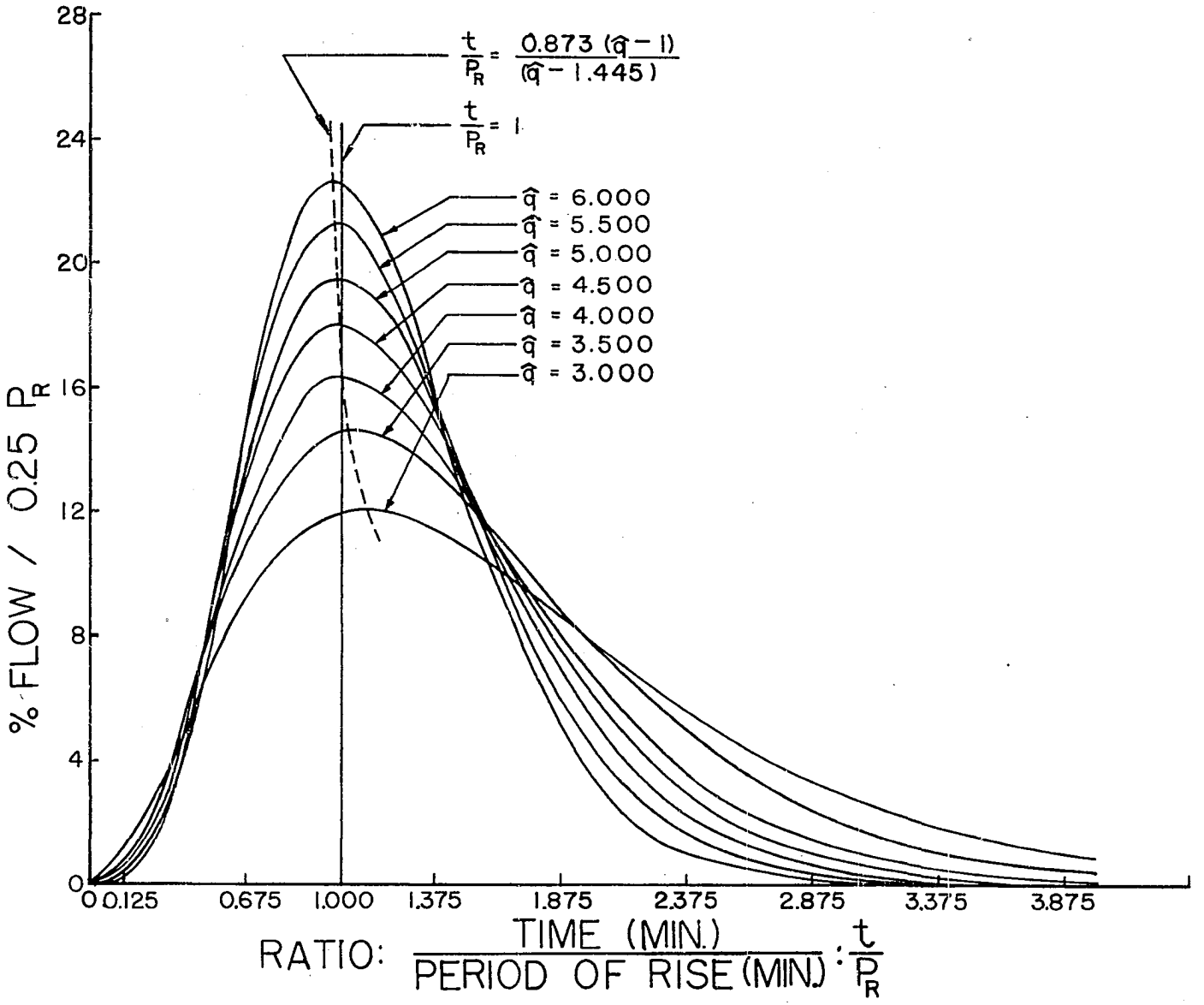
$\frac{t}{P_R} = \frac{0.873\,(\hat{q}-1)}{(\hat{q}-1.445)}$
$\frac{t}{P_R} = 1$
$\hat{q}$ = 6.000
$\hat{q}$ = 5.500
$\hat{q}$ = 5.000
$\hat{q}$ = 4.500
$\hat{q}$ = 4.000
$\hat{q}$ = 3.500
$\hat{q}$ = 3.000
% FLOW / 0.25 P_R
0
4
8
12
16
20
24
28
0 0.125
0.675
1.000
1.375
1.875
2.375
2.875
3.375
3.875
RATIO: $\frac{\text{TIME (MIN.)}}{\text{PERIOD OF RISE (MIN.)}} : \frac{t}{P_R}$

Figure 11. Inconsistencies in the positioning of the peaks of the dimensionless graphs described by the fitted gamma distributions

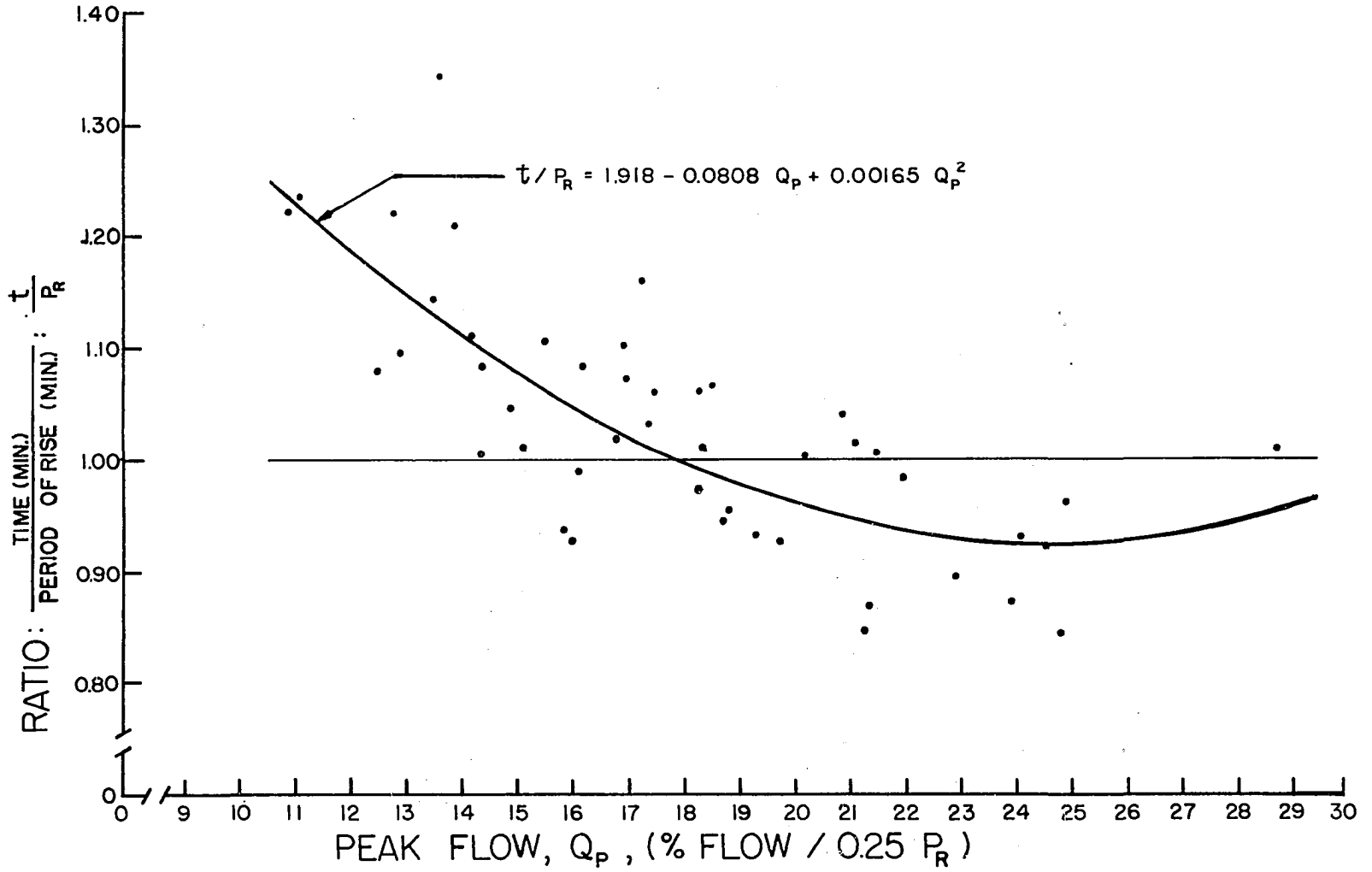
1.40
1.30
1.20
1.10
1.00
0.90
0.80
0
RATIO: TIME (MIN.) / PERIOD OF RISE (MIN.) : t/P_R
t/P_R = 1.918 - 0.0808 Q_P + 0.00165 Q_P^2
0
9
10
11
12
13
14
15
16
17
18
19
20
21
22
23
24
25
26
27
28
29
30
PEAK FLOW, Q_P , (% FLOW / 0.25 P_R)

A comparison of the variances from regression for the regression line (Equation 22) and the linear model, $t/P_R = 1$, showed a significant reduction in the sum of squares by using the curvilinear line. The statistical evidence supports the observations previously discussed; namely, that for the fitted curves, the value of t/P_R at the peak is not a constant for each watershed but varies with the magnitude of the peak ordinate in a manner described by Equation 22.

It is not believed, however, that the discrepancy is of sufficient magnitude to obviate the validity of the fitted curves. The regression line defines the mean value of t/P_R at a given Q_p-value. Percentagewise the difference between these values and the theoretical, $t/P_R = 1$, is not large especially for the range of data employed. The error becomes less significant if consideration is given to the subjectiveness involved in developing the empirical graph for a given watershed and the deviations within periods of rise of the individual hydrographs.

Estimation of the Storage Factor, P_R/γ', from Basin Characteristics

The reliability of a workable synthetic procedure depends on the success with which the empirical hydrologic results can be related to measurable physical characteristics. Edson (13) has shown that rainfall duration influences the magnitude of the parameters, m and y, of Equation 30h. He suggests that all hydrographs under consideration should be reduced to a common rainfall duration before an evaluation of the parameters is attempted.

In this study the unit-storm concept proposed by Wisler and Brater

(59, p. 38) was accepted and the representative unit hydrograph for each watershed described by the two-parameter gamma distribution defined by the parameters q and γ (see Equation 14c). According to the above principle, the parameters, q and γ, for the unit hydrograph of a given basin are relatively independent of storm duration. It would therefore appear that differences in the magnitude of these parameters for the unit hydrographs from different watersheds could be attributed mainly to differences in the physical characteristics of the watersheds.

The effect of unit-storm duration is eliminated if consideration is given only to the parameter, γ, which replaces the exponents y and k of Equations 30h and 31f. As discussed by Edson (13) and Nash (38), the exponents y and k reflect the storage properties of a given watershed. Thus, it would be expected that their magnitude would be uninfluenced by rainfall-duration effects and that they would be relatively constant for all unit graphs of a given basin.

The values of γ for the unit hydrograph or distribution graph may derived from the values for the dimensionless graph, γ', in the following manner. Since, for the dimensionless graph,

$$q/\gamma' = \bar{t}/P_R \qquad (23a)$$

where $\bar{t}$ is the mean time, by substituting, $\gamma = \gamma'/P_R$, into Equation 23a, it follows that

$$q/\gamma = \bar{t} \qquad (23b)$$

in which γ is dimensionally equal to the reciprocal of time.

The required correlation is expedited by giving consideration to the relationship between γ and k. For the instantaneous unit graph,

$$k = 1/\gamma = P_R/\gamma' \qquad (24)$$

in which γ and γ' are the parameters of the two-parameter gamma distribution for the unit hydrograph and for the dimensionless graph, respectively. The relationship is correct dimensionally.

Equation 24 suggests that the ratio, P_R/γ', measures the storage characteristics of a basin, thus was termed the storage factor. In addition, the equation shows that the ratio should be dependent on the same basin characteristics that influence the storage constant, k.

The prediction of the storage constant, k, from measurable physical characteristics has been attained only with limited success. Clark (9) and Linsley (31) have suggested relationship for this purpose. These are given by Equations 8e and 8f.

Relation of the storage factor, $P_R/\hat{\gamma}$, and the watershed parameter, $L/\sqrt{S_c}$, for 33 selected watersheds

It was assumed that the storage factor, P_R/γ', like the storage constant, k, is a measure of the lag or travel time of water through a given reach. Thus, for purely hydraulic reasons, its magnitude would vary directly with the length of the main stream, L, and inversely with some power of the channel slope, S_c. The inclusion of watershed area, A, in the relation was not considered for two reasons: first, because the watersheds used in this study were small, the storage in the tributary

streams was assumed to be negligible compared to that in the main stream; and second, because the high degree of association between L and A (see Figure 3) prohibits the development of a significantly better relation when using both factors over that which would result from the use of either L or A individually.

The experimental results showing the storage factor, $P_R/\hat{\gamma}$, plotted with their respective values of $L/\sqrt{S_c}$ for 33 selected watersheds are given in Figure 12. The "least-squares" line for these data is defined by the equation

$$P_R/\hat{\gamma} = 9.77\ (L/\sqrt{S_c})^{0.475} \qquad (25)$$

in which L, the length of the main stream, is expressed in miles and S_c, the average slope of the channel, is in percent. The percent standard error of estimate for the $P_R/\hat{\gamma}$-values was calculated to be 34.0 percent.

Relation between average channel slope, S_c, and length of main stream, L

Linsley (31) relates that the relation between the storage constant, k, and basin factors is influenced by regional differences. On the basis of these remarks, it was considered that if the relation between P_R/γ' and $L/\sqrt{S_c}$ was influenced by the same factor, greater accuracy in predicting the storage factor from the basin characteristic may be attained by stratifying the data according to region. Figure 13 shows the values of S_c for the watersheds plotted at their respective values of L. The "least-squares" line for these data is defined by the equation

$$S_c = 1.62\ L^{-0.663}\ . \qquad (26)$$

Figure 12. Relation of the storage factor, $P_R/\hat{\gamma}$, and watershed factor $L/\sqrt{S_c}$, for 33 selected watersheds

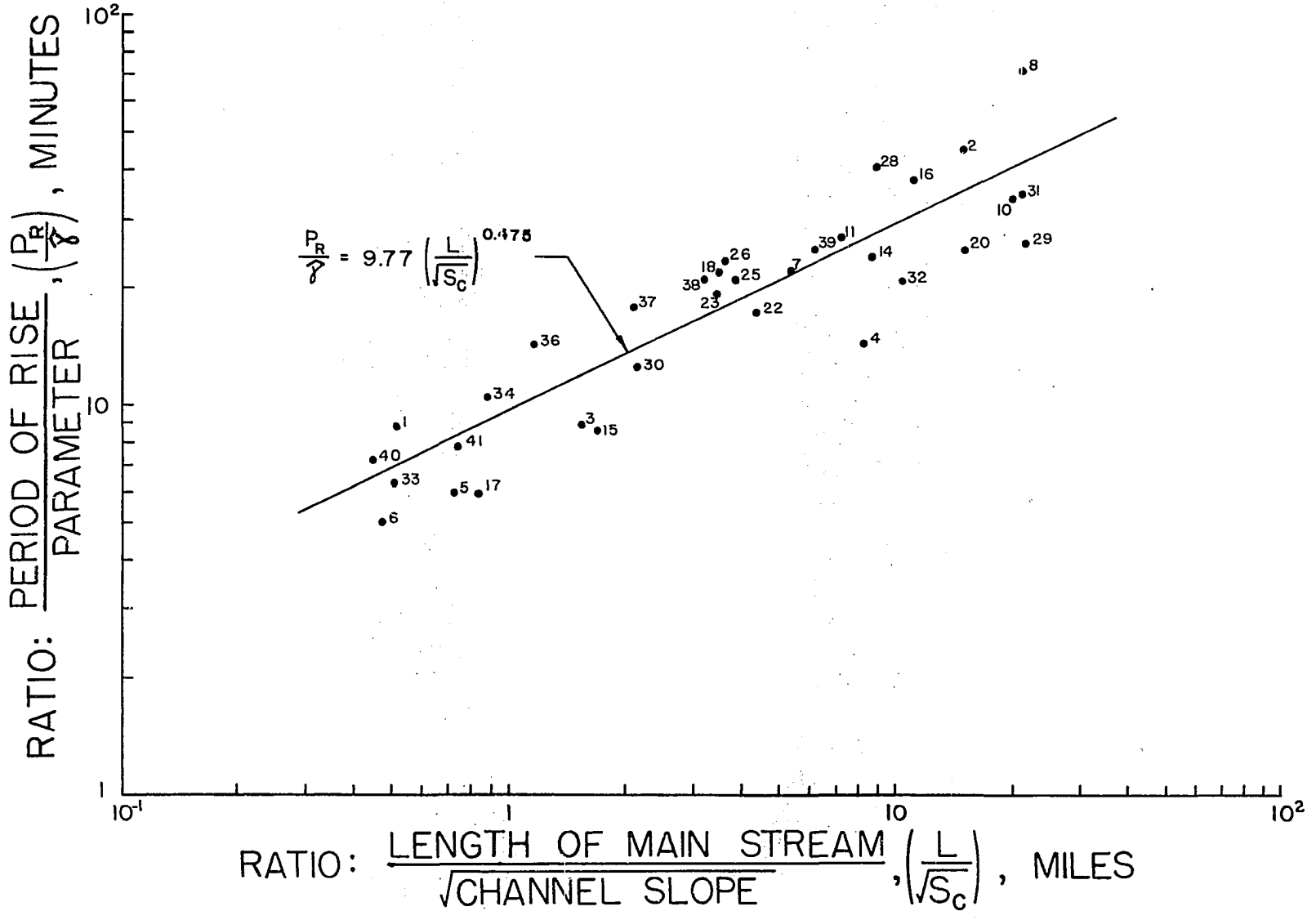
RATIO: PERIOD OF RISE / PARAMETER, $\left(\frac{P_R}{\gamma}\right)$, MINUTES
10^2
10
1
10^{-1}
1
10
10^2
$\frac{P_R}{\gamma} = 9.77 \left(\frac{L}{\sqrt{S_c}}\right)^{0.475}$
RATIO: LENGTH OF MAIN STREAM / $\sqrt{\text{CHANNEL SLOPE}}$, $\left(\frac{L}{\sqrt{S_c}}\right)$, MILES
8
2
28
16
31
10
39
11
14
20
29
18
26
7
38
25
32
23
22
37
36
4
30
34
1
3
15
41
40
33
5
17
6

Influence of region

Closer observation of these data (see Figure 13) reveal the existence of two distinct families of points for watersheds in Ohio and those in Nebraska-Western Iowa (see Figure 14). These two areas represent regions of widely-divergent geologic and climatic conditions. Probably the most distinguishing feature is between the nature of their respective predominant soil types. The soils of the Ohio watersheds are moderately-permeable, residual soils having a shallow solum underlain by shale or slate parent material (54). In contrast, the watersheds for the Nebraska-Western Iowa region occupy areas of deep, coarse, highly-permeable loessial soils (42). It is, however, the culmination of numerous factors, including the properties of the flow regime, which brings about marked differences in the erosional development of the stream channels in the two areas. Likewise, these factors produce differences in the storage characteristics of the stream channels.

From an analysis of covariance of these data, the following conclusions were effected:

1. The slopes of the two regression lines are not significantly different, and
2. The difference between the adjusted mean values of the two groups is greater than can be accounted for by sampling variation.

In essence, the analysis provides that the data can be represented by two parallel regression lines passing through the mean logarithmic values of

Figure 13. Relation of slope of the main stream, S_c, and length of the main stream, L

Figure 14. Relation of slope of the main stream, S_c, and length of the main stream, L, for watersheds in the two regions: Nebraska--Western Iowa, and Ohio

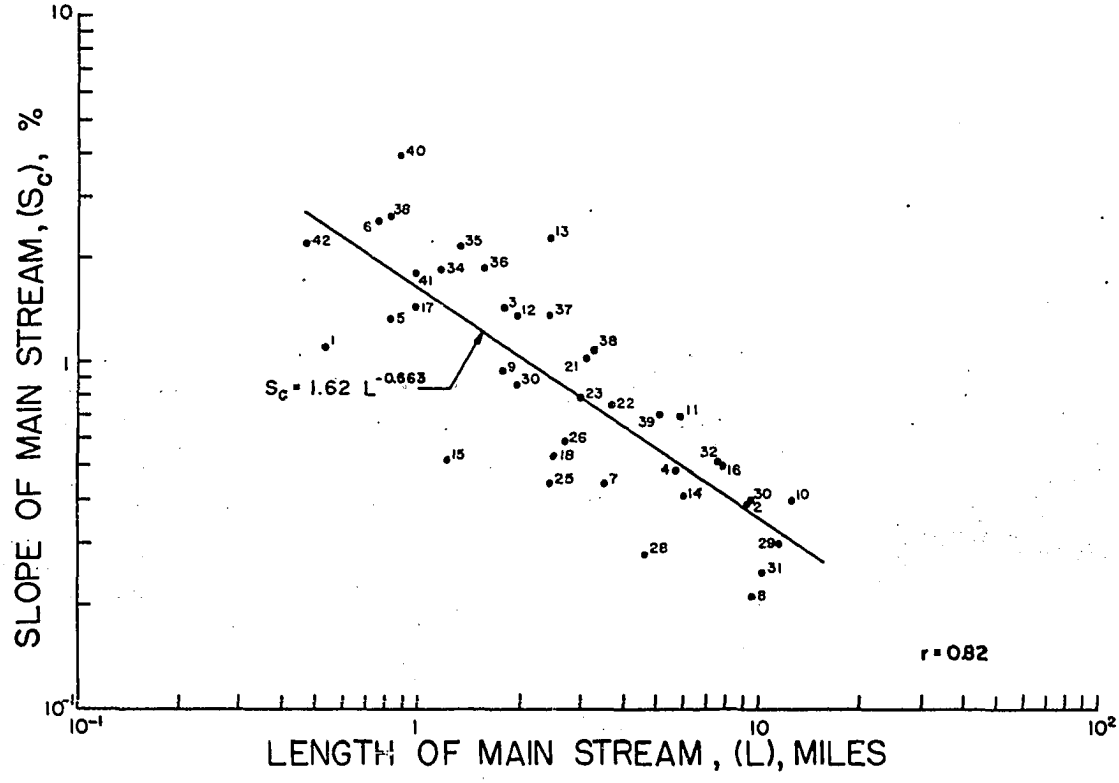
SLOPE OF MAIN STREAM, (Sc), %
LENGTH OF MAIN STREAM, (L), MILES
Sc = 1.62 L^-0.663
r = 0.82

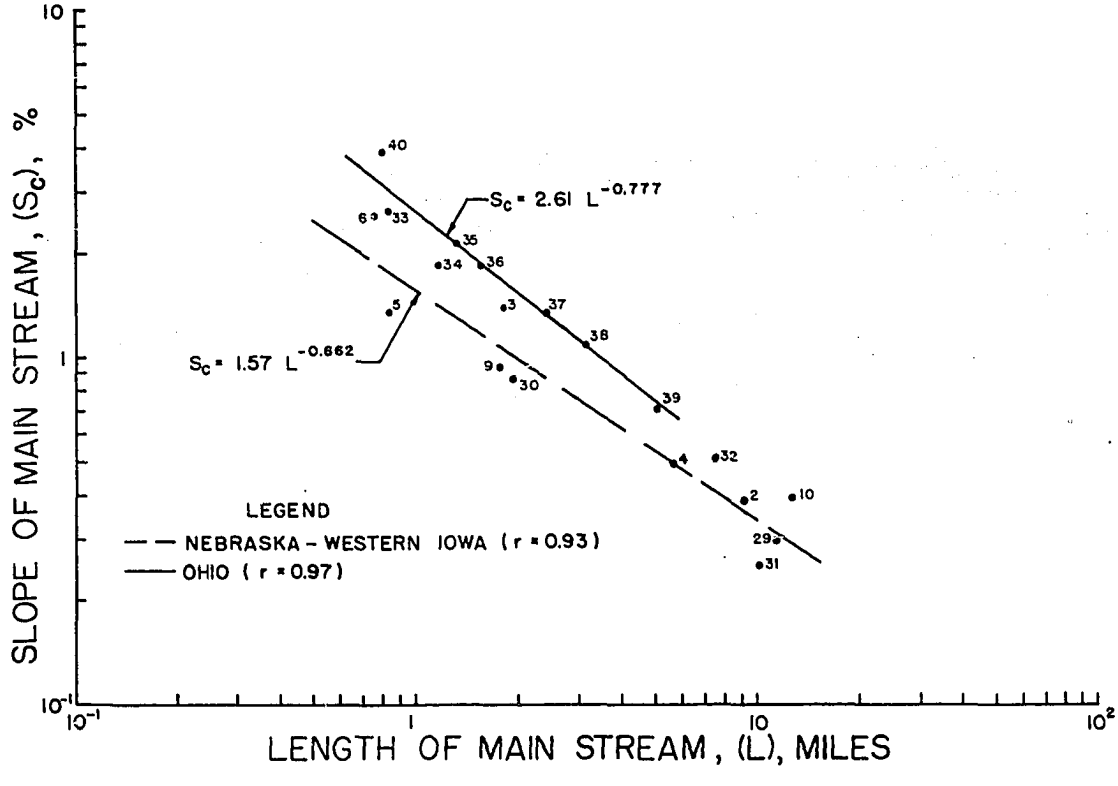
SLOPE OF MAIN STREAM, (Sc), %
LENGTH OF MAIN STREAM, (L), MILES
Sc = 2.61 L^-0.777
Sc = 1.57 L^-0.662
LEGEND
NEBRASKA - WESTERN IOWA (r = 0.93)
OHIO (r = 0.97)

S_c and L for the Ohio and Nebraska-Western Iowa watersheds. The above result gives evidence that the relationship between S_c and L varies with region.

Figure 13 illustrates that the plotted data for the other watersheds in Illinois, Central Iowa, Missouri, and Wisconsin adopt no general pattern but vary appreciably in their relative positions. In some cases they approach the regression line for the Ohio watersheds; in others, that of the Nebraska-Western Iowa region, or appear to occur in their own individual class. Since the characteristics of these basins were not available, the development of a complete family of curves was not attempted.

Selected grouping of watersheds for the prediction of the storage factor, P_R/γ'

Considering the evidence that the relationship between S_c and L varies from region to region, it follows therefrom that in predicting P_R/γ' from the ratio, $L/\sqrt{S_c}$, those watersheds from areas in which S_c and L vary in the same proportion should be combined. Otherwise, the results obtained would be inconsistent. In this study the following grouping appeared to be the most appropriate:

1. Nebraska-Western Iowa,
2. Central Iowa-Missouri-Illinois-Wisconsin, and
3. Ohio.

Figures 15a, 15b and 15c show the storage factor, $P_R/\hat{\gamma}$, plotted with the ratio $L/\sqrt{S_c}$ for these three groups. The regression equations

Figure 15a. Relation of storage factor, $P_R/\hat{\gamma}$, and watershed parameter, $L/\sqrt{S_c}$, for watersheds in Nebraska-Western Iowa

Figure 15b. Relation of storage factor, $P_R/\hat{\gamma}$, and watershed parameter, $L\sqrt{S_c}$, for watersheds in Central Illinois-Missouri-Illinois-Wisconsin

Figure 15c. Relation of storage factor, $P_R/\hat{\gamma}$, and watershed parameter, $L\sqrt{S_c}$, for watersheds in Ohio

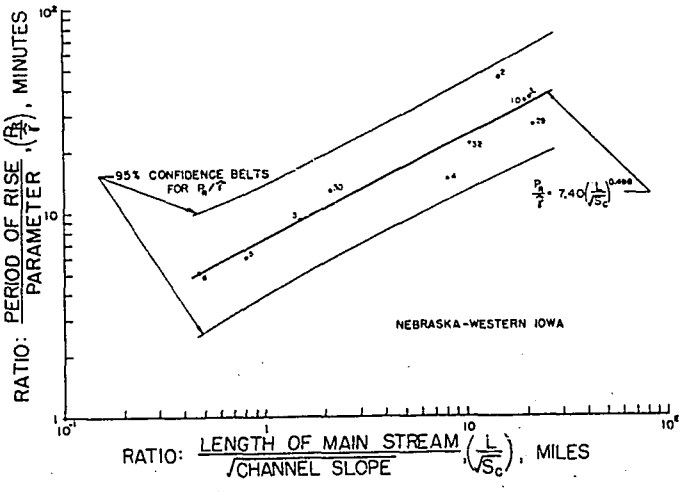
RATIO: PERIOD OF RISE / PARAMETER, (Pr/T), MINUTES
95% CONFIDENCE BELTS FOR Pr/T
Pr/T = 7.40(L/√Sc)^0.466
NEBRASKA-WESTERN IOWA
RATIO: LENGTH OF MAIN STREAM / √CHANNEL SLOPE, (L/√Sc), MILES

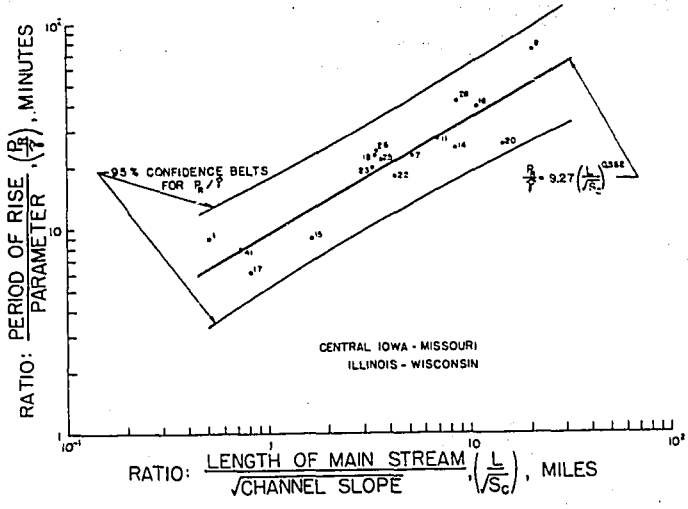
RATIO: PERIOD OF RISE / PARAMETER, (Pr/T), MINUTES
95% CONFIDENCE BELTS FOR Pr/T
Pr/T = 9.27(L/√Sc)^0.388
CENTRAL IOWA - MISSOURI
ILLINOIS - WISCONSIN
RATIO: LENGTH OF MAIN STREAM / √CHANNEL SLOPE, (L/√Sc), MILES

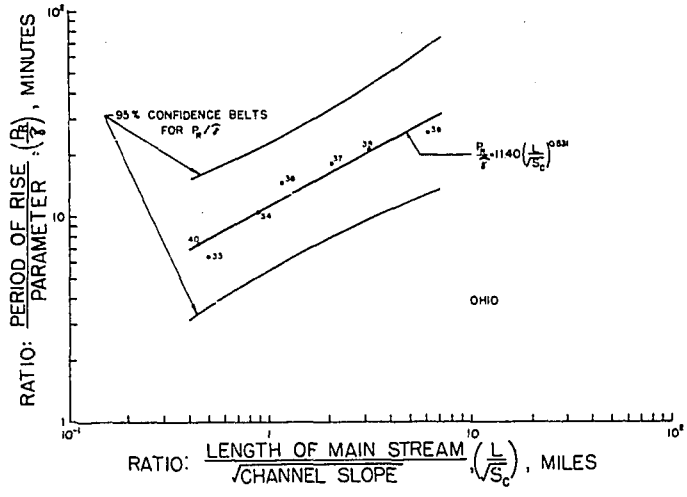
RATIO: PERIOD OF RISE / PARAMETER, (Pr/T), MINUTES
95% CONFIDENCE BELTS FOR Pr/T
Pr/T = 11.40(L/√Sc)^0.634
OHIO
RATIO: LENGTH OF MAIN STREAM / √CHANNEL SLOPE, (L/√Sc), MILES

calculated by the method of least squares were respectively

Nebraska-Western Iowa

$$P_R/\hat{\gamma} = 7.40\ (L/\sqrt{S_c})^{0.498} \tag{27a}$$

Central Iowa-Missouri-Illinois-Wisconsin

$$P_R/\hat{\gamma} = 9.27\ (L/\sqrt{S_c})^{0.562} \tag{27b}$$

Ohio

$$P_R/\hat{\gamma} = 11.4\ (L/\sqrt{S_c})^{0.531} . \tag{27c}$$

The coefficients of variation were respectively, 28.0 percent, 30.7 percent, and 29.1 percent.

An analysis of covariance of these data yielded the following results:

1. The slopes of the regression lines for the three regions do not differ significantly.
2. The adjusted mean values of $P_R/\hat{\gamma}$ for the Ohio watersheds and the Nebraska-Western Iowa watersheds are significantly different.
3. The adjusted mean value of $P_R/\hat{\gamma}$ for the watersheds in Central Iowa-Missouri-Illinois-Wisconsin is not significantly different from the adjusted mean values of either of the other two groups.

The analysis gives statistical confirmation that storage factors computed from a given value of $L/\sqrt{S_c}$ differ significantly because of regional influence, provided the regions exhibit distinct differences in their characteristics as those exhibited between Ohio and Nebraska-Western Iowa. The fact that the watersheds in Central Iowa-Missouri-

Illinois-Wisconsin adopt storage properties common to both the above regions in indicative by the non-significance between the adjusted mean value and slope for this group, and the same properties for the others. The entire data can be expressed by two parallel lines passing through the respective mean logarithmic values of $P_R/\hat{\gamma}$ and $L/\sqrt{S_c}$ for the Ohio and Nebraska-Western Iowa groups. However, due to the inability to associate particular basins within the Central Iowa-Missouri-Illinois-Wisconsin area with either of the other regions, these data were retained separately as presented in Figure 15b. The 95-percent confidence belts have been added to facilitate the use of Equations 27a, 27b, and 27c as prediction equations.

Discussion

It is evident from Figures 15a and 15c that for the same value of $L/\sqrt{S_c}$ the storage factor, $P_R/\hat{\gamma}$, is higher for the Ohio watersheds than for the Nebraska-Western Iowa watersheds. This difference is compatible with the differences associated with the geometry of the stream channels in the two regions. In Ohio, low flows are confined to shallow, vee-shaped channels that top to a narrow, rounded valley bottom. Even in the case of small flood waves, characteristic of those originating from a unit storm, overbank storage would be appreciable. In contrast, stream channels in the loessial area are in the form of deeply-entrenched, U-shaped gullies. For these areas, most flood flows from unit storms would be confined within the channel.

The use of the prediction equation (see Equation 27b) applied to

watersheds in Illinois and Wisconsin may be questioned because only one watershed from each state was included in the analysis. The $P_R/\hat{\gamma}$-values obtained fall intermediary between those for Ohio and the Nebraska-Western Iowa region. This positioning appears to correspond to that which would be found if the general geologic, physiographic and climatic conditions of the three areas were compared. For this reason, the prediction equation should give reasonable results. However, additional data are desired from these areas in order to test this assumption.

In summary, it can be stated that the storage factor, P_R/γ', can be predicted satisfactorily from the watershed parameter, $L/\sqrt{S_c}$, only after attention is given to the effect of regional influence. A possible method of accounting for this influence is to stratify the data into groups in which S_c and L have the same relation. Additional study is required to exploit this possibility.

Three prediction equations for Nebraska-Western Iowa, Central Iowa-Missouri-Illinois-Wisconsin, and Ohio have been presented from which an estimate of the P_R/γ' can be obtained for small watersheds within the size group of the experimental data. In estimating this property for different regions, the hydrologist must select the most appropriate curve, giving consideration to the similarity of geologic, topographic, and climatic conditions.

Relation of Period of Rise, P_R, and Parameter, γ'

Two analyses have been presented in previous sections to describe the relationships between dimensionless-graph properties, and the

relationships between these properties and basin characteristics. These equations may be written in the general forms

$$q = \emptyset\ (\gamma')$$

$$\text{and}\quad P_R/\gamma' = \emptyset'\ (L)/\sqrt{S_c}$$

where $\emptyset$ and $\emptyset'$ designate the function. The equations contain three unknown factors, P_R, q and γ'; thus, an additional expression is required to allow simultaneous solution. Two possibilities for meeting this requirement are:

1. Relating the variables either individually or in combination with some watershed characteristics other than L or S_c, or
2. Relating q or γ' with P_R.

The use of the first alternative is questionable, however, in view of the association of the watershed characteristics and the bias that would be introduced into the relation by using dependent terms.

Equations 19 and 23a can be combined to the following result

$$(1 + \gamma')/\gamma' = \overline{t}/P_R \qquad (28)$$

where $\overline{t}/P_R$ is the mean t/P_R-value of the dimensionless graph. Obviously, if $\overline{t}/P_R$ were a constant, γ' would also be a constant, and a common graph could be employed to describe all dimensionless graphs. The experimental results have shown that this is not the case. Equation 28 suggests, however, that if $\overline{t}/P_R$ can be expressed as a function of P_R, then P_R and γ' would be related. Figure 16 shows the two variables $\hat{\gamma}$ and P_R for the experimental data plotted on rectangular coordinate paper. An

Figure 16. Relation of parameter, $P_R/\hat{\gamma}$, and period of rise, P_R, for 33 selected watersheds

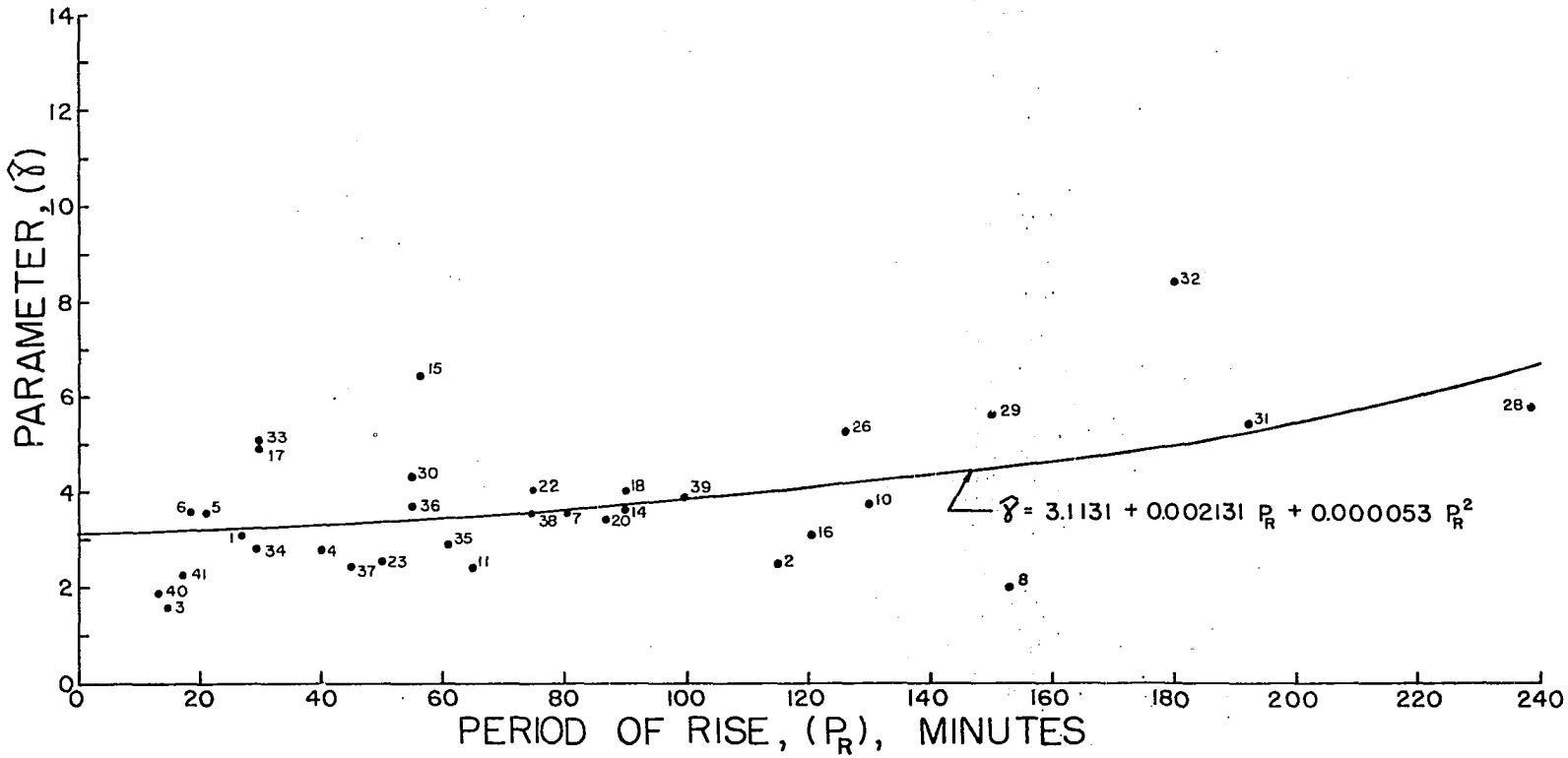
PARAMETER, ($\hat{\gamma}$)
PERIOD OF RISE, (P_R), MINUTES
$\hat{\gamma} = 3.1131 + 0.002131\ P_R + 0.000053\ P_R^2$
0
2
4
6
8
10
12
14
0
20
40
60
80
100
120
140
160
180
200
220
240
1
2
3
4
5
6
7
8
10
11
14
15
16
17
18
20
22
23
26
28
29
30
31
32
33
34
35
36
37
38
39
40
41

initial attempt to fit a linear regression model of the form, $\hat{\gamma} = a + bP_R$, proved unsuccessful. However, the use of a curvilinear regression model, $\hat{\gamma} = a + bP_R + cP_R^2$, resulted in a significant reduction in the sum of squares of deviations from regression over that obtained with the linear model. The quadratic equation obtained by the method of least squares is of the form

$$\hat{\gamma} = 3.1131 + 0.02131P_R + 0.000053P_R^2 . \qquad (29a)$$

An analysis of variance of the regression indicated a high level of significance, $F = 6.41$[1]. The standard error of estimate was calculated to be equal to 33.7 percent.

Discussion

In practical cases, the values of γ' will not continue to increase indefinitely with P_R in accordance with Equation 29a, but will attain or approach a finite maximum. It follows that the assumed model does not describe the true functional relationship between the variables. Regardless, within the range of empirical data tested it may be employed successfully. The use of a higher power polynomial would appear of little value due to the low coefficient of the quadratic term.

The curvilinear regression line does, however, impose a restriction on the allowable range of application of the prediction equations for the storage factor. Rearranging Equation 29a and setting the first differen-

---

[1]Significant at the 0.01 percent level.

tial, d $(\hat{\gamma}/P_R) = 0$, a minimum, one obtains

$$\hat{\gamma}/P_R = (3.1131/P_R) + 0.002131 + 0.000053P_R \qquad (29b)$$

$$\frac{d\ (\hat{\gamma}/P_R)}{d\ P_R} = 0 = \frac{-3.1131}{P_R{}^2} + 0.000053\ .$$

The ratio, $\hat{\gamma}/P_R$, is a minimum when P_R = 242.4 minutes. Therefore, the inverse, $P_R/\hat{\gamma}$, attains a maximum at

$$P_R/\hat{\gamma} = \frac{1}{\frac{3.1131}{242.4} + 0.002131 + (0.000053)\ (242.4)} = 36 \text{ minutes.}$$

This result infers that the excessive scatter of the data prohibits the use of Equation 29a for areas having storage constants exceeding 36 minutes.

Figure 17 is presented as a computational aid to determine the value for P_R from a known value of the storage factor, $P_R/\hat{\gamma}$.

It would appear that the mathematical limitations imposed on the results would be a limitation. However, a greater appreciation for this restriction can be obtained by considering the relation between $P_R/\hat{\gamma}$ and $L/\sqrt{S_c}$ for each region plotted on rectangular coordinate paper (see Figure 18). The figure shows there is a definite tendency for the empirical $P_R/\hat{\gamma}$-values to show wider deviations from the regression lines at the larger values of $L/\sqrt{S_c}$. A possible reason for this increased discrepancy may be obtained from remarks made by Wisler and Brater (59, p. 305),

> The term, "large watersheds," applies to basins having an area greater than 10 sq. miles. However, the distinguishing feature of large watersheds is not that their area is greater than some arbitrary limit, but rather that they

Figure 17. Relation of storage factor, $P_R/\hat{\gamma}$, and period of rise, P_R

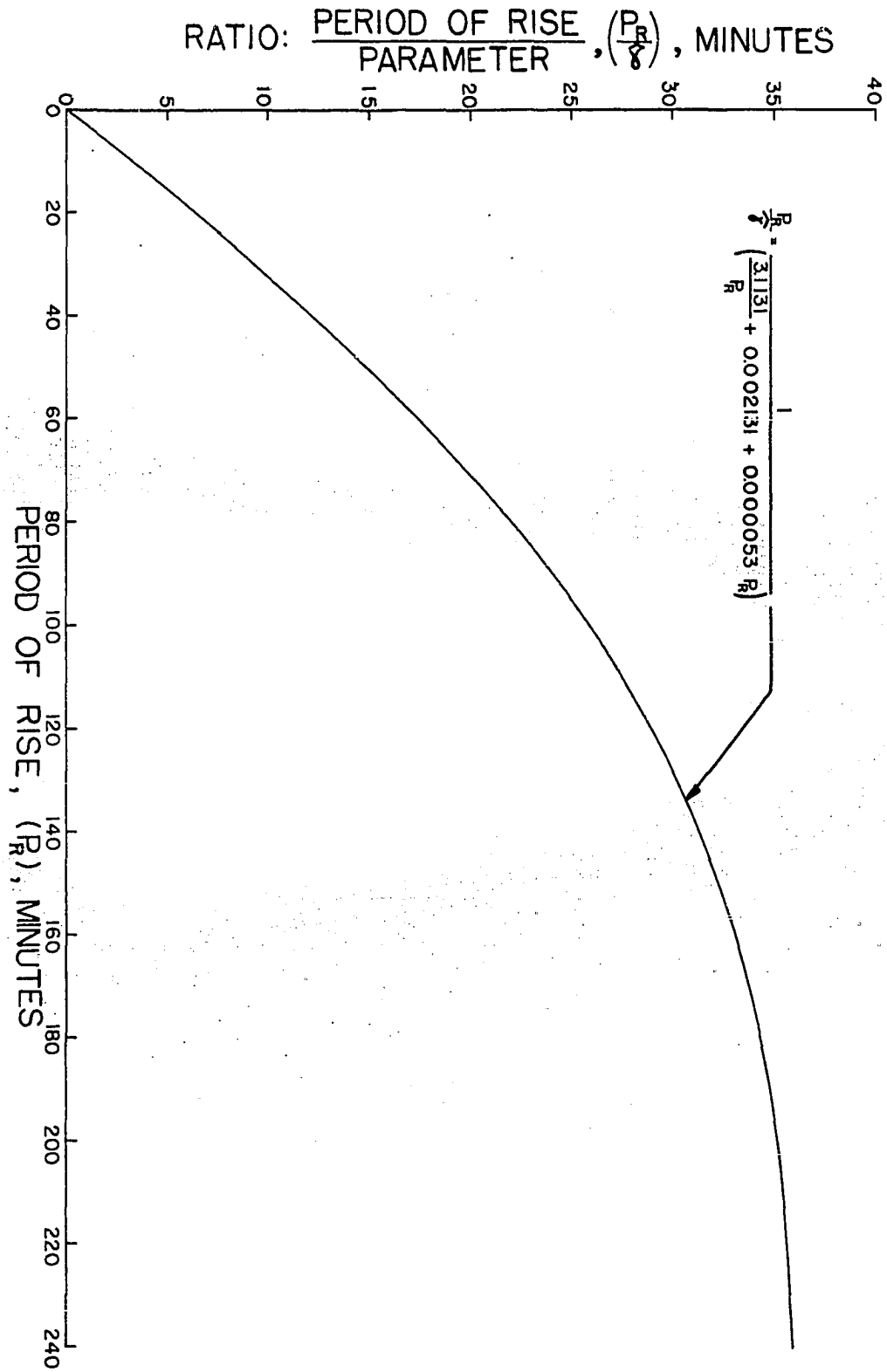
RATIO: PERIOD OF RISE / PARAMETER, (P_R/δ), MINUTES
0
5
10
15
20
25
30
35
40
PERIOD OF RISE, (P_R), MINUTES
0
20
40
60
80
100
120
140
160
180
200
220
240
P_R/δ = 1 / (3.1131/P_R + 0.002131 + 0.000053 P_R)

Figure 18. Relation of storage factor, $P_R/\hat{\gamma}$, and watershed parameter, $L/\sqrt{S_c}$, on rectangular coordinate paper

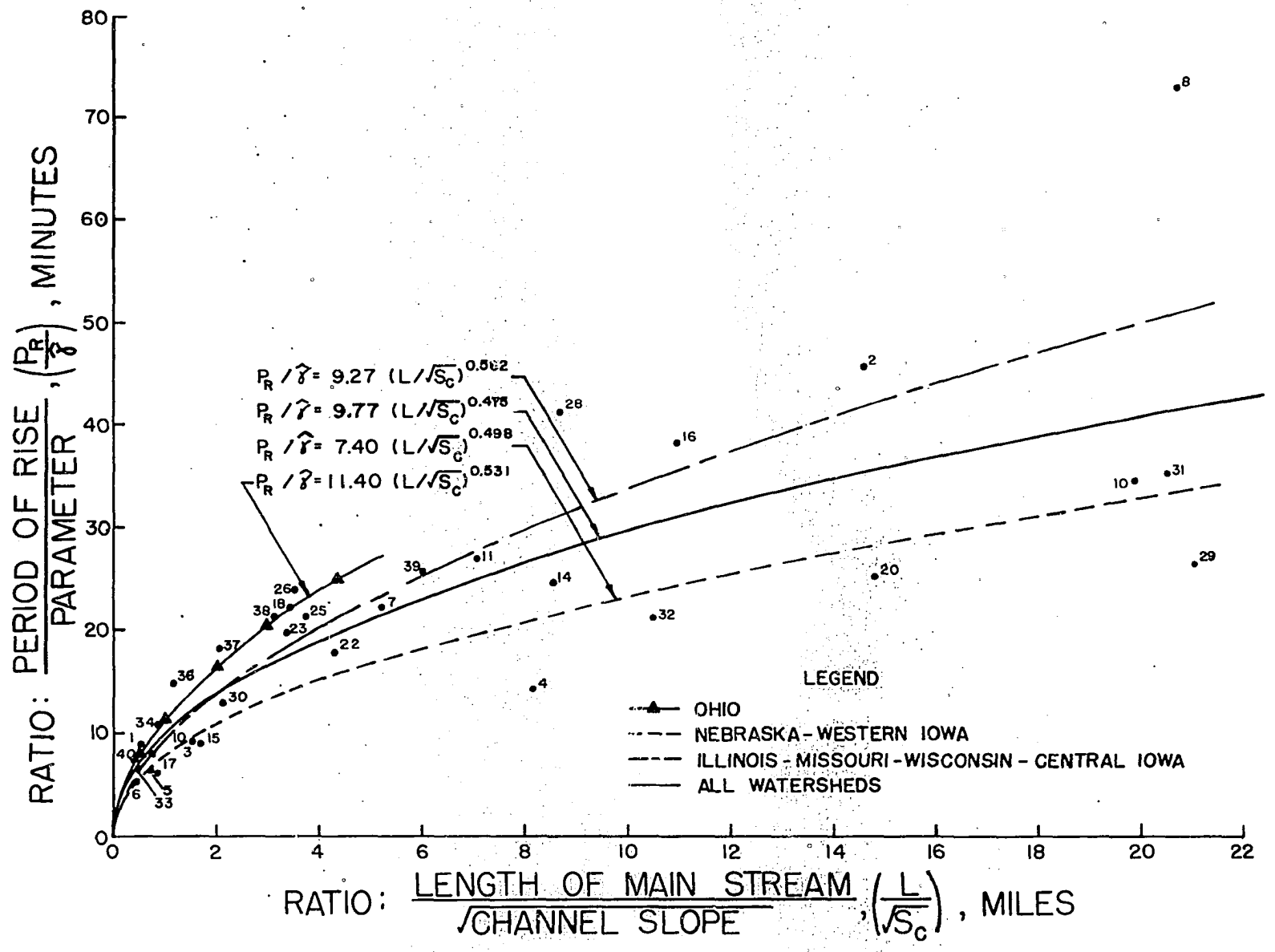
RATIO: PERIOD OF RISE / PARAMETER, (P_R/γ̂), MINUTES
RATIO: LENGTH OF MAIN STREAM / √CHANNEL SLOPE, (L/√S_c), MILES
P_R/γ̂ = 9.27 (L/√S_c)^0.562
P_R/γ̂ = 9.77 (L/√S_c)^0.478
P_R/γ̂ = 7.40 (L/√S_c)^0.498
P_R/γ̂ = 11.40 (L/√S_c)^0.531
LEGEND
OHIO
NEBRASKA - WESTERN IOWA
ILLINOIS - MISSOURI - WISCONSIN - CENTRAL IOWA
ALL WATERSHEDS

> are of such size that, within the basin, there are likely to be major differences in rainfall duration and intensity and in soil permeability. On large watersheds, major floods are frequently the result of high rates of surface runoff from only a portion of the basin. Consequently, it is usually necessary to determine unit hydrographs for several different rainfall-distribution patterns.

Equations 9 and 26 were solved for an area, A, equal to 10 square miles to obtain a value of $L/\sqrt{S_c}$ equal to approximately seven miles. Figure 18 shows that for values of $L/\sqrt{S_c}$ less than seven, the empirical data agree with the regression lines very well. Within this range, the values of P_R, $\hat{\gamma}$ and $\hat{q}$ could be reproduced successfully. In contrast, at the higher $L/\sqrt{S_c}$-values, corresponding to larger watersheds, their reproducibility became erratic.

The remarks by Wisler and Brater that no sharp, distinct arbitrary limit can be established to define the boundary between large and small watersheds may be reiterated. The coincidence of the results indicate that reproducible results can be reasonably assured when unit-hydrograph techniques as discussed herein are confined to areas less than ten square miles in size. For areas of greater size, additional factors must be considered.

In using the prediction equations presented, the hydrologist should be aware of the chance of greater error with increased basin size. The use of Equation 29a, however, forcibly restricts the use of these relationships to synthesize unit hydrographs or distribution graphs to areas less than the approximate sizes given in Table 2.

Table 2. Approximate maximum watershed size for which the prediction equations are applicable

Region	Watershed area (square miles)
Nebraska-Western Iowa	48.5
Central Iowa-Missouri-Illinois-Wisconsin	19.0
Ohio	16.4

Application of Results

An illustrative example showing the synthesis of a unit hydrograph for an area from basin characteristics using the relationships established in this thesis is given in Appendix F.

SUMMARY AND CONCLUSIONS

Topographic and hydrologic characteristics from 42 selected watersheds varying in size from 0.23-30.00 square miles and located in the states of Illinois, Iowa, Missouri, Nebraska, Ohio, and Wisconsin were studied. The listed general conclusions are valid only for topographic and hydrologic conditions comparable to those used in the study.

Topographic Characteristics

Five watershed properties: drainage-area size, A; length of the main stream, L; length to center of area, L_{ca}; slope of the main stream, S_c; and mean land slope, S_L; were obtained for each watershed where the data permitted. From analyses of these data, the following general conclusions were formed.

1. The factors L, L_{ca}, and A are highly correlated and thus their use as independent terms in dimensional analysis techniques is prohibited.
2. For practical purposes, the value of L_{ca} may be taken equal to one-half the value of L.
3. The general shape of small watersheds is intermediary between ovoid and pear-shape.
4. For watersheds in a given region, the factors S_c and L show a distinct relation.
5. The mean land slope, S_L, of a given basin can be estimated with reasonable accuracy from the mean slope of a representative sample of first-order streams, S_1, taken from the same basin.

Hydrologic Characteristics

The rainfall and runoff characteristics from a number of selected unit storms occurring over each watershed were studied. For each basin, a representative distribution graph, the so-called empirical graph, was derived and modified to a dimensionless form based on the period of rise, P_R, as the time parameter.

The two-parameter, gamma distribution described by the parameters, q and γ', was fitted to each dimensionless graph and the maximum likelihood estimators, $\hat{q}$ and $\hat{\gamma}$, of the parameters obtained. Relationships were established so that the parameters P_R, q and γ' could be evaluated from the topographic characteristics L and S_c of a given basin. With P_R, q and γ' known, the dimensionless graph, distribution graph, and unit hydrograph for the basin can be described.

The following conclusions were derived from this study.

1. For practical purposes, the period of rise may be taken equal to the lag time.
2. The period of rise can be employed to replace lag time as a time parameter.
3. In general, the two-parameter gamma distribution can be used to describe the dimensionless graph, distribution graph, or unit hydrograph.
4. Additional work is required on the methodology of fitting the two-parameter gamma distribution to the unit hydrograph and in the evaluation of the goodness of fit in terms of hydrologic

acceptance.

5. The storage factor, P_R/γ', can be predicted with reasonable success from the watershed factor, $L/\sqrt{S_c}$, provided consideration is given to regional influence.
6. The parameter, γ', of the two-parameter gamma distribution describing the dimensionless graph can be estimated from the period of rise.
7. For a given watershed, the dimensionless graph, distribution graph, and unit hydrograph can be derived from the watershed characteristic, $L/\sqrt{S_c}$.

SELECTED BIBLIOGRAPHY

1. Allen, E. S. Six place tables. 7th ed. New York, N. Y., McGraw-Hill Book Co., Inc. 1947.

2. Barger, G. L. and Thom, H. C. S. Evaluation of drought hazard. Agronomy J. 41:519-526. 1949.

3. Barnes, B. S. Consistency in unitgraphs. Proc. Am. Soc. Civil Eng. Vol. 85, No. HY8, pp. 39-63. Aug. 1959.

4. _____. The structure of discharge-recession curves. Trans. Am. Geophys. Union 20:721-725. 1939.

5. Bernard, M. M. An approach to determinate stream flow. Trans. Am. Soc. Civil Eng. 100:347-395. 1935.

6. Brater, E. F. An application of the unit hydrograph principle to small watersheds. Unpublished Ph.D. Thesis. Ann Arbor, Michigan, University of Michigan Library. 1937.

7. _____. The unit hydrograph principle applied to small watersheds. Proc. Am. Soc. Civil Eng. 65:1191-1215. 1939.

8. Butler, S. S. Engineering hydrology. Englewood Cliffs, N. J., Prentice-Hall, Inc. 1957.

9. Clark, C. O. Storage and the unit hydrograph. Proc. Am. Soc. Civil Eng. 69:1419-1447. 1943.

10. Commons, G. Flood hydrographs. Civil Engin. 12:571-572. 1942.

11. Chow, Ven Te, chm. Report of the Committee on Runoff. Trans. Am. Geophys. Union 38:379-384. 1957.

12. Dooge, J. C. I. Synthetic unit hydrographs based on triangular inflow. Unpublished M.S. Thesis. Iowa City, Iowa, State University of Iowa Library. 1956.

13. Edson, C. G. Parameters for relating unit hydrographs to watershed characteristics. Trans. Am. Geophys. Union 32:591-596. 1951.

14. Elderton, W. P. Frequency curves and correlation. 2nd ed. London, Charles and Edwin Layton. 1927.

15. Ezekiel, M. Methods of correlation analysis. New York, N. Y., J. Wiley and Sons, Inc. 1930.

16. Hartley, H. O. and Lewish, W. T. Fitting of data to the two-parameter gamma distribution with special reference to rainfall data. Ames, Iowa. Iowa State University of Science and Technology. Statistical Laboratory. (Mimeo.) 1959.

17. Hickok, R. B., Keppel, R. V. and Rafferty, B. R. Hydrograph synthesis for small arid-land watersheds. Agr. Engin. 40:608-611,615. 1959.

18. Holtappel, H. W. Tafels van E^x. Groningen, P. Noordhoff, N. V. 1938.

19. Horner, W. W. and Flynt, F. L. Relation between rainfall and run-off from urban areas. Trans. Am. Soc. Civil Eng. 101:140-206. 1936.

20. Horton, R. E. Drainage-basin characteristics. Trans. Am. Geophys. Union 13:350-361. 1932.

21. _____. Erosional development of streams and their drainage basins: hydro-physical approach to quantitative morphology. Bul. Geol. Soc. Am. 56:275-370. 1945.

22. _____. The interpretation and application of runoff plat experiments with reference to soil erosion problems. Proc. Soil Science Soc. Am. 3:340-349. 1938.

23. _____. Surface runoff phenomena. Part I: Analysis of the hydrograph. Voorheesville, N. Y. Horton Hydrological Laboratory. (Microfilm.) 1935.

24. _____. Virtual channel-inflow graphs. Trans. Am. Geophys. Union 22:811-820. 1941.

25. Hoyt, W. G. Studies of relations of rainfall and runoff in the United States. U. S. Dept. of Interior. Geological Survey Water-Supply Paper 772:123-247. 1936.

26. Johnstone, D. and Cross, W. P. Elements of applied hydrology. New York, N. Y., The Roland Press Co. 1949.

27. Kirpich, Z. P. Time of concentration of small agricultural watersheds. Civil Engin. 10:132. 1940.

28. Langbein, W. B. Channel storage and unit hydrograph studies. Trans. Am. Geophys. Union 21:620-627. 1940

29. _____. Storage in relation to flood waves. In Meinzer, O., ed. Hydrology. pp. 561-571. New York, N. Y., Dover Publications, Inc. 1949.

30. Langbein, W. B. and others. Topographic characteristics of drainage basins. U. S. Dept. of Interior Geological Survey Water-Supply Paper 968-C:125-155. 1947.

31. Linsley, R. K. Discussion of storage and the unit hydrograph. Trans. Am. Soc. Civil Eng. 110:1452-1455. 1945.

32. _____, Kohler, M. A. and Paulhus, J. L. H. Applied hydrology. New York, N. Y., McGraw-Hill Book Co., Inc. 1949.

33. _____, _____ and _____. Hydrology for engineers. New York, N. Y., McGraw-Hill Book Co., Inc. 1958.

34. Mitchell, W. D. Unit hydrographs in Illinois. Springfield, Ill., State of Illinois. Division of Waterways. 1948.

35. Mockus, V. Use of storm and watershed characteristics in synthetic hydrograph analysis and application. Paper presented at Am. Geophys. Union, Southwest Region Meeting, Sacramento, Calif. (Mimeo.) Febr. 1957.

36. Morisawa, M. Accuracy of determination of stream lengths from topographic maps. Trans. Am. Geophys. Union 38:86-88. 1957.

37. Murphy, G. Similitude in engineering. New York, N. Y., The Roland Press Co. 1950.

38. Nash, J. E. The form of the instantaneous hydrograph. Int. Assoc. Hydrology, International Union of Geodesy and Geophys., Toronto, Ont., 1957. Comptes Rendus 3:114-121. 1958.

39. _____. Systematic determination of unit hydrograph parameters. J. Geophys. Res. 64:111-115. 1959.

40. Ostle, B. Statistics in research. Ames, Iowa, Iowa State College Press. 1956.

41. Ramser, C. E. Runoff from small agricultural areas. J. Agric. Res. 34:797-823. 1927.

42. Riecken, F. F. and Smith, Guy D. Principal upland soils of Iowa. Iowa State College. Ext. Service. Agron. 49 (rev.) (Mimeo.) 1949.

43. Sherman, L. K. The hydraulics of surface runoff. Civil Engin. 10:165-166. 1940.

44. _____. The relation of runoff to size and character of drainage basins. Trans. Am. Geophys. Union 13:332-339. 1932.

45. Sherman, L. K. Streamflow from rainfall by the unit-graph method. Engin. News-Record 108:501-505. 1932.

46. _____. The unit hydrograph method. In Meinzer, O., ed. Hydrology. pp. 514-526. New York, N. Y., Dover Publications, Inc. 1949.

47. Snedecor, G. W. Statistical methods; applied to experiments in agriculture and biology. 5th ed. Ames, Iowa, Iowa State College Press. 1957.

48. Snyder, F. F. Synthetic unit graphs. Trans. Am. Geophys. Union 19:447-454. 1938.

49. Snyder, W. M. Hydrograph analysis by the method of least squares. Proc. Am. Soc. Civil Eng., J. Hydraulic Div. Paper 793:1-25. Sept. 1955.

50. Strahler, A. N. Dimensional analysis applied to fluvially eroded landforms. Bul. Geol. Soc. Am. 69:279-300. 1958.

51. _____. Quantitative analysis of watershed geomorphology. Trans. Am. Geophys. Union 38:913-920. 1957.

52. Taylor, A. B. and Schwarz, H. E. Unit hydrograph lag and peak flow related to basin characteristics. Trans. Am. Geophys. Union 33:235-246. 1952.

53. Thom, H. C. S. A note on the gamma distribution. U. S. Weather Bureau. Monthly Weather Review 86:117-122. 1958.

54. U. S. Dept. of Agr., Soil Conservation Service. Hydrologic data; north appalachian experimental watershed, Coshocton, Ohio. U. S. Dept. of Agr., Soil Conservation Service Hydrologic Bul. 1. 1941.

55. U. S. Dept. of Agr., Soil Conservation Service. Engineering Handbook, Section 4, Hydrology, Supplement A. Washington, D. C., Author. 1957.

56. U. S. Dept. of Army, Corps of Eng., Office of the Chief of Eng. Hydrologic and hydrograph analyses; flood hydrograph analyses and computations. Washington, D. C., Author. 1948.

57. Warnock, R. G. A study of the relationship between watershed characteristics and distribution graph properties. Unpublished M.S. Thesis. Iowa City, Iowa, State University of Iowa Library. 1952.

58. Winsor, C. P. and Clarke, G. L. A statistical study of variation in the catch of plankton nets. J. Marine Res. 3:1-27. 1940.

59. Wisler, C. O. and Brater, E. F. Hydrology. New York, N. Y., John Wiley and Sons, Inc. 1949.

ACKNOWLEDGMENTS

The author is indebted to Professor Hobart Beresford and Professor M. G. Spangler, professors in charge of his graduate program, for their cooperative leadership and encouragement throughout the study.

The author also wishes to express his sincere appreciation for the contributions of the following:

Dr. Don Kirkham, Dr. J. F. Timmons and Professor P. E. Morgan, members of the committee, for their comments and suggestions related to this study;

Dr. R. K. Frevert and Dr. E. R. Baumann for their assistance in setting up the graduate program and initiating the study;

Dr. H. P. Johnson for his counsel, helpful suggestions and review of certain sections of this thesis;

Mr. W. P. Lewish and Mr. D. Grosvenor of the statistical laboratory, who assisted in processing the data to the IBM 650 computer;

Mr. L. Glymph, USDA, ARS, Beltsville, Maryland; Mr. L. L. Harrold, USDA, ARS, Coshocton, Ohio; Mr. J. Allis, USDA, ARS, Hastings, Nebraska; Mr. M. S. Petersen, USGS, Rolla, Missouri; Mr. V. R. Bennion, USGS, Iowa City, Iowa; Mr. H. D. Brice, USGS, Lincoln, Nebraska; and Professor J. W. Howe, SUI, Iowa City, Iowa, who contributed voluntarily of their time in assisting with the selection of the basic data; and

Iowa Agricultural and Home Economics Experiment Station, Ames, Iowa, for the financial support.

APPENDIX A: GLOSSARY OF TERMS AND SYMBOLS

Centroid of precipitation - mass center of the unit-storm rainfall histogram about which the sum of the product moments of rainfall volume times time are equal to zero

cfs - cubic feet per second

Channel storage - the volume of water confined within a stream channel

Dimensionless graph - see p. 50

Distribution graph - see p. 20

Drainage-area size, A - plane area of the watershed in square miles which is enclosed within the topographic divide above the gaging station

Excess precipitation - that portion of rainfall which is in excess of soil infiltration and other losses, and appears as surface runoff at the gaging station

First-order streams - the smallest, unbranched, finger-tip tributary streams of a drainage net

Lag time, t_L - time difference in minutes between the centroid of precipitation and the peak discharge rate of the hydrograph

Length of main stream, L - distance in miles along the main stream from the gaging station to the outermost point defined on the topographic map

Length to center of area, L_{ca} - distance in miles along the main stream from the gaging station to the point nearest the mass center of the area

Main stream - stream of the highest order which passes through the gaging station. To delineate the main stream at bifurcations the following rules established by Horton (21, p. 281) were used:

1. Starting below the junction, the main stream was projected upstream from the bifurcation in the same direction. The stream joining the main stream at the greatest angle was taken as the lower order.
2. If both streams were at about the same angle to the main stream at the junction, the shorter was taken as the lower order.

Mean land slope, S_L - mean land slope in percent determined by the grid-intersection method

Mean slope of first-order streams, S_1 - slope in percent obtained by averaging the slopes from a representative number of first-order streams in a given watershed

% flow/0.25P_R - see p. 50

Period of rise - time lapse in minutes from the beginning of surface run-off to the occurrence of the peak discharge rate

q, γ - shape and scale parameters, respectively, of the two-parameter gamma distribution which describes the distribution graph or unit hydrograph of a given watershed

q, γ' - dimensionless parameters of the two-parameter gamma distribution which describes the dimensionless graph of a given watershed

$\hat{q}$, $\hat{\gamma}$ - maximum likelihood estimators of q and γ' obtained by fitting the two-parameter gamma distribution to the empirically-derived

dimensionless graph of a given watershed

Q_t - ordinate of the unit hydrograph in cfs

Q_{t/P_R} - ordinate of the dimensionless graph in % flow/0.25P_R

Slope of the main stream, S_c - slope in percent of a line drawn along the longitudinal section of the main channel in such a manner that the area between the line and a horizontal line drawn through the channel outlet elevation is equal to the area between the channel grade line and the same horizontal line

r - correlation coefficient

Unit hydrograph - see p. 15

Unit storm - see p. 17

APPENDIX B: EQUATIONAL FORMS OF THE UNIT HYDROGRAPH

Basic Elements of "Mathematical Interpretation of the Unit Hydrograph" by Edson (13)

If isochrones could be drawn to represent the time required for each local element of effective rainfall to reach the mouth of a watershed, the culmination of area, A, with time, t, would result in an approximate parabola

$$A \propto t^x, \quad x > 1$$

so that the runoff discharge rate, Q, might become

$$Q \propto t^x, \quad x > 1 \tag{30a}$$

However, the time of travel required for each component is so affected by other components that the hypothetical isochrones are invalidated. It is regarded that the consequent delay in delivery is the result of valley storage. The discharge from storage is known to decrease exponentially with time

$$Q \propto e^{-yt} \tag{30b}$$

where y is the recession constant whose magnitude is greater than zero.

Thus, the reservoir action of the valley storage is seen to have a dampening effect on the flow implied by proportion 30a. Accordingly, proportion 30a must continue in effect indefinitely. On the other hand, since valley storage must exist for even a small amount of discharge,

proportion 30b is seen to be in effect from the very inception of runoff. The combined effect becomes

$$Q \propto t^{x} e^{-yt} \tag{30c}$$

The fact that the recession limb of a unit hydrograph becomes approximately linear when plotted on semi-logarithmic paper simply means proportion 30b is dominate sometime after the peak discharge. At no time prior to the peak discharge, however, is proportion 30b dominated by proportion 30a so that proportion 30c cannot be developed by the usual curve-fitting methods.

The total discharge volume, V, is obtained from

$$V = \int_{0}^{\infty} Q dt \tag{30d}$$

but

$$Q = Bt^{x} e^{-yt} \tag{30e}$$

where B is a proportionality constant. Substituting Equation 30e into Equation 30d

$$V = \int_{0}^{\infty} Bt^{x} e^{-yt} dt \tag{30f}$$

To facilitate the integration of Equation 30f, let

$x = m-1$,

$z = yt$, and

$dz = ydt$.

By substitution, Equation 30f becomes

$$V = \int_0^{\infty} B(z/y)^{m-1} e^{-z} \, dz/y$$

$$= By^{-m} \int_0^{\infty} z^{m-1} e^{-z} \, dz \, .$$

The quantity, $\int_0^{\infty} z^{m-1} e^{-z} \, dz$, is recognized as the gamma function of m, $\Gamma(m)$. Therefore

$$\bar{V} = By^{-m} \Gamma(m)$$

$$\text{and } B = \frac{V}{y^{-m} \Gamma(m)} \, . \qquad (30g)$$

By substituting Equation 30g into Equation 30e and making the appropriate substitutions

$$Q = \frac{V y^m}{\Gamma(m)} e^{-yt} t^{m-1} \, . \qquad (30h)$$

Basic Elements of "The Form of the Instantaneous Hydrograph" by Nash (38)

It is assumed that any watershed may be replaced by a series of n reservoirs each having the storage characteristics

$$S = kQ \qquad (31a)$$

where S = storage volume,

k = proportionality constant having dimensions of time, and

Q = discharge rate.

When an instantaneous inflow of volume, V, takes place to the first reservoir, its level is raised by an amount sufficient to accommodate the increased storage. The discharge rises instantaneously from zero to V/k and diminishes with time according to the equation

$$Q_1 = \frac{V}{k} e^{-t/k} \tag{31b}$$

where t is the time and e is the base of the natural logarithms. Q_1 becomes the inflow, I, to the second reservoir. Therefore, the discharge from the second reservoir, Q_2, is

$$Q_2 = \frac{1}{k} e^{-t/k} \int_0^t I e^{t/k} \, dt$$

$$Q_2 = \frac{1}{k} e^{-t/k} \int_0^t \frac{V}{k} \, dt$$

$$Q_2 = \frac{V}{k^2} e^{-t/k} \, t \, . \tag{31c}$$

With successive routings through n reservoirs, the discharge rate, Q_n, becomes

$$Q_n = \frac{V}{k^n (n-1)!} e^{-t/k} \, t^{n-1} \, . \tag{31d}$$

But, $(n-1)! = \Gamma(n)$ (31e)

where Γ is the gamma function. Substituting the equality 31e into Equation 31d, the relation can be written

$$Q_n = \frac{V}{\Gamma(n)} \; k^{-n} \; e^{-t/k} \; t^{n-1} \quad . \tag{31f}$$

APPENDIX C: TOPOGRAPHIC AND HYDROLOGIC DATA

In an effort to alleviate overcrowding of tables and illustrations arising from employing watershed names, each watershed was given a number designation (see Table 3). The number designation was employed exclusively to define the watersheds and to associate topographic and hydrologic properties with a given watershed throughout the thesis.

Table 3. Watershed name and corresponding number designation

State	Number	Watershed
Illinois	1	W-IV, Edwardsville
Iowa	2	Davids Creek near Hamlin
	3	Hayworth Main Outlet near Climbing Hill
	4	Indian Creek at Council Bluffs
	5	Muckey Creek near Mapleton
	6	Nepper Main Outlet near Mapleton
	7	Ralston Creek near Iowa City
	8	Rapid Creek near Iowa City
	9	Renneker Main Outlet near Anthon
	10	Waubonsie Creek near Bartlett
Missouri	11	Beaver Creek near Rolla
	12	Behmke Branch near Rolla
	13	Big Creek near Yukon
	14	Bourbeuse Creek near St. James
	15	Coyle Branch at Houston
	16	East Fork Fishing River at Excelsior Springs
	17	Green Acre Branch near Rolla
	18	Jenkins Branch at Gower

Table 3. (Continued)

State	Number	Watershed
Missouri	19	Lanes Fork near Rolla
	20	Lanes Fork near Vichy
	21	Little Beaver Creek near Rolla
	22	Lost Creek at Elsberry
	23	Mill Creek at Oregon
	24	Oak Grove Branch near Brighton
	25	Shiloh Branch near Marshall
	26	Stahl Creek near Miller
	27	Stark's Creek at Preston
	28	White Cloud Creek near Maryville
Nebraska	29	Dry Creek near Curtis
	30	W-3, Hastings
	31	New York Creek near Herman
	32	Tekamah Creek at Tekamah
Ohio	33	W-5, Coshocton
	34	W-11, Coshocton
	35	W-91, Coshocton
	36	W-92, Coshocton
	37	W-94, Coshocton
	38	W-95, Coshocton
	39	W-97, Coshocton
	40	W-196, Coshocton
Wisconsin	41	W-I, Fennimore
	42	W-II, Fennimore
North Carolina	43	W-7, Coweeta
	44	W-8, Coweeta
	45	W-9, Coweeta
	46	W-10, Coweeta

Table 4. Collection agencies for raw topographic and hydrologic data

Letter designation	Agency and location
ARS	United States Department of Agriculture, Agricultural Research Service, Soil and Water Conservation Divisions: Beltsville, Maryland; Hastings, Nebraska; and Coshocton, Ohio
FS	United States Department of Agriculture Forest Service, Coweeta Hydrology Laboratory, Dillard, Georgia
ISU	Iowa State University of Science and Technology, Agricultural Engineering Department, Ames, Iowa
SUI	State University of Iowa, Department of Mechanics and Hydraulics, Iowa City, Iowa
USGS	United States Department of Interior Geological Survey, Topographic and Water Resources Divisions; States of Iowa, Missouri, Nebraska and Ohio
USWB	United States Department of Commerce Weather Bureau, National Weather Records Center, Asheville, North Carolina

Table 5. Summary of topographic characteristics

Watershed number[a]	Collection agencies[b]	A (sq.miles)	L (miles)	L_{ca} (miles)	S_c (percent)	S_L (percent)
1	ARS	0.45	0.54	0.28	1.10	5.68[c]
2	ISU, USGS	26.01	9.14	4.95	0.39	4.15[c]
3	ISU	0.91	1.80	0.85	1.41	8.05[c]
4	USGS	7.56	5.69	2.08	0.49	8.45[c]
5	ISU	0.69	0.83	0.45	1.34	12.30[c]
6	ISU	0.35	0.75	0.43	2.56	
7	SUI	3.00	3.50	2.80	0.45	7.76[d]
8	ISU, USGS	24.57	9.50	4.15	0.21	4.10[c]
9	ISU	0.89	1.78	0.68	0.94	5.26[c]
10	ISU, USGS	32.64	12.50	5.30	0.40	2.90[c]
11	USGS	13.70	5.95	2.90	0.70	10.30[d]
12	USGS	1.03	1.95	1.15	1.37	7.05[d]
13	USGS	8.36	2.45	1.65	2.28	
14	USGS	21.30	6.00	3.02	0.41	
15	USGS	1.30	1.21	0.80	0.52	7.18[d]
16	USGS	20.00	7.80	3.60	0.50	6.31[c]
17	USGS	0.62	0.98	0.60	1.45	
18	USGS	2.72	2.50	1.20	0.53	5.06[c]
19	USGS	0.23				
20	USGS	24.10	9.40	3.10	0.40	
21	USGS	6.27	3.10	1.60	1.02	7.86[d]
22	USGS	12.20	3.70	1.98	0.74	8.69[d]

[a]Refer to Table 3 for code designation.

[b]Refer to Table 4 for interpretation.

[c]Mean land slope computed from regression equation 13.

[d]Slope determination by grid-intersection method (21).

Table 5. (continued)

Watershed number[a]	Collection agencies[b]	A (sq.miles)	L (miles)	L_{ca} (miles)	S_c (percent)	S_L (percent)
23	USGS	4.90	3.00	1.60	0.79	6.56[c]
24	USGS	1.00	1.00	0.75		
25	USGS	2.87	2.45	1.60	0.45	3.72[c]
26	USGS	3.86	2.70	1.40	0.59	2.93[d]
27	USGS	4.72	1.98	1.10		
28	USGS	6.06	4.60	2.60	0.28	4.46[d]
29	USGS	20.00	11.59	5.49	0.30	4.74[c]
30	ARS	0.75	1.96	1.54	0.86	5.44[d]
31	USGS	30.00	10.25	5.45	0.25	3.88[c]
32	USGS	21.53	7.50	4.25	0.52	5.01[c]
33	USGS, ARS	0.55	0.82	0.48	2.64	18.90[c]
34	USGS, ARS	0.46	1.17	0.74	1.83	24.60[c]
35	USGS, ARS	0.46	1.31	0.57	2.13	25.60[c]
36	USGS, ARS	1.44	1.56	0.72	1.84	25.40[c]
37	USGS, ARS	2.37	2.41	1.02	1.37	14.80[d]
38	USGS, ARS	4.02	3.25	1.45	1.09	22.60[c]
39	USGS, ARS	7.15	5.11	2.44	0.72	20.40[c]
40	ARS	0.47	0.88	0.42	3.94	15.60[d]
41	ARS	0.52	0.99	0.55	1.80	8.10[c]
42	ARS	0.27	0.46	0.29	2.20	5.77[d]
43	FS					51.20[d]
44	FS					45.50[d]
45	FS					46.10[d]
46	FS					43.30[d]

Table 6. Summary of storm characteristics and hydrograph properties

Watershed number[a]	Raingage: Collection agency[b]	Raingage: Station	Storm characteristics: Storm date	Storm characteristics: Rainfall: Excess period (min.)	Storm characteristics: Rainfall: Total depth (in.)	Hydrograph properties: Collection agency	Hydrograph properties: Period of rise (min.)	Hydrograph properties: Peak discharge (cfs)	Hydrograph properties: Lag time (min.)
1	ARS	Weighted average R-1, R-2, R-3, R-4, R-5, R-6, R-7	July 8-9, 1942	56	2.11	ARS	28	423	22
			Aug. 14-15, 1946	53	1.98		39	667	39
			Aug. 15-16, 1946	40	1.00		25	260	17
2	USWB	Coon Rapids	Aug. 15, 1952			USGS	120	840	
			June 4-5, 1953				120	362	
			June 6-7, 1956	100	1.57		105	533	93
3	ISU	Weighted average H-1, H-2	June 15, 1950	20	1.57	ISU	15	860	14
			June 23, 1951	30	1.01		14	320	10
			June 25, 1951	15	0.98		16	980	14
4			July 8-9, 1955			USGS	51	540	
			July 13, 1956				50	712	
			June 15-16, 1957				40	2,050	
5	ISU	Weighted average M-1, M-2	June 19, 1951	20	0.60	ISU	23	420	20
			1. Aug. 17, 1951	15	0.85		20	600	17
			2. Aug. 17, 1951	15	0.71		26	592	30
			June 24, 1953	25	1.05		20	557	14

[a]Refer to Table 3 for code designation.

[b]Refer to Table 4 for interpretation.

Table 6. (continued)

Watershed number[a]	Raingage: Collection agency[b]	Raingage: Station	Storm characteristics: Storm date	Storm characteristics: Rainfall: Excess period (min.)	Storm characteristics: Rainfall: Total depth (in.)	Hydrograph properties: Collection agency	Hydrograph properties: Period of rise (min.)	Hydrograph properties: Peak discharge (cfs)	Hydrograph properties: Lag time (min.)
6	ISU	Weighted average N-1,N-2, N-3	June 17-18, 1951	25	2.02	ISU	20	700	25
			1. June 24, 1953	25	1.36		17	426	23
			2. June 24, 1953	20	0.86		14	290	18
7	SUI[c]		June 27, 1941	55	2.34	SUI	63	1,345	64
			June 30, 1941	45	1.01		90	817	73
			July 30, 1950	25	0.84		67	241	58
			May 24, 1953				80	290	
8	USWB	Morse 1N	July 12, 1943	20	0.23	USGS	153	279	
			June 1, 1945	20	0.47		121	377	
			July 31-Aug. 1, 1950	25	0.76		153	261	
			July 31, 1956				243	1,025	
9	ISU	Weighted average R-1,R-2	Apr. 30, 1951	10	0.52	ISU	16	493	13
			June 23, 1951	25	0.84		18	765	17
			July 2, 1951	20	1.18		20	1,450	12
10			Aug. 23, 1954			USGS	135	3,500	
			July 15-16, 1956				90	4,200	
			July 1, 1957				165	2,460	
			June 7, 1957				70	2,448	

[c]Raingage station unknown, available from SUI.

Table 6. (continued)

Watershed number[a]	Raingage: Collection agency[b]	Raingage: Station	Storm characteristics: Storm date	Rainfall: Excess period (min.)	Rainfall: Total depth (in.)	Hydrograph properties: Collection agency	Period of rise (min.)	Peak discharge (cfs)	Lag time (min.)
11	USWB	Rolla 7S	Apr. 23, 1950			USGS	35	742	
			Aug. 9-10, 1951	60	1.54		30	1,080	32
			Aug. 15-16, 1951	15	0.70		75	640	
			July 7, 1955	50	0.95		60	1,047	
12	USWB	Rolla 4SE	June 9, 1950	40	1.41	USGS	45	1,190	44
			June 9, 1954	65	2.17		45	845	36
13	USWB	Tyrone 2N	Sept. 12, 1949	30	1.35	USGS	55	351	
			May 31, 1957	45	0.35		60	940	
			July 14, 1957	50	1.70		60	490	75
14	USWB	St.James 3NW	June 20-21, 1948	60	1.20	USGS	105	4,050	77
			July 12, 1948	45	1.08		90	3,270	80
			June 26, 1949	45	1.00		90	1,090	107
			May 25, 1957	30	0.82		90	3,400	123
15	USWB	Houston 1SE	June 9-10, 1950			USGS	47	265	
			Apr. 6, 1951	90	2.16		43	648	45
			June 29, 1951	57	1.80		67	315	84
			June 30, 1951	50	1.45		55	996	40
16			June 21, 1951			USGS	99	1,030	
			Aug. 8, 1951				135	5,550	
			May 1, 1954				126	833	
			June 24, 1955				123	1,450	

Table 6. (continued)

Watershed number[a]	Raingage: Collection agency[b]	Raingage: Station	Storm characteristics: Storm date	Rainfall: Excess period (min.)	Rainfall: Total depth (in.)	Hydrograph properties: Collection agency	Period of rise (min.)	Peak discharge (cfs)	Lag time (min.)
17	USWB	Rolla 5SE	Apr. 23, 1953	13	0.94	USGS	30	577	26
			June 9, 1954	30	1.89		31	821	19
			May 12, 1955	35	1.15		15	337	15
18	USWB	Gower 2N	July 16-17, 1950			USGS	90	385	
			June 2, 1954	75	1.49		90	657	122
			June 24, 1955	45	1.10		90	463	107
19	USWB[d]		Apr. 23-24, 1953			USGS	58	120	
			June 10, 1954				60	120	
			May 25, 1957	25	0.63		45	48	35
20	USWB	Vichy 2SE	Aug. 15, 1950	60	1.54	USGS	60	1,790	85
			July 23, 1955	60	1.66		70	1,530	
			May 22, 1957	35	2.30		90	6,230	98
21	USWB	Rolla 3W	July 22, 1951			USGS	60	864	
			Apr. 23, 1953	15	1.31		75	2,050	65
			July 6-7, 1955	15	0.75		50	950	74
			Aug. 7, 1955	15	1.45		72	564	60
22			Oct. 11, 1954			USGS	80	1,325	
			May 28, 1955				66	400	
			Aug. 7, 1955				79	1,600	

[d]Raingage station unknown, rainfall chart for storm on May 25, 1957 obtained from USGS, Rolla, Missouri.

Table 6. (continued)

Watershed number[a]	Raingage: Collection agency[b]	Raingage: Station	Storm characteristics: Storm date	Rainfall: Excess period (min.)	Rainfall: Total depth (in.)	Hydrograph properties: Collection agency	Period of rise (min.)	Peak discharge (cfs)	Lag time (min.)
23	USWB	Oregon 1NE	Aug. 14, 1951	45	0.60	USGS	60	548	50
			Aug. 15, 1951	25	0.45		60	680	52
			Aug. 21, 1954	45	1.25		45	580	28
24	USWB	Brighton	May 22, 1957	25	1.85	USGS	71	845	73
25	USWB	Marshall	May 27-28, 1955	30	1.40	USGS	70	658	71
			June 2, 1955				45	885	
			June 29, 1957				68	503	
26	USWB	Miller 2SE	June 7, 1956	70	2.25	USGS	90	747	118
			June 24-25, 1956	40	1.34		130	432	126
			May 22, 1957	30	1.00		165	556	165
27	USWB	Preston	Apr. 21, 1957	70	1.15	USGS	150	832	141
			May 9, 1957	25	0.70		75	160	81
			May 22, 1957	55	0.60		65	635	69
28	USWB	Maryville 7NW	June 24, 1949	25	0.55	USGS	164	158	150
			May 25, 1951	75	0.60		238	171	193
			June 19, 1951	45	1.10		238	396	253
			June 20-21, 1951				361	443	
			June 21-22, 1951				419	410	

Table 6. (continued)

Watershed number[a]	Raingage: Collection agency[b]	Raingage: Station	Storm characteristics: Storm date	Storm characteristics: Rainfall: Excess period (min.)	Storm characteristics: Rainfall: Total depth (in.)	Hydrograph properties: Collection agency	Hydrograph properties: Period of rise (min.)	Hydrograph properties: Peak discharge (cfs)	Hydrograph properties: Lag time (min.)
29	USWB	Curtis 4N	May 30-31, 1951	30	0.86	USGS	165	2,375	129
		Curtis 4N	June 8, 1951	40	1.62		150	4,430	136
		Stockville 6SSW	June 21-22, 1951	45	1.51		70	3,956	60
30	ARS	B-32R	June 18, 1947	38	1.00	ARS	55	143	64
			May 5-6, 1949	29	0.88		60	307	65
			June 8, 1949				63	288	
			July 10, 1951	50	1.84		41	845	42
31	USWB	Spiker 4NW	May 31, 1951	50	1.82	USGS	190	2,980	198
			Aug. 14, 1951	30	0.60		200	1,046	160
			Aug. 20, 1951	30	0.60		185	3,151	160
32	USWB	Rosalie	May 27-28, 1954	100	0.32	USGS	180	1,676	
			May 31-June 1, 1954	55	0.42		90	1,135	
			May 12-13, 1956	25	0.79		210	1,294	
33	ARS	91	June 4, 1941	53	1.00	ARS	32	293	34
34	ARS	27	Sept. 23, 1945	32	1.21	ARS	26	310	23
			July 21, 1956	45	1.61		30	134	27
			June 12, 1957	23	1.60		25	88	37
			July 14, 1958	33	1.13		32	110	41

Table 6. (continued)

Watershed number[a]	Raingage: Collection agency[b]	Raingage: Station	Storm characteristics: Storm date	Storm characteristics: Rainfall: Excess period (min.)	Storm characteristics: Rainfall: Total depth (in.)	Hydrograph properties: Collection agency	Hydrograph properties: Period of rise (min.)	Hydrograph properties: Peak discharge (cfs)	Hydrograph properties: Lag time (min.)
35	ARS	91	June 4, 1941	52	1.00	ARS	28	214	29
			Sept. 23, 1945	30	1.20		26	130	29
			June 28, 1946	22	0.86		17	235	30
			July 14, 1958	27	1.08		36	86	34
36	ARS	27	Sept. 23, 1945	30	1.75	ARS	45	212	38
			June 16, 1946	16	0.57		55	192	69
			July 11, 1946				70	404	
			June 12, 1957				40	262	
37	ARS	27	June 18, 1940	26	0.98	ARS	45	248	46
38	ARS	27	June 4, 1941	35	1.02	ARS	74	880	93
			June 21, 1946	20	0.75		75	753	102
			June 12, 1957	53	2.00		82	896	99
39	ARS	27	Aug. 4, 1938	64	1.34	ARS	76	410	94
			July 11, 1946	84	2.52		100	974	142
			July 21, 1946	60	1.18		100	840	113
			June 12, 1957				80	1,270	94
40	ARS	108	July 8, 1939	28	0.78	ARS	13	177	17
			Aug. 15, 1941				14	140	
			June 6, 1947	50	1.26		20	126	23
			Aug. 16, 1947	26	1.11		13	179	23
			July 21, 1949	28	1.14		14	116	23

Table 6. (continued)

Watershed number[a]	Raingage: Collection agency[b]	Raingage: Station	Storm characteristics: Storm date	Storm characteristics: Rainfall: Excess period (min.)	Storm characteristics: Rainfall: Total depth (in.)	Hydrograph properties: Collection agency	Hydrograph properties: Period of rise (min.)	Hydrograph properties: Peak discharge (cfs)	Hydrograph properties: Lag time (min.)
41	ARS	Weighted average R-2, R-9	Aug. 12, 1943	23	2.07	ARS	18	306	18
			June 28, 1945	16	0.93		16	340	19
			July 15-16, 1950	11	1.07		20	350	19
42	ARS	R-2	Aug. 12, 1943	23	1.89	ARS	10	212	5
			June 28, 1945	18	0.96		12	229	10
			July 15-16, 1950	10	0.93		16	183	21

APPENDIX D: DISTRIBUTION GRAPHS AND EMPIRICAL GRAPHS

Development of an Empirical Graph for a Given Watershed

A set of raw data, including a station description, rating tables and stage graphs for three storms occurring on watershed 19, are given in Figures 19a, 19b, and 20a, 20b, and 20c, respectively.

1. *Development of discharge hydrographs*

   A. The stage readings for each storm were tabulated at appropriate times to allow faithful reproduction of the original stage graph (see Tables 7, 8, and 9). In the tabulation, any major fluctuation of the curve was noted and the peak stage was always listed.

   B. Using the appropriate rating table, the stage readings were corrected for any "shift-in-control" and converted to equivalent discharges expressed in cfs (see Tables 7, 8, and 9).

   C. The discharge readings were plotted with time to produce the discharge hydrographs presented in Figures 21a, 21b and 21c.

2. Separation of base flow

   Since the distribution-graph or unit-graph principle is only applicable to surface runoff, it was necessary to separate the base flow component from each discharge hydrograph. Several techniques are available to accomplish this separation; however, the selection of one in preference to another is

Figure 19a. Station description for watershed 19

(Photostat of original data.)

UNITED STATES
DEPARTMENT OF THE INTERIOR
GEOLOGICAL SURVEY
WATER RESOURCES DIVISION

File No. | Washington ..... | Field .....

Station Prepared: 4-1-52
Date
by Perry C. Bolon

Description of Gaging Station on Lanes Fork

Near Rolla State of Missouri

Prepared in accordance with outline in Book of Forms 9-277. Plot cross section to scale. Enclose 9-275 for each discharge measurement. Initial and date sheets.

LOCATION.--Lat 37°59'33", long. 91°43'36", in NE¼SE¼ sec. 30, T. 38 N., R. 7 W., on left bank 100 ft upstream from farm road bridge in lane leading to farmhouse of Jack Rice, 500 ft west of Highway V, 1 mile north of U. S. Highway 66 at Dunivan Crossing, and 4½ miles northeast of Rolla. Lane to Rice residence is first lane north of point where highline crosses Highway V.

ESTABLISHMENT.--Mar. 1, 1952.

AREA.--0.225 sq mi, by transit and stadia survey.

GAGE.--Stevens water-stage recorder in small wooden box on 12-inch corrugated pipe well on concrete base and fastened to overhanging locust tree on left bank. Bottom of pipe at gage height 1.0 ft. Clean-out door at gage height 2.0 ft. Top of pipe 9.0 ft. Recorder equipped with spined tape and set to read zero as inside enameled staff section 1.10 to 3.34 ft bolted to inside of gage well.

Staff gage 0-3.34 ft fastened to steel angle posts at right and left water's edge 5 ft upstream from concrete V-notch control and 5 ft downstream from recorder.

All gages set to same datum. Inside staff is base gage.

HISTORY.--Recorder installed Mar. 1, 1951, by H. C. Bolon and son to study time of travel of peaks. Readings not comparable due to installation of V-notch weir.

RAIN GAGE AND SOIL MOISTURE BLOCKS.--Recording rain gage and soil moisture blocks installed 600 ft west southwest of water-stage recorder. Observer is Mrs. Betty Prior Rice who changes rain charts and takes soil moisture readings.

BENCH MARKS.--B.M. 1 Head of 20-penny spike driven vertically into top of right-upstream root of double 14-inch locust tree on right bank 60 ft downstream from gage. Elevation, 4.81 ft.

B.M. 2 Head of 20-penny spike driven horizontally 1 foot above ground into upstream side of 9-inch hickory tree on left bank 60 ft downstream from gage. Elevation, 4.99 ft.

B.M. 3 Head of 20-penny spike 3 ft above ground driven horizontally into upstream side of 12-inch locust tree on right bank 10 ft right of gage. Elevation, 6.91 ft.

B.M. 4 Top of right edge of weir. Elevation, 4.48 ft.

B.M. 5 Top of left edge of weir. Elevation, 4.45 ft.

CONTROL.--V-notch weir made by setting grader blades in concrete wall, 10 ft below recorder. Bottom of V-notch is elevation 1.91 ft. Top of weir at elevation 4.40 ft. Channel about 12 ft wide and 4 ft deep in hardpan. Irregular banks flanked by narrow stripe of trees and brush on each side. Broad level fields beyond. 8-foot farm bridge in lane 100 ft downstream may control extreme high stages. Channel shifting.

DISCHARGE MEASUREMENTS.--Extreme low measurements by bucket. Low and medium measurements by wading near gage. Extreme measurements by wading along farm lane or by indirect method.

FLOODS.--No record.

POINT OF ZERO FLOW.--1.91 (Bottom of V-notch).

REGULATION.--None.

WATER DISCHARGE.--Should be good. Oil cylinder used.

DIVERSIONS.--None.

ACCURACY.--Good to excellent.

COOPERATION.--State Highway Commission of Missouri. Missouri School of Mines and Metallurgy furnished materials and labor for control.

PHOTOGRAPHS.--Some stage pictures of gage, channel and control.

Figure 19b. Rating tables for watershed 19

(Photostat of original data.)

UNITED STATES DEPARTMENT OF THE INTERIOR
GEOLOGICAL SURVEY (WATER RESOURCES DIVISION)

Rating table for Lanes Fork near Rolla, Mo. Dated 1-15, 1954

from Mar. 1, 1952 to ... from ... to ...

Gage height	.00	.01	.02	.03	.04	.05	.06	.07	.08	.09	Difference
1.8	Sec. R.	0	.001	.002	.003	.004	.006	.008	.012	.016	Sec. R.
1.9	.020	.025	.030	.036	.043	.050	.059	.069	.079	.089	Direct from Curve
2.0	.100	.111	.122	.134	.147	.160	.174	.190	.206	.223	
.1	.24	.250	.270	.300	.322	.345	.369	.396	.422	.451	
.2	.48	.520	.560	.600	.640	.680	.720	.760	.800	.840	.60
.3	.88	.926	.972	1.05	1.10	1.16	1.22	1.27	1.33	1.38	.56
.4	1.44	1.51	1.57	1.64	1.71	1.78	1.84	1.91	1.98	2.04	.67
.5	2.11	2.20	2.29	2.38	2.47	2.56	2.64	2.73	2.82	2.91	.89
.6	3.00	3.11	3.23	3.34	3.46	3.57	3.68	3.80	3.91	4.03	1.14
.7	4.14	4.28	4.42	4.56	4.70	4.84	4.98	5.12	5.26	5.40	1.43
.8	5.54	5.70	5.86	6.02	6.18	6.34	6.51	6.67	6.83	6.99	1.61
.9	7.15	7.31	7.47	7.63	7.79	7.96	8.12	8.28	8.44	8.60	1.61
3.0	8.76	8.93	9.11	9.28	9.46	9.63	9.80	9.98	10.2	10.3	1.74
.1	10.5	10.7	10.9	11.1	11.3	11.6	11.7	11.9	12.1	12.3	2.05
.2	12.55	12.8	13.0	13.3	13.5	13.8	14.0	14.3	14.5	14.8	2.45
.3	15.0	15.3	15.5	15.8	16.0	16.3	16.6	16.8	17.1	17.3	2.6
.4	17.6	17.9	18.2	18.5	18.8	19.0	19.3	19.6	19.9	20.2	2.9
.5	20.5	20.8	21.1	21.4	21.7	22.0	22.4	22.7	23.0	23.3	3.1
.6	23.6	23.9	24.3	24.6	25.0	25.3	25.6	26.0	26.3	26.7	3.4
.7	27.0	27.4	27.7	28.1	28.5	28.8	29.2	29.6	30.0	30.3	3.7
.8	30.7	31.1	31.5	31.9	32.3	32.6	33.0	33.4	33.8	34.2	3.9
.9	34.6	35.0	35.4	35.9	36.3	36.7	37.1	37.5	38.0	38.4	4.2
4.0	38.8	39.3	39.7	40.2	40.6	41.1	41.6	42.0	42.5	42.9	4.6
.1	43.4	43.9	44.4	44.8	45.3	45.8	46.3	46.8	47.2	47.7	4.8
.2	48.2	48.7	49.3	49.8	50	51	51	52	52	53	5.3
.3	53.5	54	55	55	56	56	57	58	58	59	6.0
.4	59.5	60	61	62	62	63	64	64	65	66	7.0
.5	66.5	67	68	69	70	71	72	72	73	74	8.5
.6	75.0	76	77	78	79	80	81	82	83	84	10
.7	85.0	86	87	89	90	91	92	93	95	96	12
.8	97	98	100	102	103	104	106	108	109	110	15
.9	112	114	116	118	120						20

Computed by EAR 1/15/1954; Checked by JPH 1/16/1954 Remarks

Based on measurements 1-16 (1952), disch. computed by weir formula for 122° V-notch weir, and field estimate of overflow for flood on Apr. 23, 1952 at GH 4.34 ft.

UNITED STATES DEPARTMENT OF THE INTERIOR
GEOLOGICAL SURVEY (WATER RESOURCES DIVISION)

Rating table for Lanes Fork near Rolla, Mo. Dated 2-4, 1957

from Oct. 1, 1955 to ... from ... to ...

Gage height	.00	.01	.02	.03	.04	.05	.06	.07	.08	.09	Difference
1.8	Sec. R.	0	.002	.005	.008	.012	.016	.021	.026	.031	Sec. R.
1.9	.036	.042	.048	.055	.062	.070	.078	.086	.094	.102	
2.0	.110	.119	.128	.137	.147	.157	.168	.180	.192	.205	
.1	.220	.235	.251	.267	.285	.305	.325	.345	.367	.390	Direct from Curve
.2	.415	.44	.47	.50	.53	.56	.59	.62	.66	.70	
.3	.75	.80	.85	.90	.95	1.00	1.06	1.12	1.18	1.24	
.4	1.30	1.37	1.44	1.51	1.58	1.66	1.75	1.84	1.93	2.02	
.5	2.11	2.20	2.29	2.38	2.47	2.56	2.64	2.73	2.82	2.91	.89
.6	3.00	3.11	3.23	3.34	3.46	3.57	3.68	3.80	3.91	4.03	1.14
.7	4.14	4.28	4.42	4.56	4.70	4.84	4.98	5.12	5.26	5.40	1.40
.8	5.54	5.70	5.86	6.02	6.18	6.34	6.51	6.67	6.83	6.99	1.61
.9	7.15	7.31	7.47	7.63	7.79	7.96	8.12	8.28	8.44	8.60	1.61
3.0	8.76	8.93	9.11	9.28	9.46	9.63	9.80	9.98	10.2	10.3	1.74
.1	10.6	10.7	10.9	11.1	11.3	11.5	11.7	11.9	12.1	12.3	2.05
.2	12.55	12.8	13.0	13.3	13.5	13.8	14.0	14.3	14.5	14.8	2.45
.3	15.0	15.3	15.5	15.8	16.0	16.3	16.6	16.8	17.1	17.3	2.6
.4	17.6	17.9	18.2	18.5	18.8	19.0	19.3	19.6	19.9	20.2	2.9
.5	20.5	20.8	21.1	21.4	21.7	22.0	22.4	22.7	23.0	23.3	3.1
.6	23.6	23.9	24.3	24.6	25.0	25.3	25.6	26.0	26.3	26.7	3.4
.7	27.0	27.4	27.7	28.1	28.5	28.8	29.2	29.6	30.0	30.3	3.7
.8	30.7	31.1	31.5	31.9	32.3	32.6	33.0	33.4	33.8	34.2	3.9
.9	34.6	35.0	35.4	35.9	36.3	36.7	37.1	37.5	38.0	38.4	4.2
4.0	38.8	39.3	39.7	40.2	40.6	41.1	41.6	42.0	42.5	42.9	4.6
.1	43.4	43.9	44.4	44.8	45.3	45.8	46.3	46.8	47.2	47.7	4.8
.2	48.2	48.7	49.3	49.8	50	51	51	52	52	53	5.3
.3	53.5	54	55	55	56	56	57	58	58	59	6.0
.4	59.5	60	61	62	62	63	64	64	65	66	7.0
.5	66.5	67	68	69	70	71	72	72	73	74	8.5
.6	75.0	76	77	78	79	80	81	82	83	84	10
.7	85.0	86	87	89	90	91	92	93	95	96	12
.8	97	98	100	102	103	104	106	108	109	110	15
.9	112	114	116	118	120						20

Computed by EAR 2-4-1957; Checked by WLA Remarks

Based on measurements 18-22 (1956-57) and rating dated 1-15-54 above 2.5 ft.

Same as rating dated 1-15-54 above 2.5 ft.

Figure 20a. Stage graph for storm of April 23-24, 1953 on watershed 19

(Photostat of original data.)

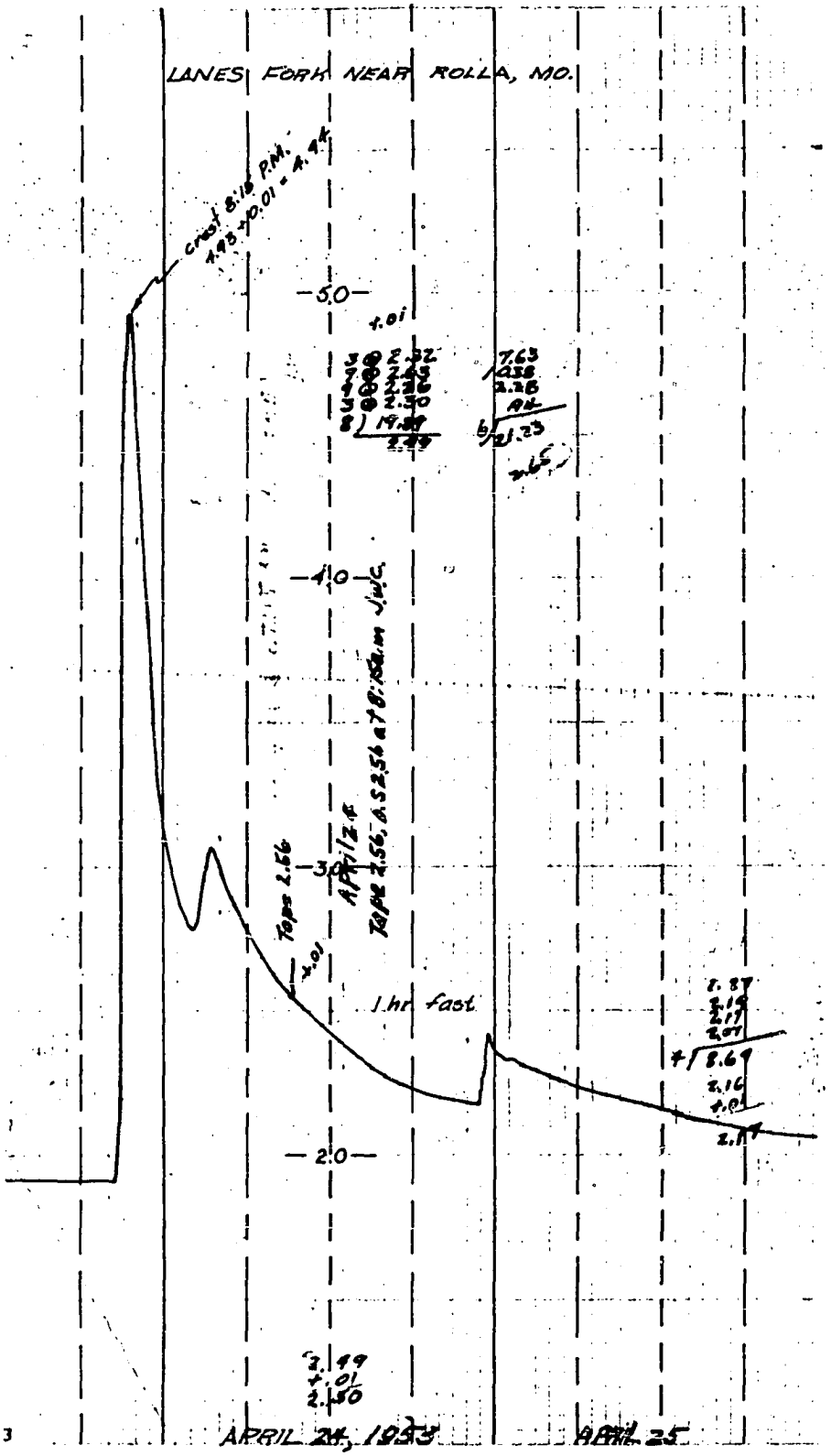
LANES FORK NEAR ROLLA, MO.
crest 8:15 P.M.
4.95 +0.01 = 4.96
5.0
4.0
3.0
2.0
Tape 2.56
+.01
1 hr fast
APRIL 24, 1953
APRIL 25

Figure 20b. Stage graph for storm of June 10, 1954 on watershed 19

(Photostat of original data.)

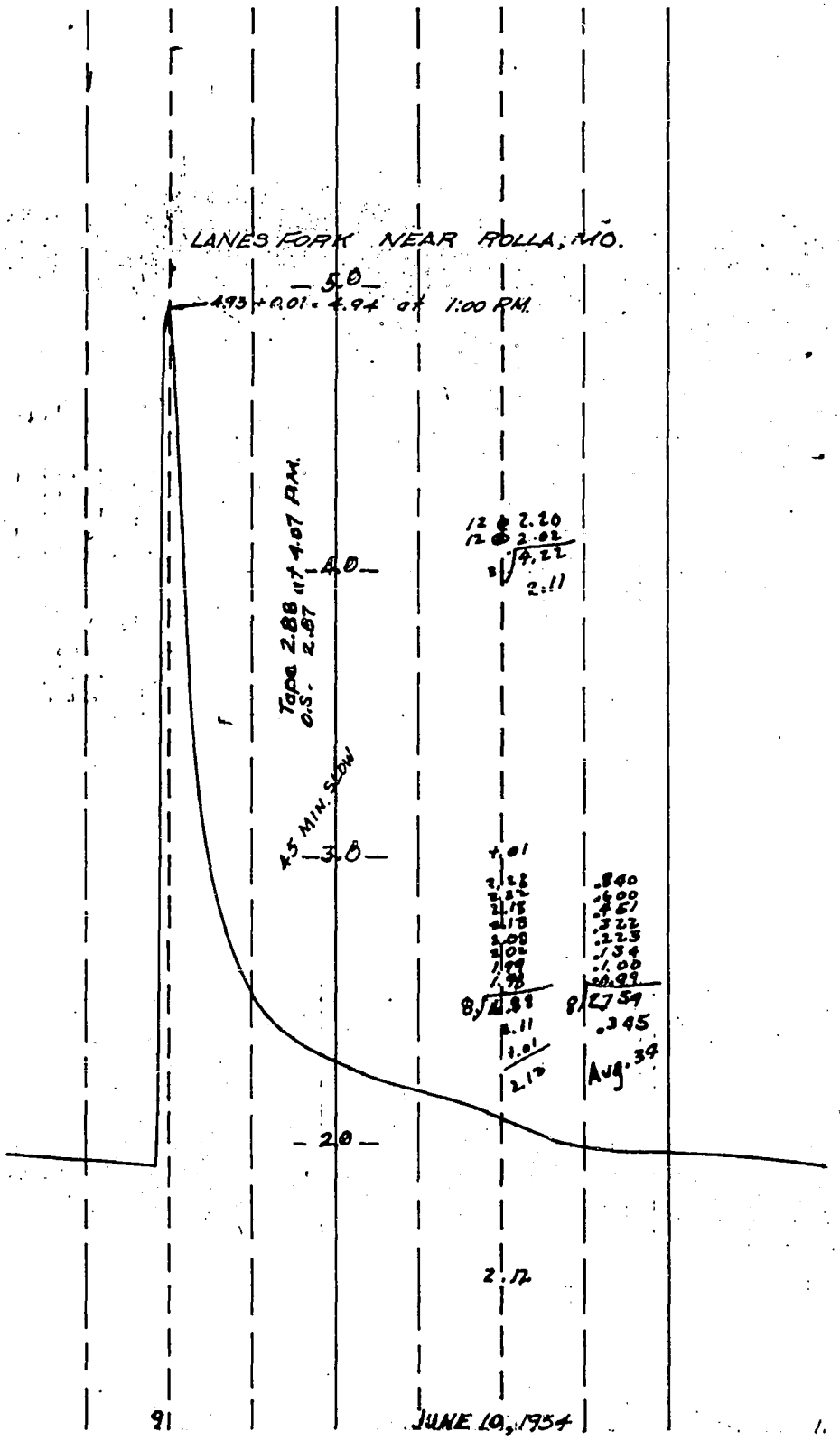
LANES FORK NEAR ROLLA, MO.
5.0
4.93 + 0.01 = 4.94 at 1:00 PM.
4.0
Tape 2.88 at 4.07 PM.
O.S. 2.87
45 MIN. SLOW
3.0
2.0
91
JUNE 10, 1954

Figure 20c. Stage graph for storm of May 25, 1957 on watershed 19

(Photostat of original data.)

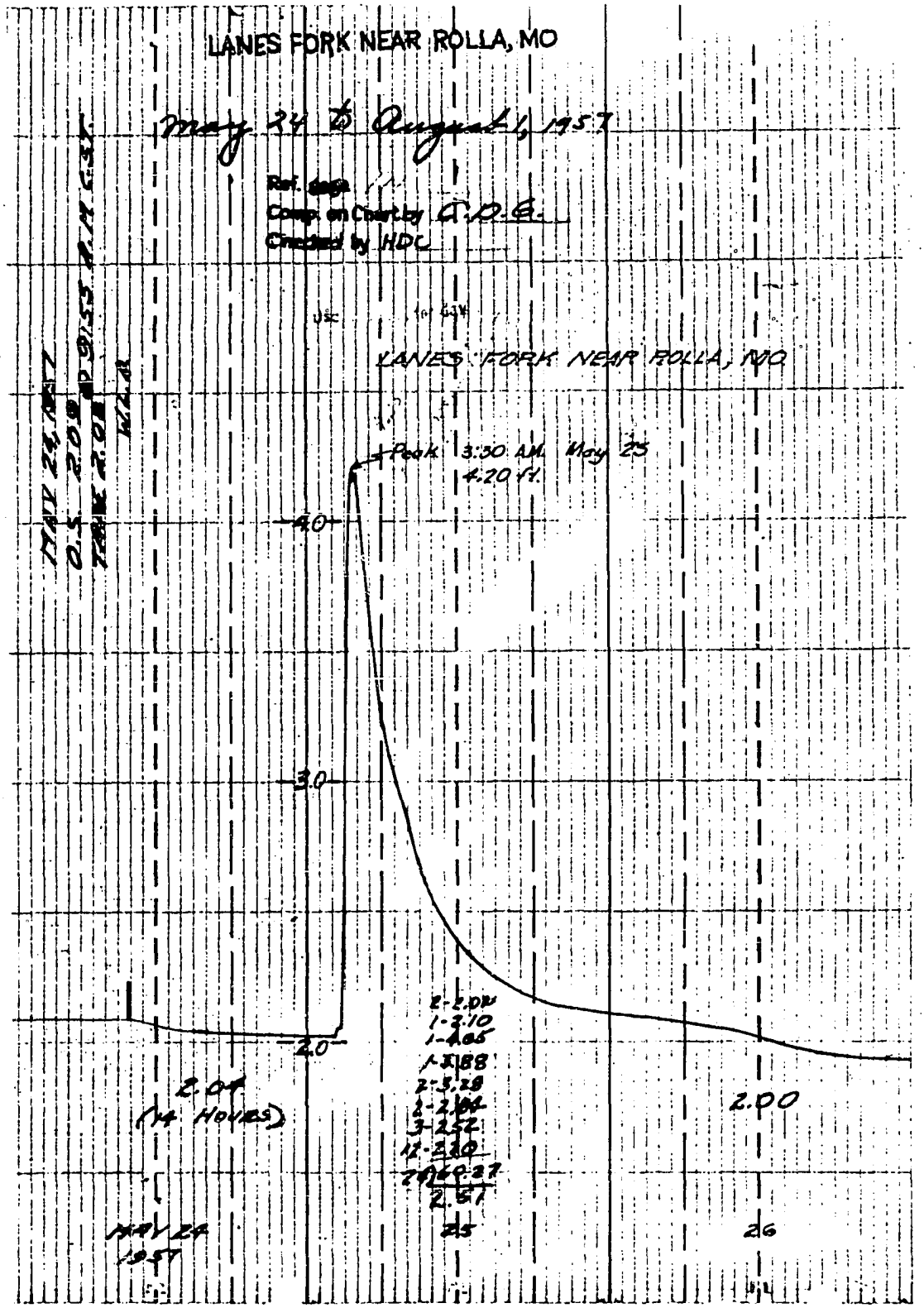
LANES FORK NEAR ROLLA, MO
May 24 to August 1, 1957
Ref. Gage
Comp. on Chart by C.O.E.
Checked by HDC
LANES FORK NEAR ROLLA, MO
Peak 3:30 AM May 25
4.20 ft.
4.0
3.0
2.0
2.04
(14 Hours)
2.00
MAY 24
1957
25
26

Table 7. Discharge readings for storm of April 23-24, 1953, on watershed 19

Accumulated time hr.	Stage ft.	Shift correction ft.	Corrected stage ft.	Discharge cfs
0.00	1.92	+0.01	1.93	0.0
0.25	3.00	"	3.01	9.3
0.50	4.30	"	4.31	54.0
1.00	4.93	"	4.94	120.0
1.50	4.55	"	4.56	72.0
2.00	4.17	"	4.18	47.0
2.50	3.75	"	3.76	29.0
3.00	3.35	"	3.36	19.0
3.50	3.25	"	3.26	14.0
4.00	3.00	"	3.01	8.9
4.50	2.90	"	2.91	7.3
5.00	2.82	"	2.83	6.0
5.50	2.79	"	2.80	5.5
6.00	2.84	"	2.85	6.3
6.50	3.00	"	3.01	8.9
7.00	3.06	"	3.07	10.0
7.50	3.00	"	3.01	8.9
8.00	2.93	"	2.94	7.8
8.50	2.87	"	2.88	6.8
9.50	2.78	"	2.79	5.4
10.00	2.73	"	2.74	4.5

Table 8. Discharge readings for storm of June 10, 1954, on watershed 19

Accumulated time hr.	Stage ft.	Shift correction ft.	Corrected stage ft.	Discharge cfs
0.00	1.92	+0.01	1.93	0.0
0.25	3.50	"	3.51	21.0
0.50	4.69	"	4.70	85.0
0.75	4.88	"	4.89	109.0
1.00	4.93	"	4.94	120.0
1.50	4.60	"	4.61	76.0
2.00	4.06	"	4.07	42.0
2.50	3.61	"	3.62	24.0
3.00	3.30	"	3.31	15.0
3.50	3.10	"	3.11	11.0
4.00	2.95	"	2.96	8.1
4.50	2.84	"	2.85	6.3
5.00	2.76	"	2.77	5.1
6.00	2.62	"	2.63	3.3
7.00	2.51	"	2.52	2.3
8.00	2.45	"	2.46	1.8
9.00	2.40	"	2.41	1.5
10.00	2.36	"	2.37	1.3

Table 9. Discharge readings for storm of May 25, 1957, on watershed 19

Accumulated time hr.	Stage ft.	Shift correction[a] ft.	Corrected stage ft.	Discharge cfs
0.00	2.02			0.0
0.25	3.00			8.8
0.50	3.89			34.0
0.75	4.20			48.0
1.25	4.10			43.0
1.75	3.87			33.0
2.25	3.65			25.0
2.75	3.43			19.0
3.25	3.26			14.0
3.75	3.14			11.0
4.25	3.03			9.3
4.75	2.94			7.8
5.25	2.87			6.7
6.25	2.66			3.7
7.25	2.55			2.6
8.25	2.47			1.8
9.00	2.41			1.3

[a]No shift correction.

Figure 21a. Discharge hydrograph for storm of April 23-24, 1953 on watershed 19

Figure 21b. Discharge hydrograph for storm of June 10, 1954 on watershed 19

Figure 21c. Discharge hydrograph for storm of May 25, 1957 on watershed 19

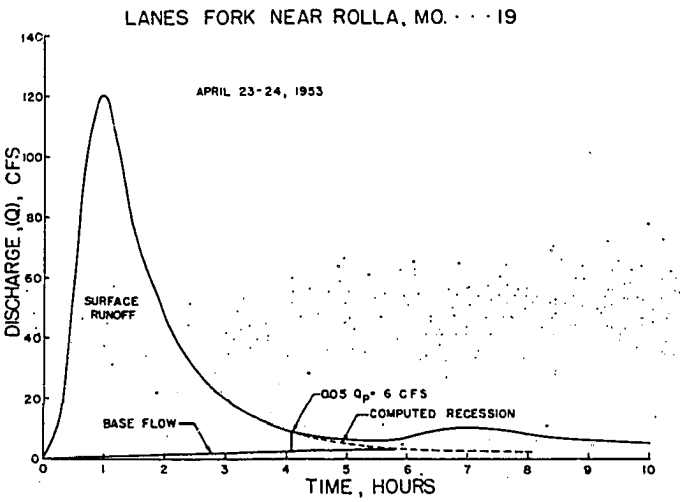
LANES FORK NEAR ROLLA, MO. · · · 19
APRIL 23-24, 1953
DISCHARGE, (Q), CFS
SURFACE RUNOFF
BASE FLOW
0.05 Qp = 6 CFS
COMPUTED RECESSION
TIME, HOURS

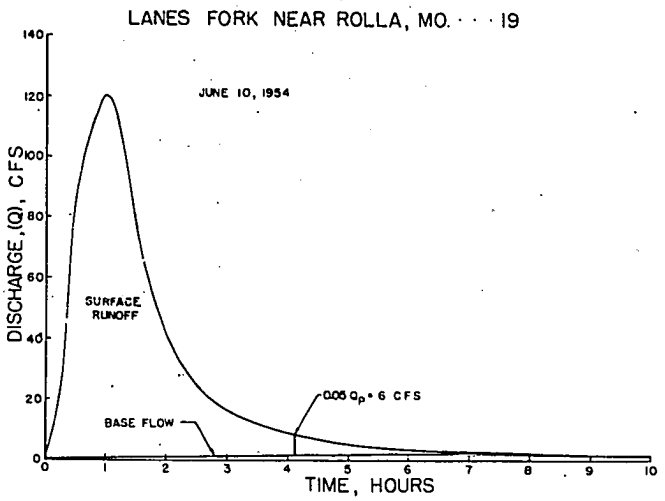
LANES FORK NEAR ROLLA, MO. · · · 19
JUNE 10, 1954
DISCHARGE, (Q), CFS
SURFACE RUNOFF
BASE FLOW
0.05 Qp = 6 CFS
TIME, HOURS

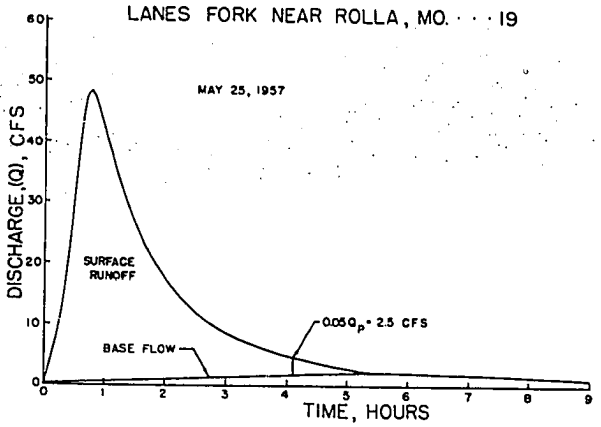
LANES FORK NEAR ROLLA, MO. · · · 19
MAY 25, 1957
DISCHARGE, (Q), CFS
SURFACE RUNOFF
BASE FLOW
0.05 Qp = 2.5 CFS
TIME, HOURS

subject to personal opinion. With reference to the methodology employed, Wisler and Brater (59, p. 30) state, "The exact location of the end of surface runoff usually cannot be determined, but this is not of great importance as long as one always follows a consistent procedure."

For the watersheds employed in this study, the contribution of base flow during the flood period was assumed to be practically negligible. It was, therefore, considered impractical to adopt a complex, time-consuming technique for base-flow separation. A simple, arbitrary procedure was developed to accomplish this purpose.

A. A straight line was drawn tangent to the recession curve where the curve showed an approximate constant depletion rate over a long period of time.

B. The initial point of rise on the recession limb was connected with the point at which the tangent line departed from the recession curve by a straight line (see Figures 21a, 21b, and 21c).

The area above this line was taken to represent surface runoff; the area below, base flow. In an attempt to obtain congruency in the time-bases of the hydrographs, the period of surface runoff was temporarily defined as the time from the initial point of rise to the point at which the surface runoff rate decreased to 5 percent of the peak discharge rate, $0.05Q_p$.

Where a parasite storm complexed the recession limb as in the hydrograph for April 23, 1953, the normal recession limb was plotted according to a composite recession curve developed from the other hydrographs of

record (see Figure 22).

3. Development of the distribution graphs

A. The time-bases of the surface-runoff hydrographs were divided into at least 10 and preferably 14-15 equal-time increments of Δt-minutes duration. To avoid irregular time increments, Δt was chosen to the nearest 5 minutes and the last increment taken to include the discharge, $0.05Q_p$. The same time unit was used for all hydrographs of a given watershed.

B. The ordinate values of the surface-runoff hydrographs were tabulated at the respective times from the beginning of surface runoff,

$$\frac{\Delta t}{2}, \quad \frac{3}{2}\Delta t, \frac{5}{2}\Delta t \cdot \cdot \cdot \cdot \cdot \frac{(2n-1)}{2}\Delta t$$

where n is the number Δt-increments.

For each hydrograph, the peak discharge was always recorded.

C. The distribution graph was developed from each hydrograph by the relationship

$$\% \text{ flow}/\Delta t\text{-increment} = \frac{\Sigma \text{cfs for a given } \Delta t\text{-period}}{\Sigma \text{cfs for n } \Delta t\text{-periods}} \times 100$$

See Tables 10, 11, and 12.

4. Development of empirical graph

The empirical graph for each watershed was developed by procedures described previously (see discussion pp. 44ff). The graph for watershed 19 is given in Figure 27.

Figure 22. Recession curve for watershed 19

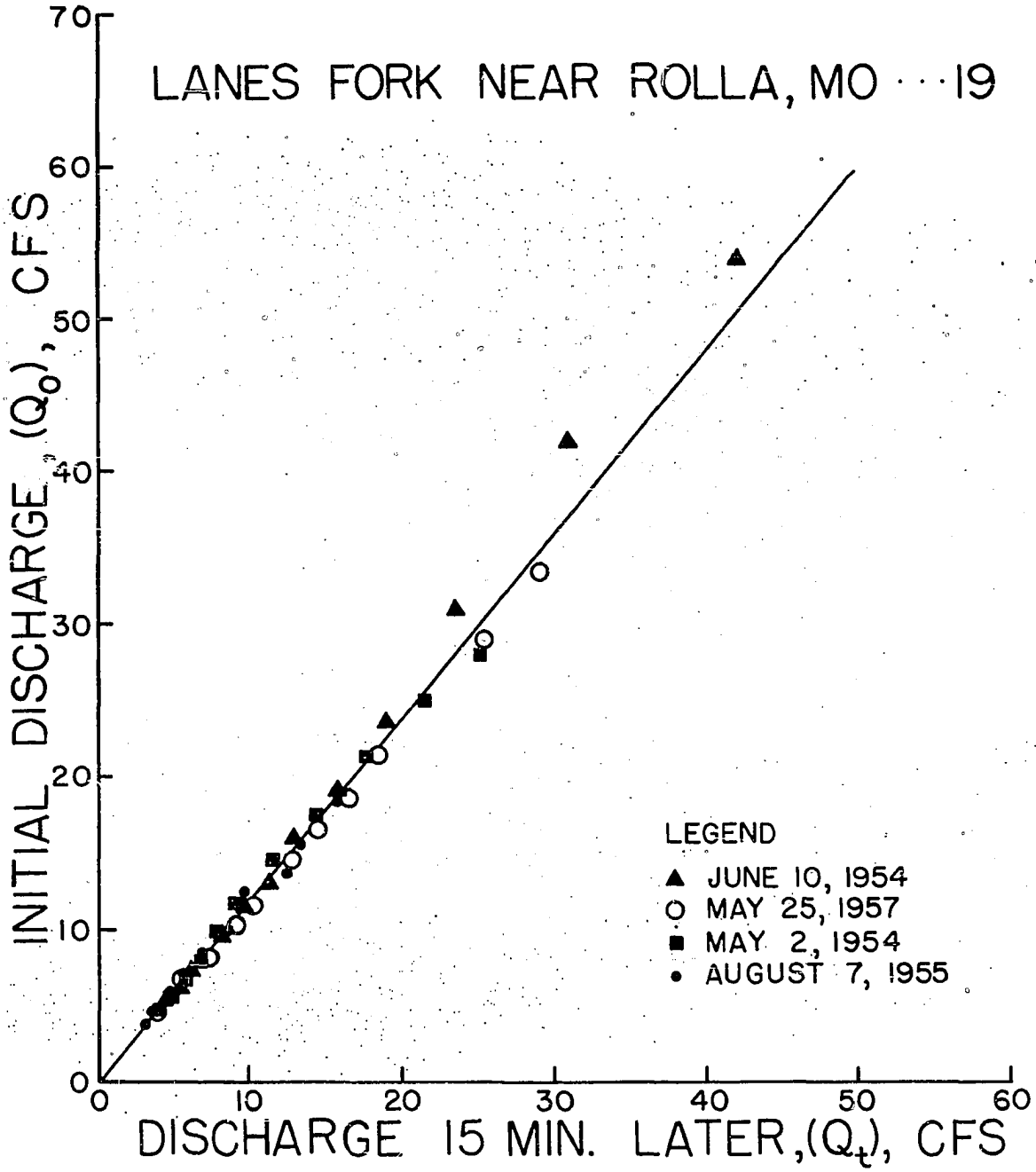
LANES FORK NEAR ROLLA, MO ···19
INITIAL DISCHARGE, (Q_0), CFS
DISCHARGE 15 MIN. LATER, (Q_t), CFS
0
10
20
30
40
50
60
70
LEGEND
JUNE 10, 1954
MAY 25, 1957
MAY 2, 1954
AUGUST 7, 1955

Table 10. Distribution graph for watershed 19 from storm of April 23-24, 1953

Accumulated time min.	Number of 15-minute periods min.	Corrected discharge cfs	Flow per 15-minute time interval percent
0.0	0	0	0.0
7.5	1	4	0.6
22.5	2	27	3.9
37.5	3	82	11.8
52.5	4	113	16.2
57.5		119[a]	17.1
67.5	5	112	16.0
82.5	6	85	12.2
97.5	7	65	9.3
112.5	8	51	7.3
127.5	9	38	5.5
142.5	10	30	4.3
157.5	11	24	3.4
172.5	12	19	2.7
187.5	13	15	2.2
202.5	14	12	1.7
217.5	15	9	1.3
232.5	16	7	1.0
247.5	17	4	0.6
	Total	697	100.0

[a]Peak discharge rate; not included in total.

Table 11. Distribution graph for watershed 19 from storm of June 10, 1954

Accumulated time min.	Number of 15-minute periods min.	Corrected discharge cfs	Flow per 15-minute time interval percent
0.0	0	0	0.0
7.5	1	8	1.1
22.5	2	50	6.9
37.5	3	98	13.6
52.5	4	115	15.9
60.0		119[a]	16.5
67.5	5	114	15.8
82.5	6	90	12.3
97.5	7	62	8.6
112.5	8	46	6.4
127.5	9	34	4.7
142.5	10	25	3.5
157.5	11	20	2.8
172.5	12	16	2.2
187.5	13	13	1.8
202.5	14	11	1.5
217.5	15	9	1.2
232.5	16	7	1.0
247.5	17	5	0.7
	Total	723	100.0

[a]Peak discharge rate; not included in total.

Table 12. Distribution graph for watershed 19 from storm of May 25, 1957

Accumulated time min.	Number of 15-minute periods min.	Corrected discharge cfs	Flow per 15-minute time interval percent
0.0	0	0	0.0
7.5	1	4	1.4
22.5	2	18	6.6
37.5	3	41	15.0
45.0		48[a]	17.5
52.5	4	44	16.0
67.5	5	36	13.1
82.5	6	28	10.2
97.5	7	22	8.1
112.5	8	18	6.6
127.5	9	15	5.5
142.5	10	12	4.2
157.5	11	9	3.5
172.5	12	7	2.6
187.5	13	6	2.2
202.5	14	5	1.8
217.5	15	4	1.4
232.5	16	3	1.1
247.5	17	2	0.7
	Total	274	100.0

[a]Peak discharge rate; not included in total.

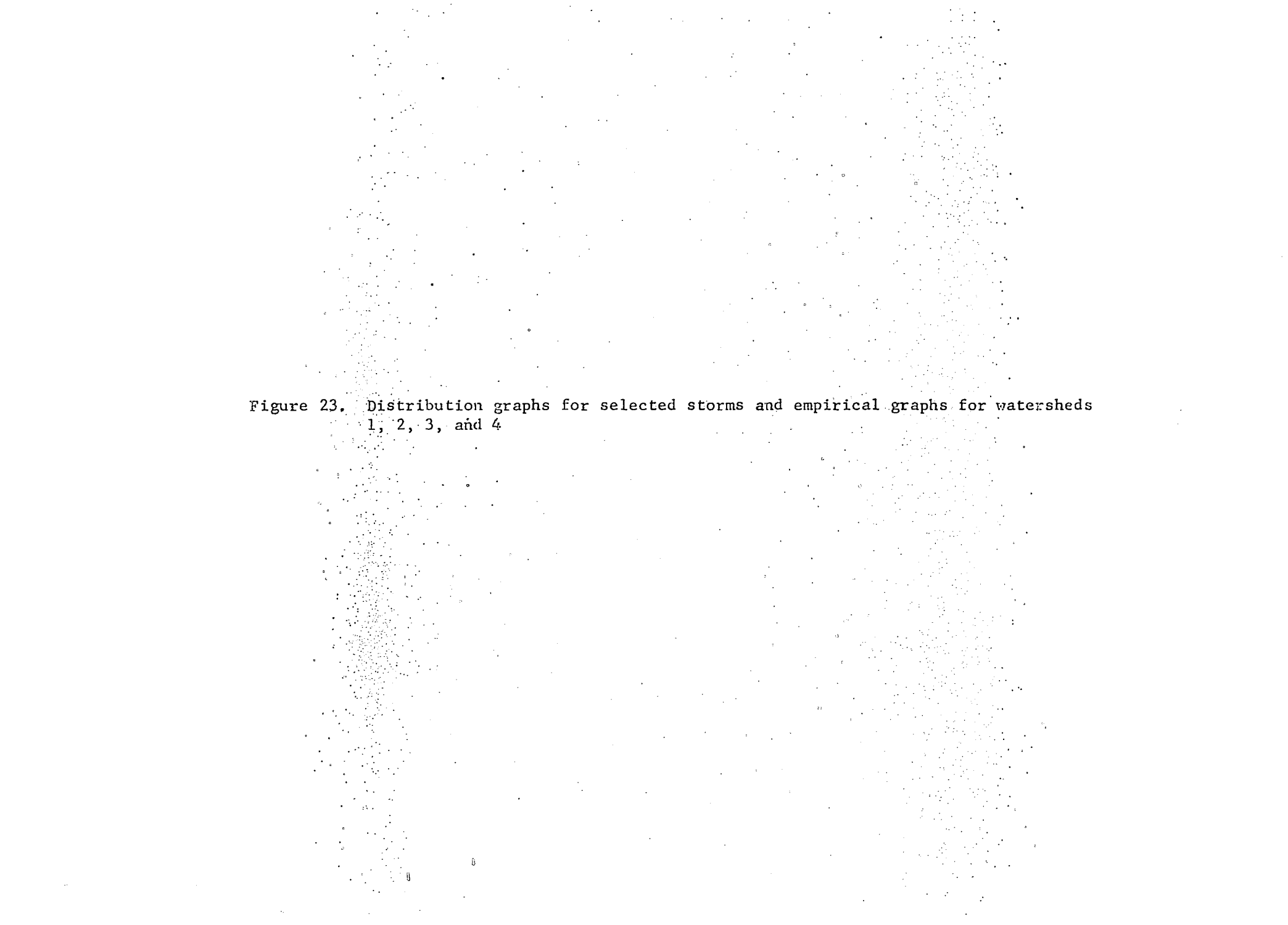

Figure 23. Distribution graphs for selected storms and empirical graphs for watersheds 1, 2, 3, and 4

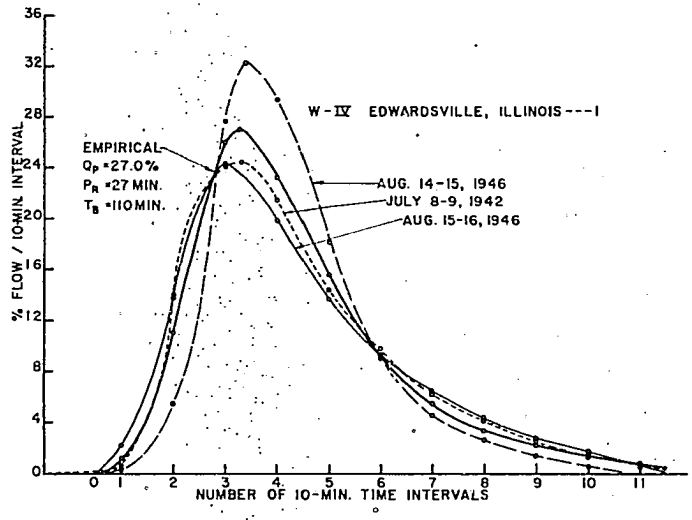
W-IV EDWARDSVILLE, ILLINOIS---1
EMPIRICAL
Q_P =27.0%
P_R =27 MIN.
T_B =110MIN.
AUG. 14-15, 1946
JULY 8-9, 1942
AUG. 15-16, 1946
% FLOW / 10-MIN. INTERVAL
NUMBER OF 10-MIN. TIME INTERVALS

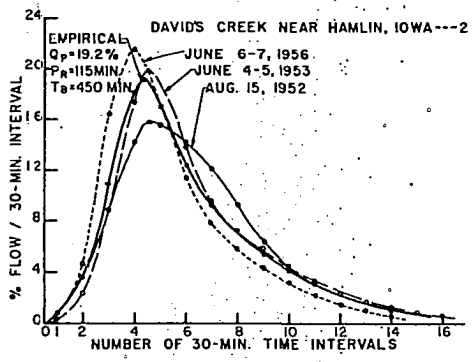
DAVIDS CREEK NEAR HAMLIN, IOWA---2
EMPIRICAL
Q_P =19.2%
P_R =115MIN.
T_B =450 MIN.
JUNE 6-7, 1956
JUNE 4-5, 1953
AUG. 15, 1952
% FLOW / 30-MIN. INTERVAL
NUMBER OF 30-MIN. TIME INTERVALS

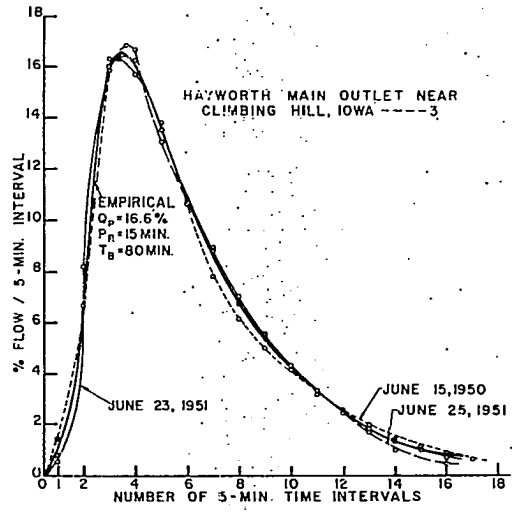
HAYWORTH MAIN OUTLET NEAR
CLIMBING HILL, IOWA ----3
EMPIRICAL
Q_P =16.6%
P_R =15 MIN.
T_B =80MIN.
JUNE 23, 1951
JUNE 15,1950
JUNE 25, 1951
% FLOW / 5-MIN. INTERVAL
NUMBER OF 5-MIN. TIME INTERVALS

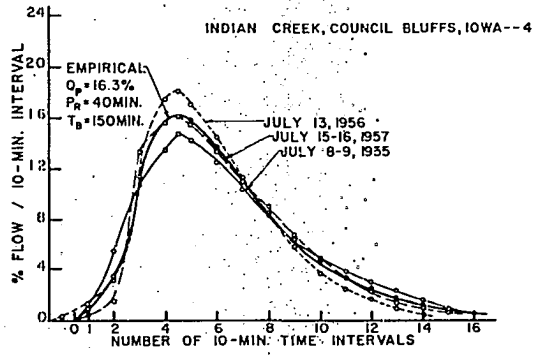
INDIAN CREEK, COUNCIL BLUFFS, IOWA--4
EMPIRICAL
Q_P =16.3%
P_R =40MIN.
T_B =150MIN.
JULY 13, 1956
JULY 15-16, 1957
JULY 8-9, 1935
% FLOW / 10-MIN. INTERVAL
NUMBER OF 10-MIN. TIME INTERVALS

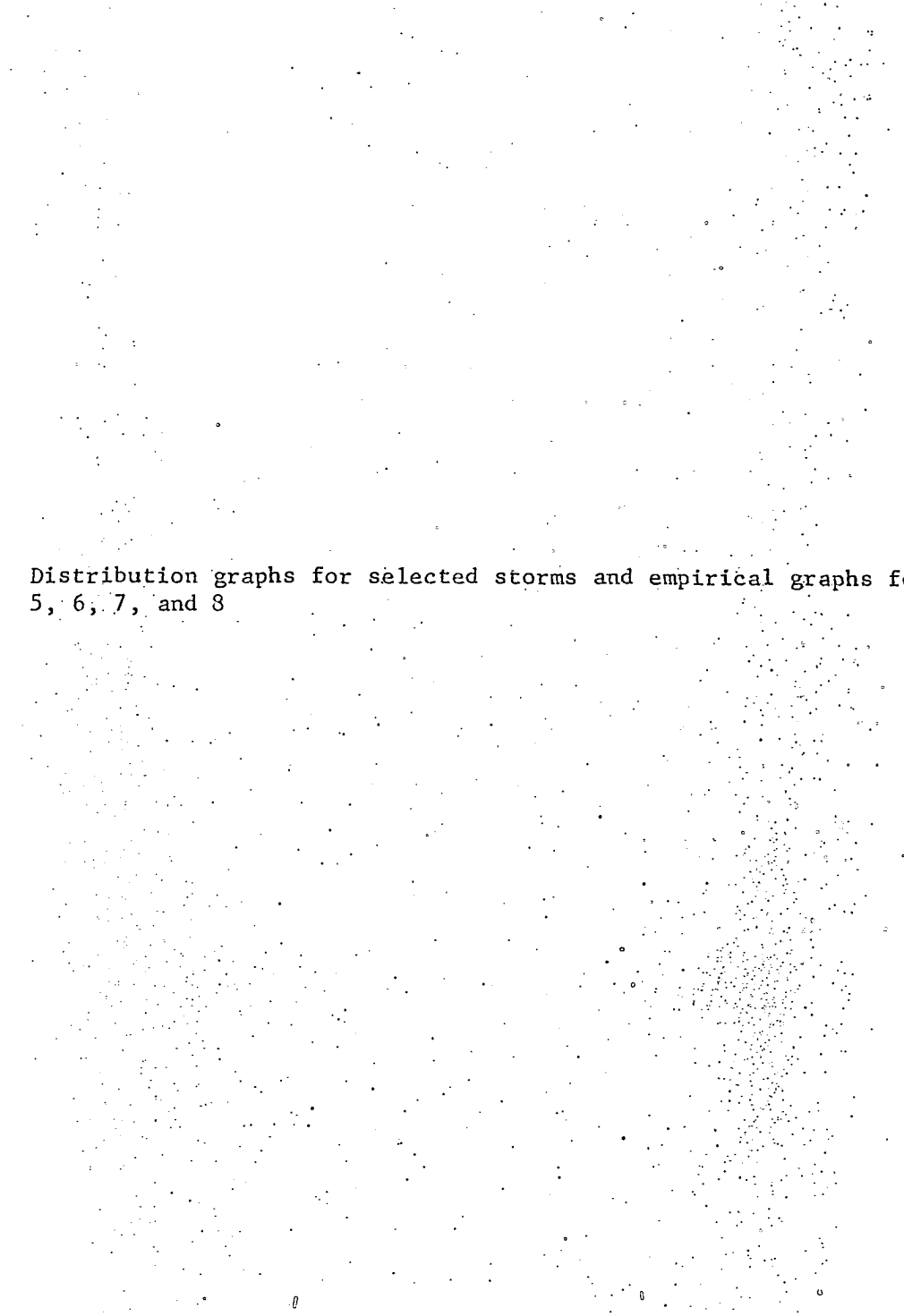

Figure 24. Distribution graphs for selected storms and empirical graphs for watersheds 5, 6, 7, and 8

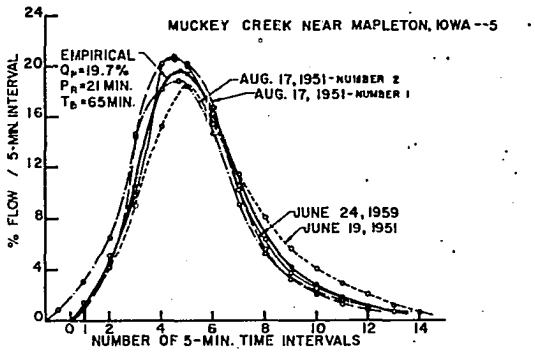
MUCKEY CREEK NEAR MAPLETON, IOWA--5
EMPIRICAL
Q_p=19.7%
P_R=21 MIN.
T_B=65 MIN.
AUG. 17, 1951-NUMBER 2
AUG. 17, 1951-NUMBER 1
JUNE 24, 1959
JUNE 19, 1951
% FLOW / 5-MIN. INTERVAL
NUMBER OF 5-MIN. TIME INTERVALS

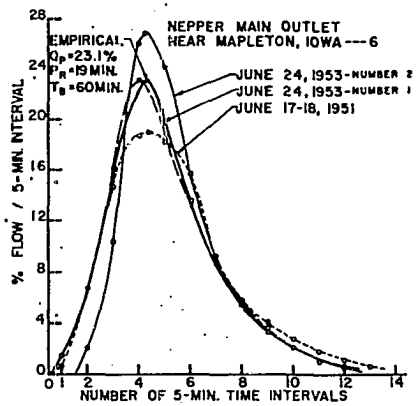
NEPPER MAIN OUTLET
NEAR MAPLETON, IOWA---6
EMPIRICAL
Q_p=23.1%
P_R=19 MIN.
T_B=60 MIN.
JUNE 24, 1953-NUMBER 2
JUNE 24, 1953-NUMBER 1
JUNE 17-18, 1951
% FLOW / 5-MIN. INTERVAL
NUMBER OF 5-MIN. TIME INTERVALS

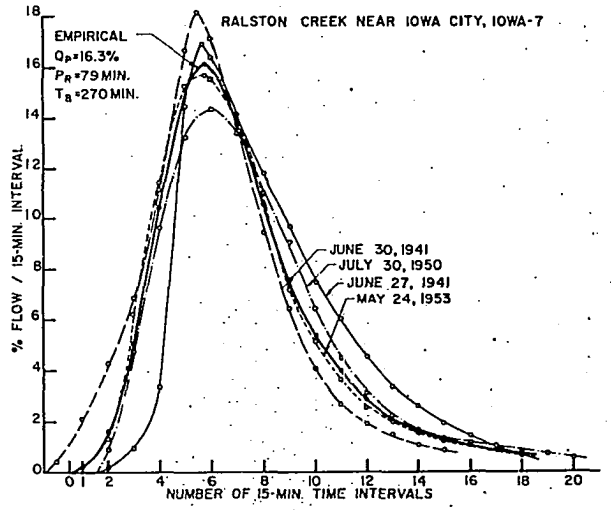
RALSTON CREEK NEAR IOWA CITY, IOWA-7
EMPIRICAL
Q_p=16.3%
P_R=79 MIN.
T_B=270 MIN.
JUNE 30, 1941
JULY 30, 1950
JUNE 27, 1941
MAY 24, 1953
% FLOW / 15-MIN. INTERVAL
NUMBER OF 15-MIN. TIME INTERVALS

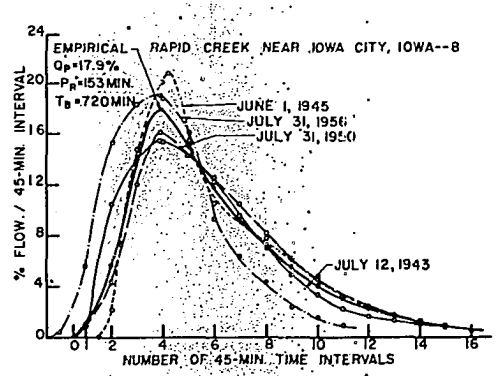
RAPID CREEK NEAR IOWA CITY, IOWA--8
EMPIRICAL
Q_p=17.9%
P_R=153 MIN.
T_B=720 MIN.
JUNE 1, 1945
JULY 31, 1956
JULY 31, 1950
JULY 12, 1943
% FLOW / 45-MIN. INTERVAL
NUMBER OF 45-MIN. TIME INTERVALS

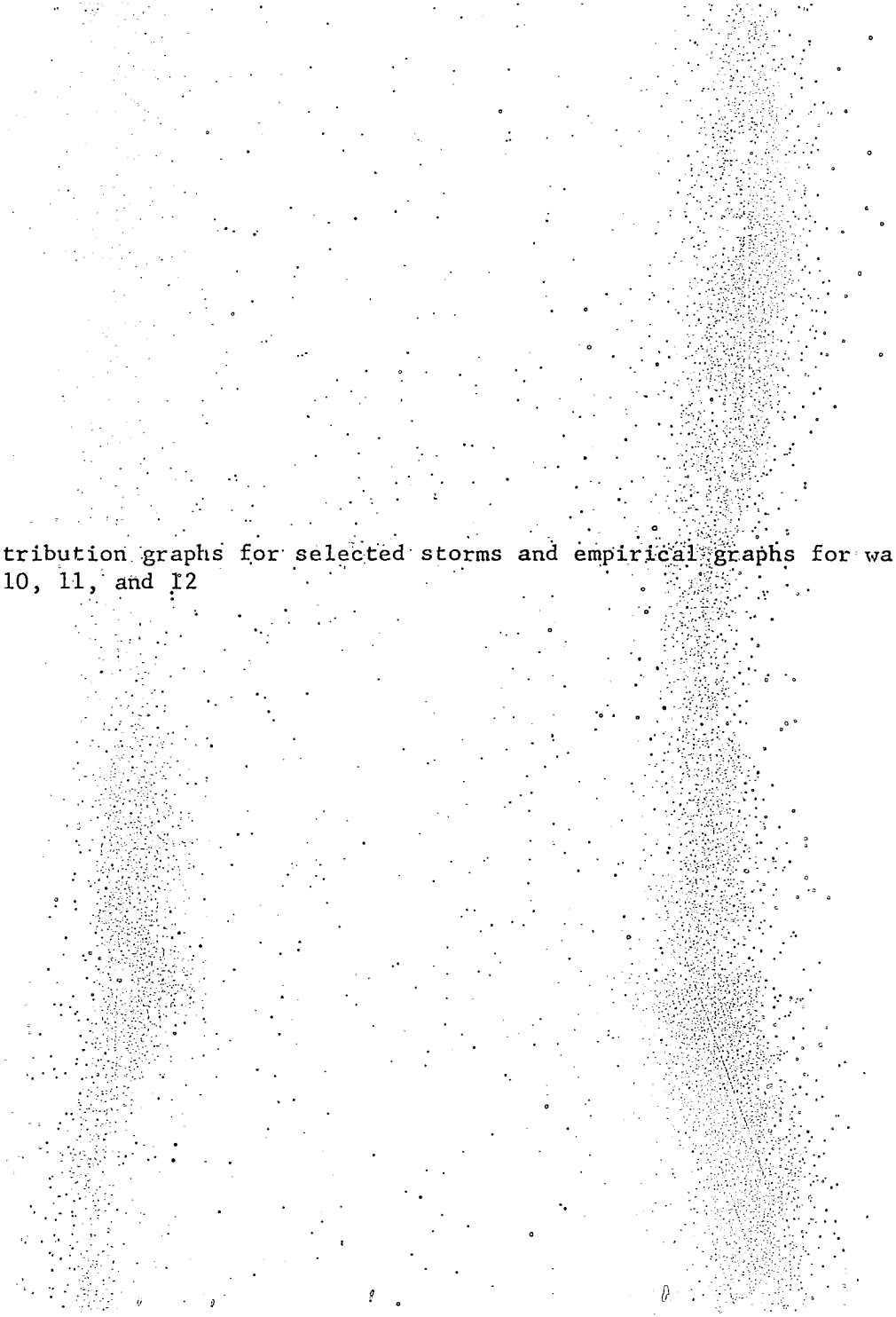

Figure 25. Distribution graphs for selected storms and empirical graphs for watersheds 9, 10, 11, and 12

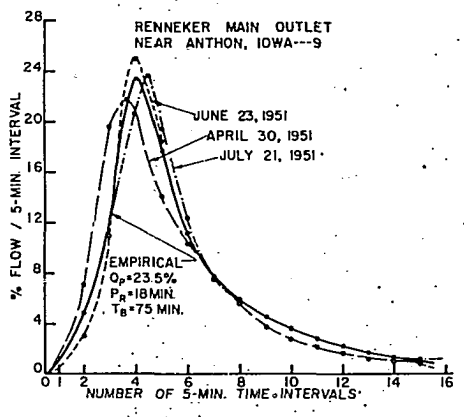
RENNEKER MAIN OUTLET
NEAR ANTHON, IOWA---9
JUNE 23, 1951
APRIL 30, 1951
JULY 21, 1951
EMPIRICAL
Q_P=23.5%
P_R=18MIN.
T_B=75 MIN.
% FLOW / 5-MIN. INTERVAL
NUMBER OF 5-MIN. TIME INTERVALS

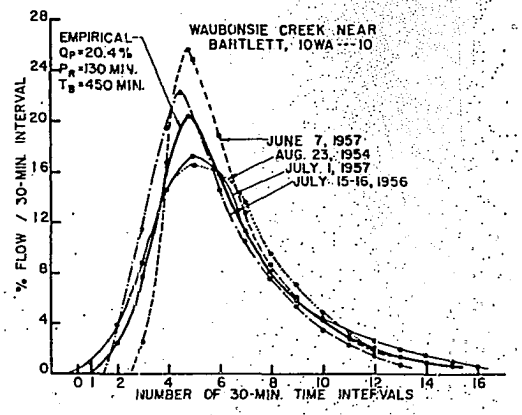
WAUBONSIE CREEK NEAR
BARTLETT, IOWA---10
EMPIRICAL
Q_P=20.4%
P_R=130 MIN.
T_B=450 MIN.
JUNE 7, 1957
AUG. 23, 1954
JULY 1, 1957
JULY 15-16, 1956
% FLOW / 30-MIN. INTERVAL
NUMBER OF 30-MIN. TIME INTERVALS

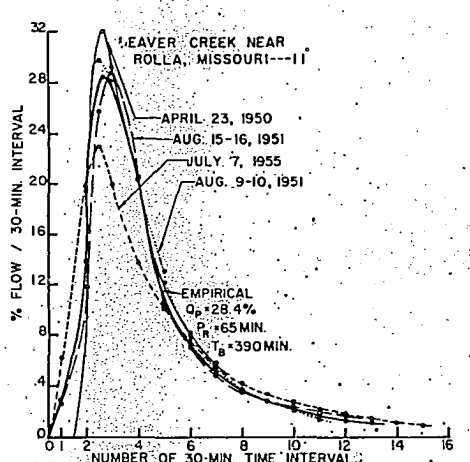
BEAVER CREEK NEAR
ROLLA, MISSOURI---11
APRIL 23, 1950
AUG. 15-16, 1951
JULY 7, 1955
AUG. 9-10, 1951
EMPIRICAL
Q_P=28.4%
P_R=65MIN.
T_B=390MIN.
% FLOW / 30-MIN. INTERVAL
NUMBER OF 30-MIN. TIME INTERVALS

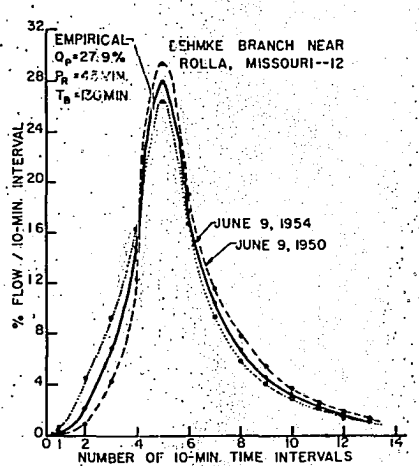
EMPIRICAL
Q_P=27.9%
P_R=45 MIN.
T_B=120MIN.
LEHMKE BRANCH NEAR
ROLLA, MISSOURI--12
JUNE 9, 1954
JUNE 9, 1950
% FLOW / 10-MIN. INTERVAL
NUMBER OF 10-MIN. TIME INTERVALS

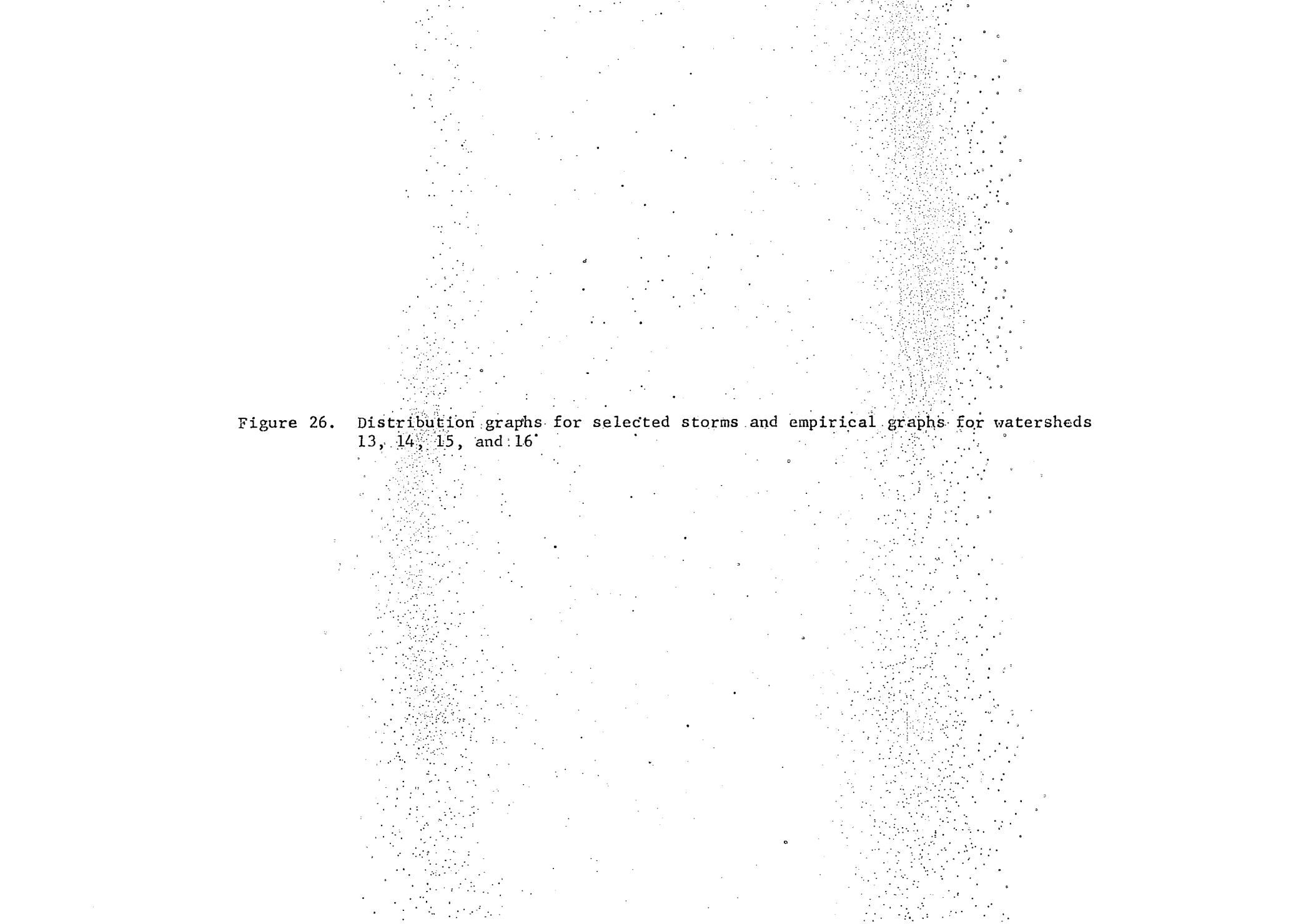

Figure 26. Distribution graphs for selected storms and empirical graphs for watersheds 13, 14, 15, and 16

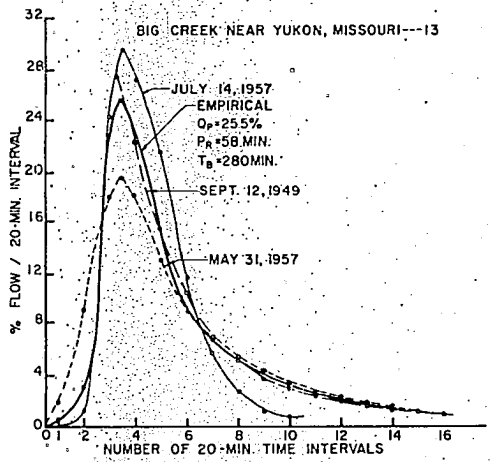
BIG CREEK NEAR YUKON, MISSOURI---13
JULY 14, 1957
EMPIRICAL
Q_P=25.5%
P_R=58 MIN.
T_B=280 MIN.
SEPT. 12, 1949
MAY 31, 1957
% FLOW / 20-MIN. INTERVAL
NUMBER OF 20-MIN. TIME INTERVALS

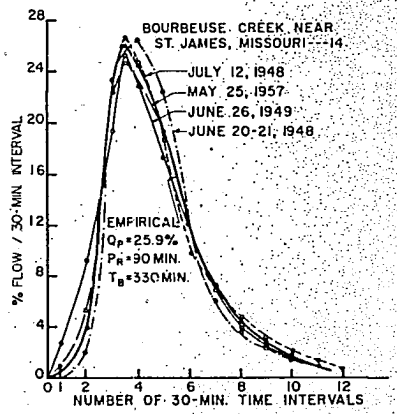
BOURBEUSE CREEK NEAR ST. JAMES, MISSOURI---14
JULY 12, 1948
MAY 25, 1957
JUNE 26, 1949
JUNE 20-21, 1948
EMPIRICAL
Q_P=25.9%
P_R=90 MIN.
T_B=330 MIN.
% FLOW / 30-MIN. INTERVAL
NUMBER OF 30-MIN. TIME INTERVALS

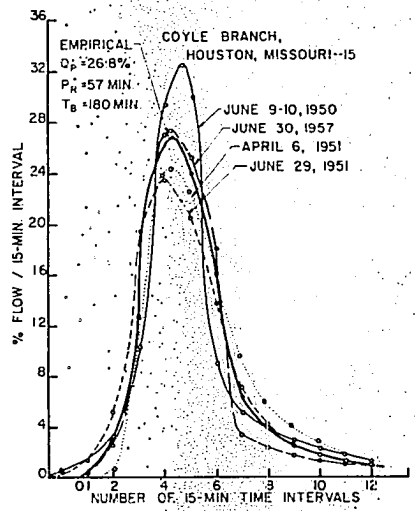
COYLE BRANCH, HOUSTON, MISSOURI--15
EMPIRICAL
Q_P=26.8%
P_R=57 MIN.
T_B=180 MIN.
JUNE 9-10, 1950
JUNE 30, 1957
APRIL 6, 1951
JUNE 29, 1951
% FLOW / 15-MIN. INTERVAL
NUMBER OF 15-MIN TIME INTERVALS

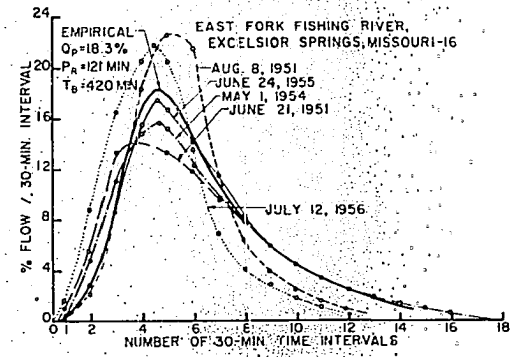
EAST FORK FISHING RIVER, EXCELSIOR SPRINGS, MISSOURI-16
EMPIRICAL
Q_P=18.3%
P_R=121 MIN.
T_B=420 MIN.
AUG. 8, 1951
JUNE 24, 1955
MAY 1, 1954
JUNE 21, 1951
JULY 12, 1956
% FLOW / 30-MIN. INTERVAL
NUMBER OF 30-MIN. TIME INTERVALS

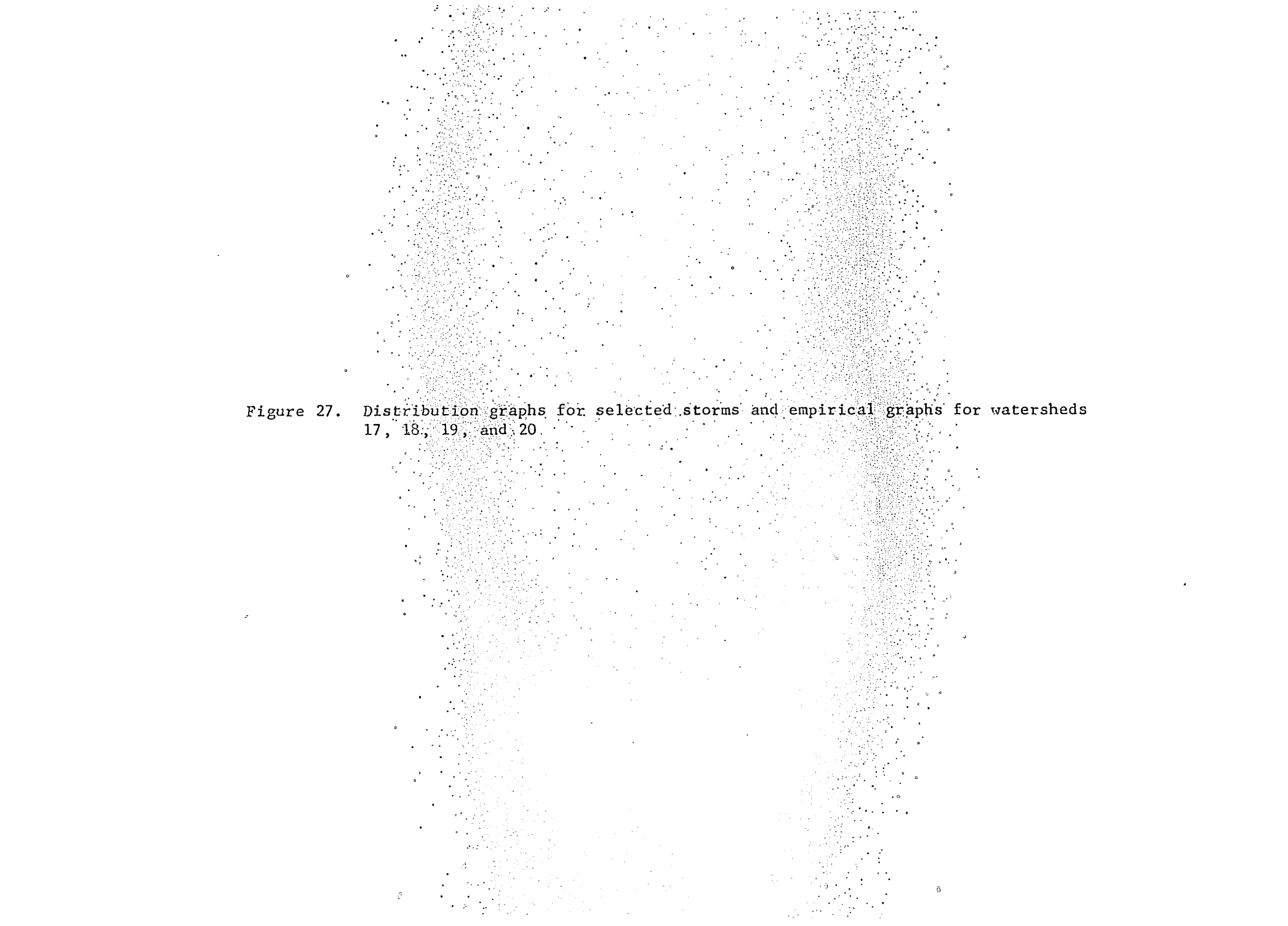

Figure 27. Distribution graphs for selected storms and empirical graphs for watersheds 17, 18, 19, and 20

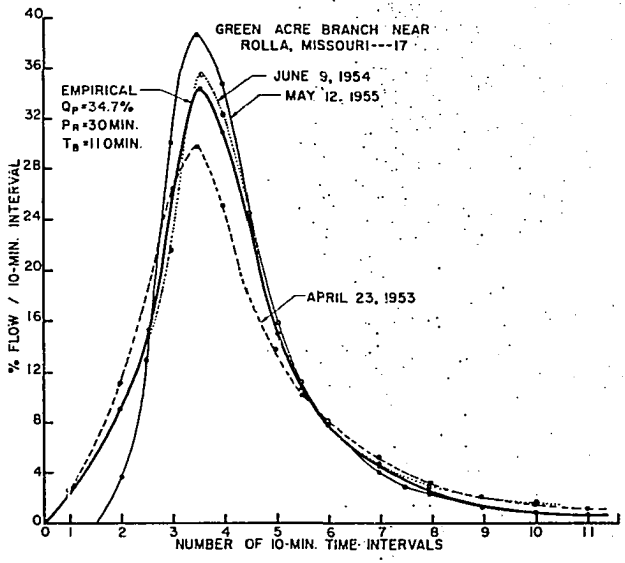
GREEN ACRE BRANCH NEAR
ROLLA, MISSOURI---17
EMPIRICAL
Q_P=34.7%
P_R=30 MIN.
T_B=110 MIN.
JUNE 9, 1954
MAY 12, 1955
APRIL 23, 1953
% FLOW / 10-MIN. INTERVAL
NUMBER OF 10-MIN. TIME INTERVALS

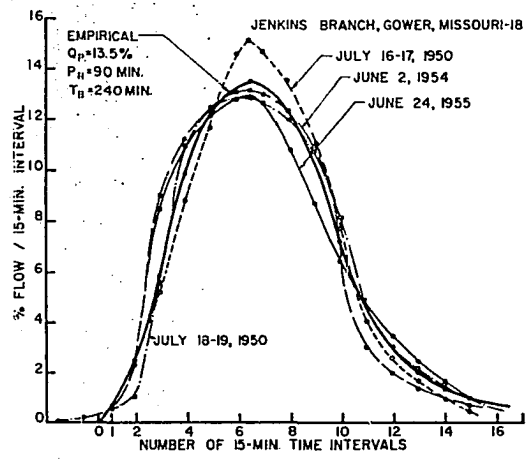
JENKINS BRANCH, GOWER, MISSOURI-18
EMPIRICAL
Q_P=13.5%
P_H=90 MIN.
T_B=240 MIN.
JULY 16-17, 1950
JUNE 2, 1954
JUNE 24, 1955
JULY 18-19, 1950
% FLOW / 15-MIN. INTERVAL
NUMBER OF 15-MIN. TIME INTERVALS

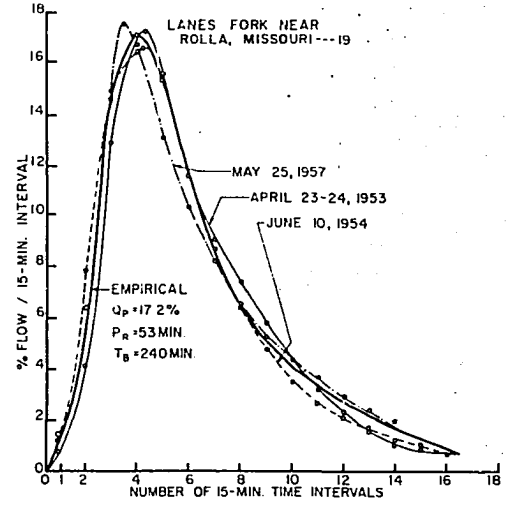
LANES FORK NEAR
ROLLA, MISSOURI---19
MAY 25, 1957
APRIL 23-24, 1953
JUNE 10, 1954
EMPIRICAL
Q_P=17.2%
P_R=53 MIN.
T_B=240 MIN.
% FLOW / 15-MIN. INTERVAL
NUMBER OF 15-MIN. TIME INTERVALS

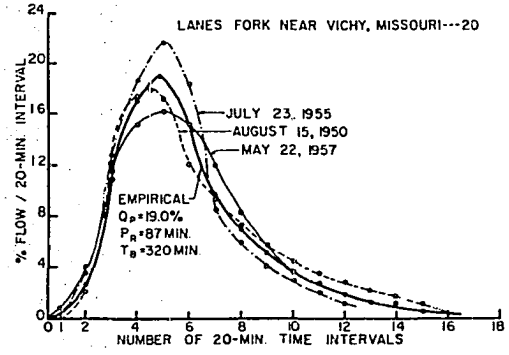
LANES FORK NEAR VICHY, MISSOURI---20
JULY 23, 1955
AUGUST 15, 1950
MAY 22, 1957
EMPIRICAL
Q_P=19.0%
P_R=87 MIN.
T_B=320 MIN.
% FLOW / 20-MIN. INTERVAL
NUMBER OF 20-MIN. TIME INTERVALS

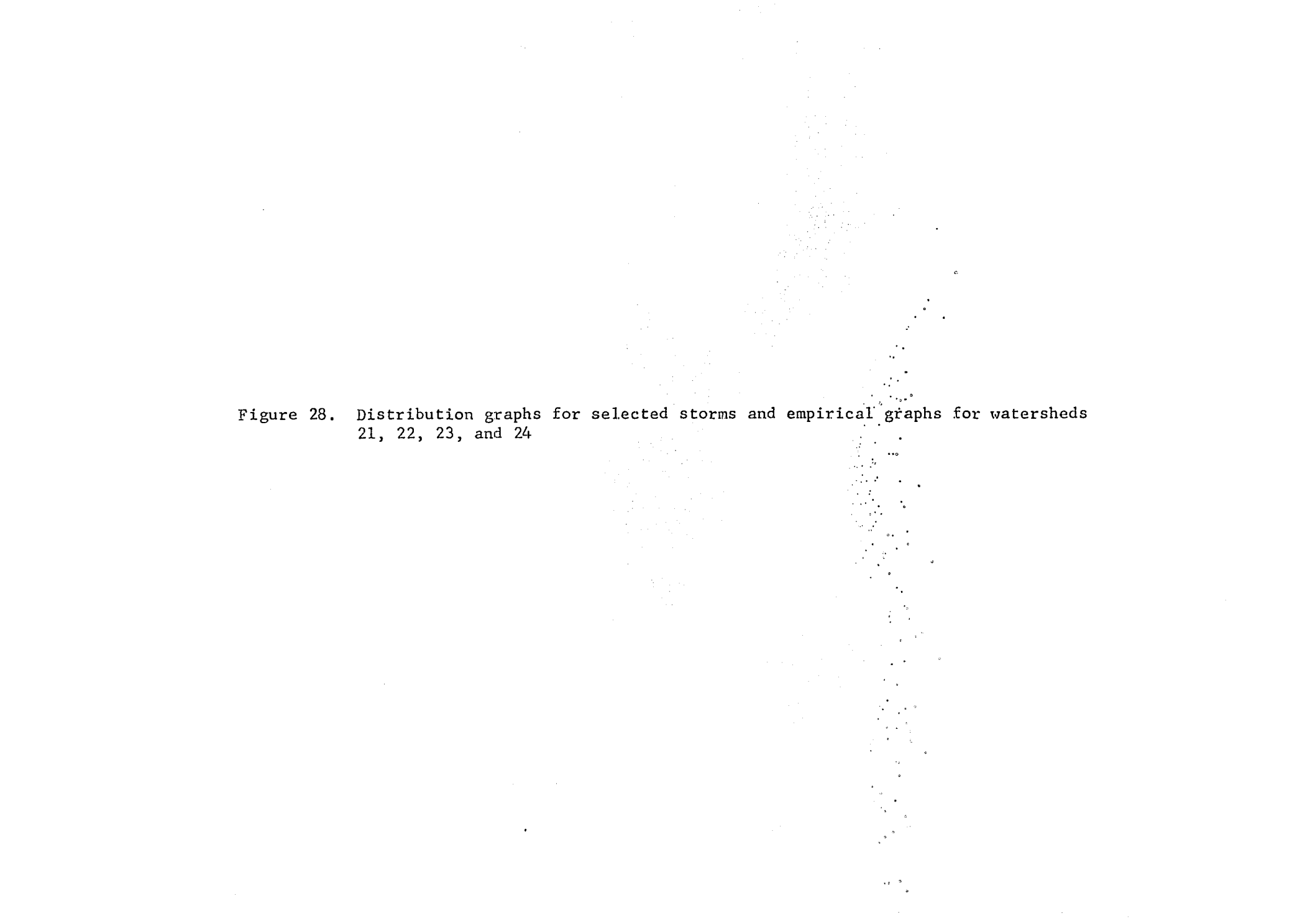

Figure 28. Distribution graphs for selected storms and empirical graphs for watersheds 21, 22, 23, and 24

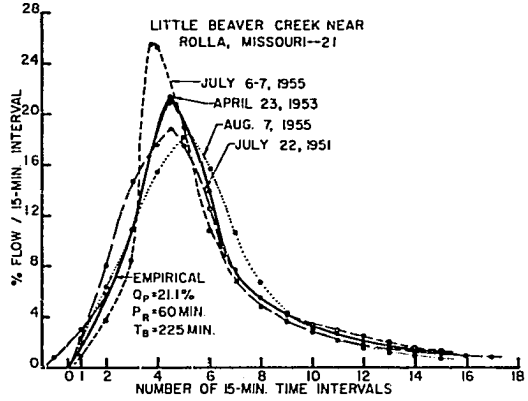
LITTLE BEAVER CREEK NEAR
ROLLA, MISSOURI--21
JULY 6-7, 1955
APRIL 23, 1953
AUG. 7, 1955
JULY 22, 1951
EMPIRICAL
Q_P=21.1%
P_R=60 MIN.
T_B=225 MIN.
% FLOW / 15-MIN. INTERVAL
NUMBER OF 15-MIN. TIME INTERVALS

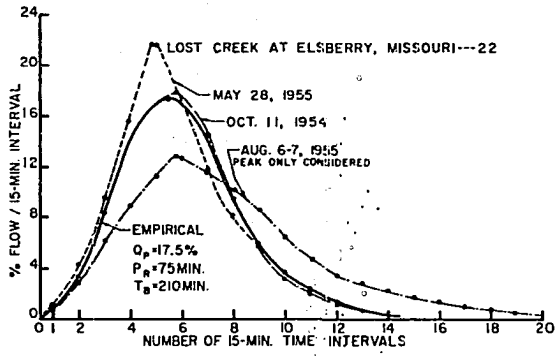
LOST CREEK AT ELSBERRY, MISSOURI---22
MAY 28, 1955
OCT. 11, 1954
AUG. 6-7, 1955
PEAK ONLY CONSIDERED
EMPIRICAL
Q_P=17.5%
P_R=75 MIN.
T_B=210 MIN.
% FLOW / 15-MIN. INTERVAL
NUMBER OF 15-MIN. TIME INTERVALS

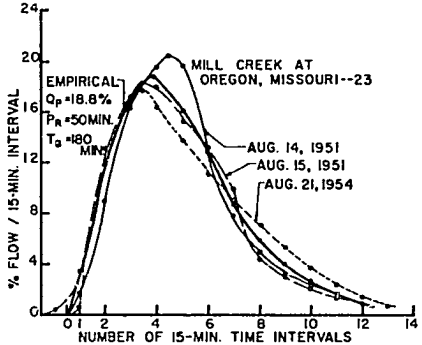
MILL CREEK AT
OREGON, MISSOURI--23
EMPIRICAL
Q_P=18.8%
P_R=50 MIN.
T_B=180 MIN.
AUG. 14, 1951
AUG. 15, 1951
AUG. 21, 1954
% FLOW / 15-MIN. INTERVAL
NUMBER OF 15-MIN. TIME INTERVALS

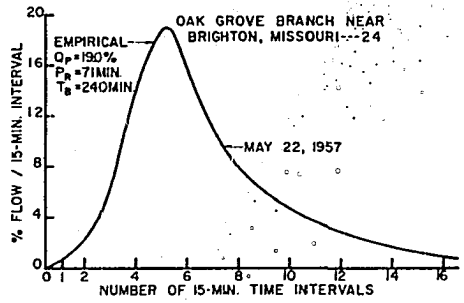
OAK GROVE BRANCH NEAR
BRIGHTON, MISSOURI---24
EMPIRICAL
Q_P=19.0%
P_R=71 MIN.
T_B=240 MIN.
MAY 22, 1957
% FLOW / 15-MIN. INTERVAL
NUMBER OF 15-MIN. TIME INTERVALS

Figure 29. Distribution graphs for selected storms and empirical graphs for watersheds 25, 26, 27, and 28

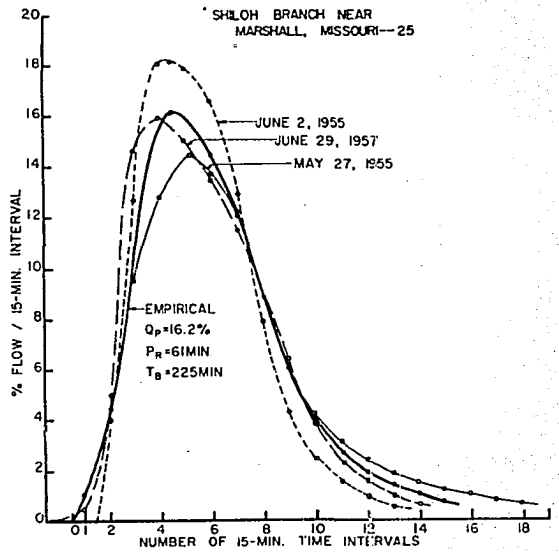
SHILOH BRANCH NEAR
MARSHALL, MISSOURI--25
JUNE 2, 1955
JUNE 29, 1957
MAY 27, 1955
EMPIRICAL
Q_p=16.2%
P_R=61MIN
T_B=225MIN
% FLOW / 15-MIN. INTERVAL
NUMBER OF 15-MIN. TIME INTERVALS

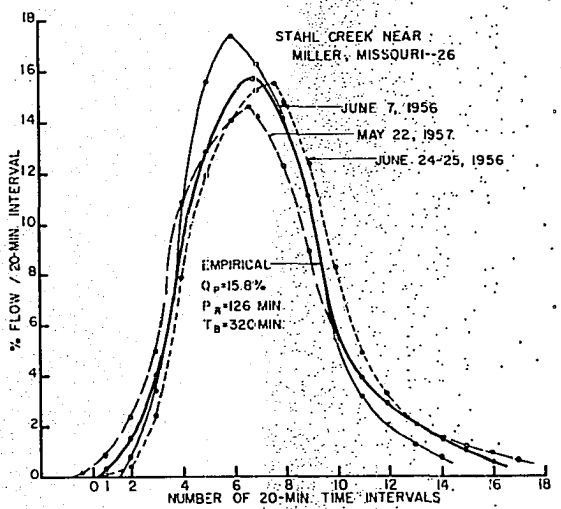
STAHL CREEK NEAR
MILLER, MISSOURI--26
JUNE 7, 1956
MAY 22, 1957
JUNE 24-25, 1956
EMPIRICAL
Q_p=15.8%
P_R=126 MIN.
T_B=320 MIN.
% FLOW / 20-MIN. INTERVAL
NUMBER OF 20-MIN. TIME INTERVALS

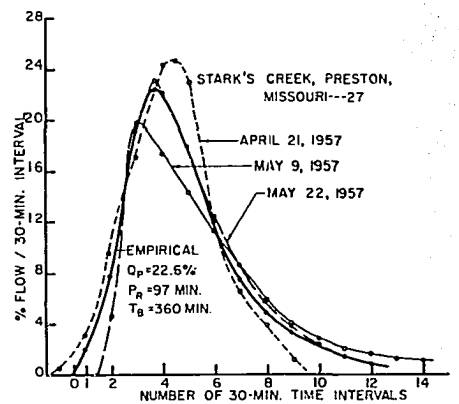
STARK'S CREEK, PRESTON,
MISSOURI---27
APRIL 21, 1957
MAY 9, 1957
MAY 22, 1957
EMPIRICAL
Q_p=22.6%
P_R=97 MIN.
T_B=360 MIN.
% FLOW / 30-MIN. INTERVAL
NUMBER OF 30-MIN. TIME INTERVALS

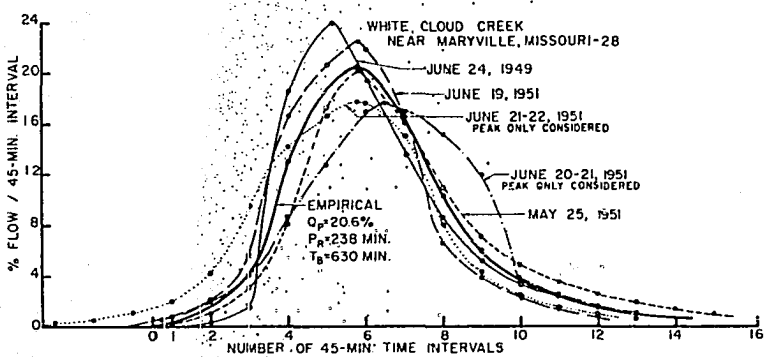
WHITE CLOUD CREEK
NEAR MARYVILLE, MISSOURI-28
JUNE 24, 1949
JUNE 19, 1951
JUNE 21-22, 1951
PEAK ONLY CONSIDERED
JUNE 20-21, 1951
PEAK ONLY CONSIDERED
MAY 25, 1951
EMPIRICAL
Q_p=20.6%
P_R=238 MIN.
T_B=630 MIN.
% FLOW / 45-MIN. INTERVAL
NUMBER OF 45-MIN. TIME INTERVALS

Figure 30. Distribution graphs for selected storms and empirical graphs for watersheds 29, 30, 31, and 32

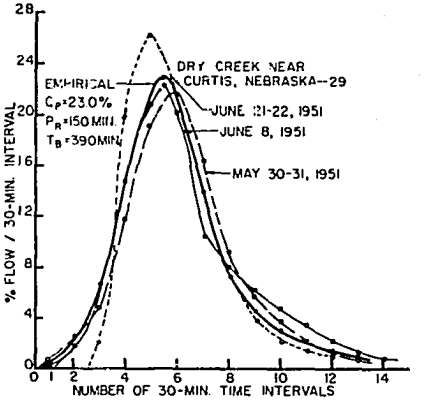
DRY CREEK NEAR CURTIS, NEBRASKA--29
EMPIRICAL
C_p=23.0%
P_R=150 MIN.
T_B=390 MIN.
JUNE 21-22, 1951
JUNE 8, 1951
MAY 30-31, 1951
% FLOW / 30-MIN. INTERVAL
NUMBER OF 30-MIN. TIME INTERVALS

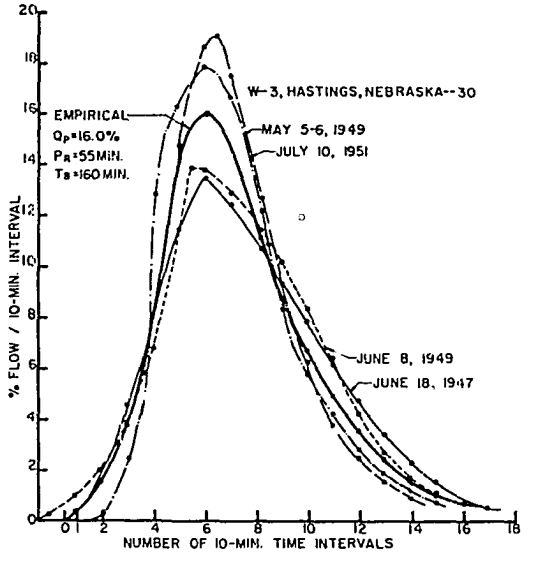
W-3, HASTINGS, NEBRASKA--30
EMPIRICAL
Q_p=16.0%
P_R=55 MIN.
T_B=160 MIN.
MAY 5-6, 1949
JULY 10, 1951
JUNE 8, 1949
JUNE 18, 1947
% FLOW / 10-MIN. INTERVAL
NUMBER OF 10-MIN. TIME INTERVALS

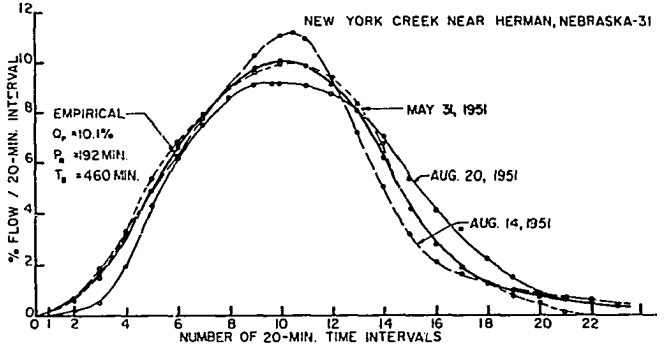
NEW YORK CREEK NEAR HERMAN, NEBRASKA-31
EMPIRICAL
Q_p=10.1%
P_R=192 MIN.
T_B=460 MIN.
MAY 31, 1951
AUG. 20, 1951
AUG. 14, 1951
% FLOW / 20-MIN. INTERVAL
NUMBER OF 20-MIN. TIME INTERVALS

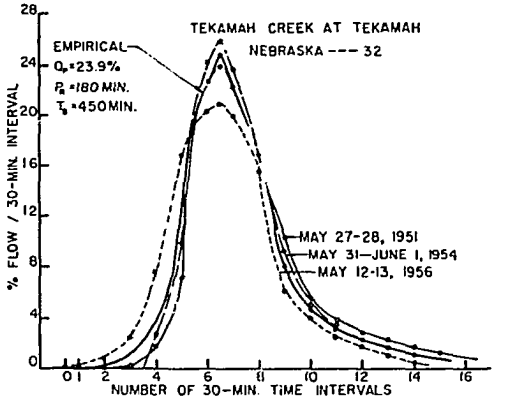
TEKAMAH CREEK AT TEKAMAH NEBRASKA --- 32
EMPIRICAL
Q_p=23.9%
P_R=180 MIN.
T_B=450 MIN.
MAY 27-28, 1951
MAY 31—JUNE 1, 1954
MAY 12-13, 1956
% FLOW / 30-MIN. INTERVAL
NUMBER OF 30-MIN. TIME INTERVALS

Figure 31. Distribution graphs for selected storms and empirical graphs for watersheds 33, 34, 35, and 36

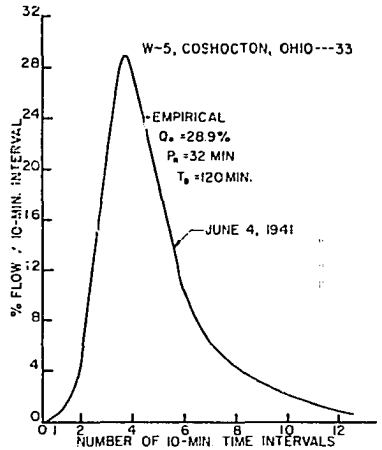
W-5, COSHOCTON, OHIO---33
EMPIRICAL
Q_p =28.9%
P_R =32 MIN
T_B =120 MIN.
JUNE 4, 1941
% FLOW / 10-MIN. INTERVAL
NUMBER OF 10-MIN. TIME INTERVALS

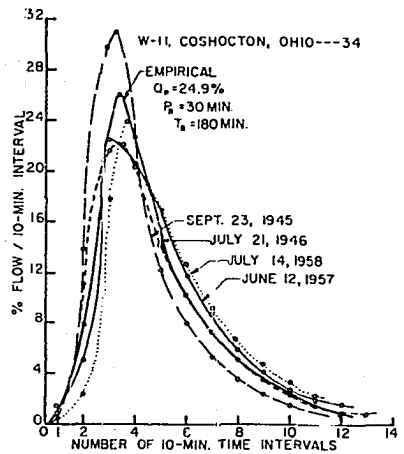
W-11, COSHOCTON, OHIO---34
EMPIRICAL
Q_p =24.9%
P_R =30 MIN.
T_B =180 MIN.
SEPT. 23, 1945
JULY 21, 1946
JULY 14, 1958
JUNE 12, 1957
% FLOW / 10-MIN. INTERVAL
NUMBER OF 10-MIN. TIME INTERVALS

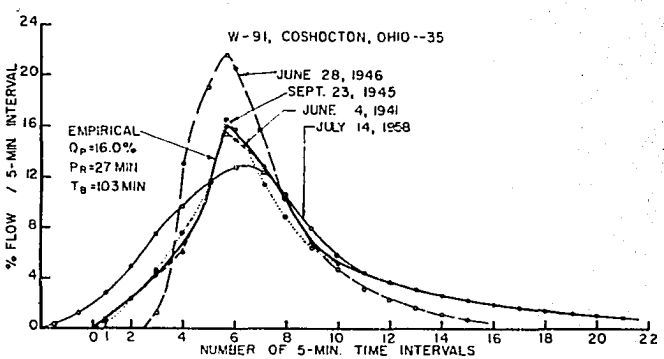
W-91, COSHOCTON, OHIO--35
JUNE 28, 1946
SEPT. 23, 1945
JUNE 4, 1941
JULY 14, 1958
EMPIRICAL
Q_p =16.0%
P_R =27 MIN
T_B =103 MIN
% FLOW / 5-MIN INTERVAL
NUMBER OF 5-MIN. TIME INTERVALS

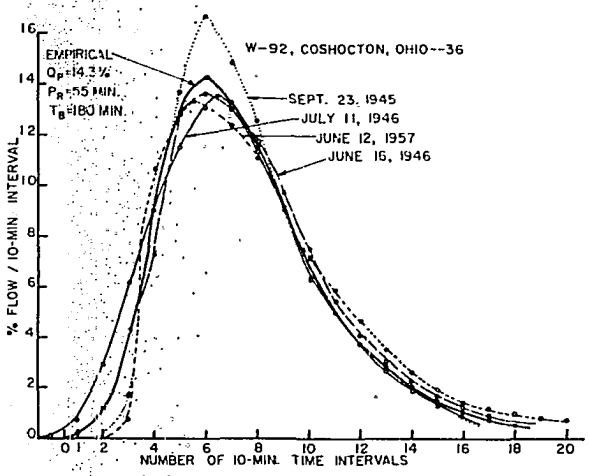
W-92, COSHOCTON, OHIO--36
EMPIRICAL
Q_p =14.3%
P_R =55 MIN.
T_B =180 MIN.
SEPT. 23, 1945
JULY 11, 1946
JUNE 12, 1957
JUNE 16, 1946
% FLOW / 10-MIN. INTERVAL
NUMBER OF 10-MIN. TIME INTERVALS

Figure 32. Distribution graphs for selected storms and empirical graphs for watersheds 37, 38, 39, and 40

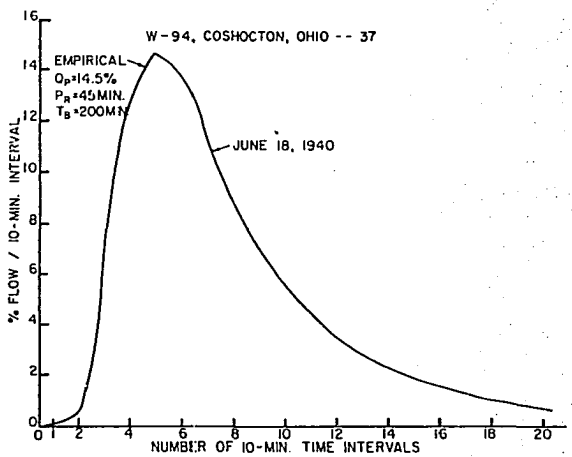
W-94, COSHOCTON, OHIO -- 37
EMPIRICAL
Q_P=14.5%
P_R=45MIN.
T_B=200MIN.
JUNE 18, 1940
% FLOW / 10-MIN. INTERVAL
NUMBER OF 10-MIN. TIME INTERVALS

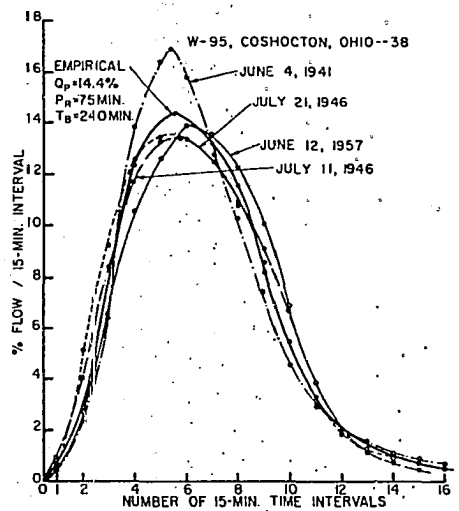
W-95, COSHOCTON, OHIO--38
EMPIRICAL
Q_P=14.4%
P_R=75MIN.
T_B=240MIN.
JUNE 4, 1941
JULY 21, 1946
JUNE 12, 1957
JULY 11, 1946
% FLOW / 15-MIN. INTERVAL
NUMBER OF 15-MIN. TIME INTERVALS

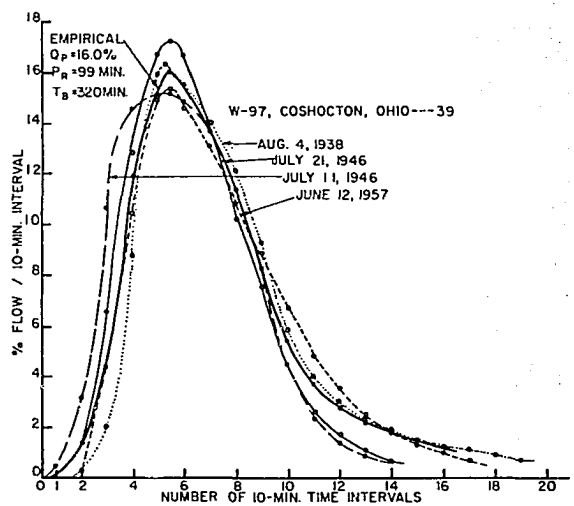
EMPIRICAL
Q_P=16.0%
P_R=99 MIN.
T_B=320MIN.
W-97, COSHOCTON, OHIO---39
AUG. 4, 1938
JULY 21, 1946
JULY 11, 1946
JUNE 12, 1957
% FLOW / 10-MIN. INTERVAL
NUMBER OF 10-MIN. TIME INTERVALS

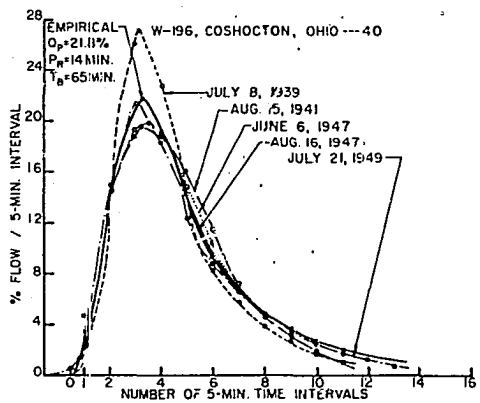
EMPIRICAL
Q_P=21.1%
P_R=14MIN.
T_B=65MIN.
W-196, COSHOCTON, OHIO---40
JULY 8, 1939
AUG. 15, 1941
JUNE 6, 1947
AUG. 16, 1947
JULY 21, 1949
% FLOW / 5-MIN. INTERVAL
NUMBER OF 5-MIN. TIME INTERVALS

Figure 33. Distribution graphs for selected storms and empirical graphs for watersheds 41 and 42

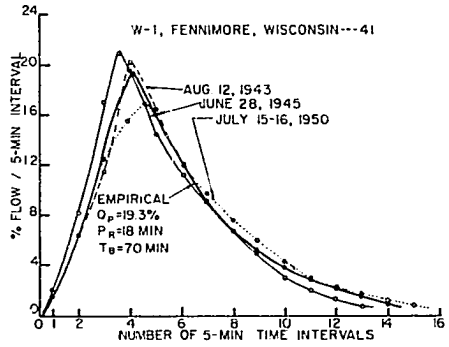
W-1, FENNIMORE, WISCONSIN---41
AUG 12, 1943
JUNE 28, 1945
JULY 15-16, 1950
EMPIRICAL
Q_P=19.3%
P_R=18 MIN
T_B=70 MIN
% FLOW / 5-MIN INTERVAL
NUMBER OF 5-MIN TIME INTERVALS

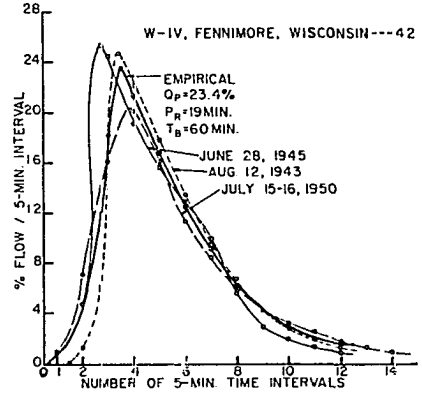
W-IV, FENNIMORE, WISCONSIN---42
EMPIRICAL
Q_P=23.4%
P_R=19MIN.
T_B=60MIN.
JUNE 28, 1945
AUG 12, 1943
JULY 15-16, 1950
% FLOW / 5-MIN INTERVAL
NUMBER OF 5-MIN. TIME INTERVALS

APPENDIX E: DIMENSIONLESS GRAPHS

Determination of the "Best-Fit" Two-Parameter Gamma Distribution Describing the Dimensionless Graphs

With the particular program employed, the input capacity of the IBM 650 was restricted to 999 numbers of 10 digits or less. In order to accommodate the entire capacity, the following procedures were applied to the dimensionless graphs of each of the 42 watersheds included in this study.

1. The ordinate values of Q_1, Q_2, Q_3, Q_4, ... Q_n, expressed in % flow/$0.25P_R$, for the respective increments, $t/P_R = 0.125$, along the base of the dimensionless graph were listed and summed. This sum must be 200 percent because the number of abscissa values chosen has been doubled. A dimensionless graph expressed in this manner may be represented as a histogram as shown in Figure 34.
2. The ordinate values given in 1 above were increased by a multiple of five, to give a sum of 1,000 percent.
3. Each value of the ratio, t/P_R, was punched on the predetermined number of IBM cards given by the ordinate value in 2 above. The correction for odd values of the ordinates, for example, 14.5 percent, was accomplished by placing 14 cards of the respective t/P_R-value into the distribution and placing an additional card of the value, t/P_R, for the next odd ordinate nearest the peak. A card from the group for the largest recorded value of t/P_R was removed to reduce the deck to 999 cards.

Figure 34. Dimensionless graph of watershed 19 as a histogram

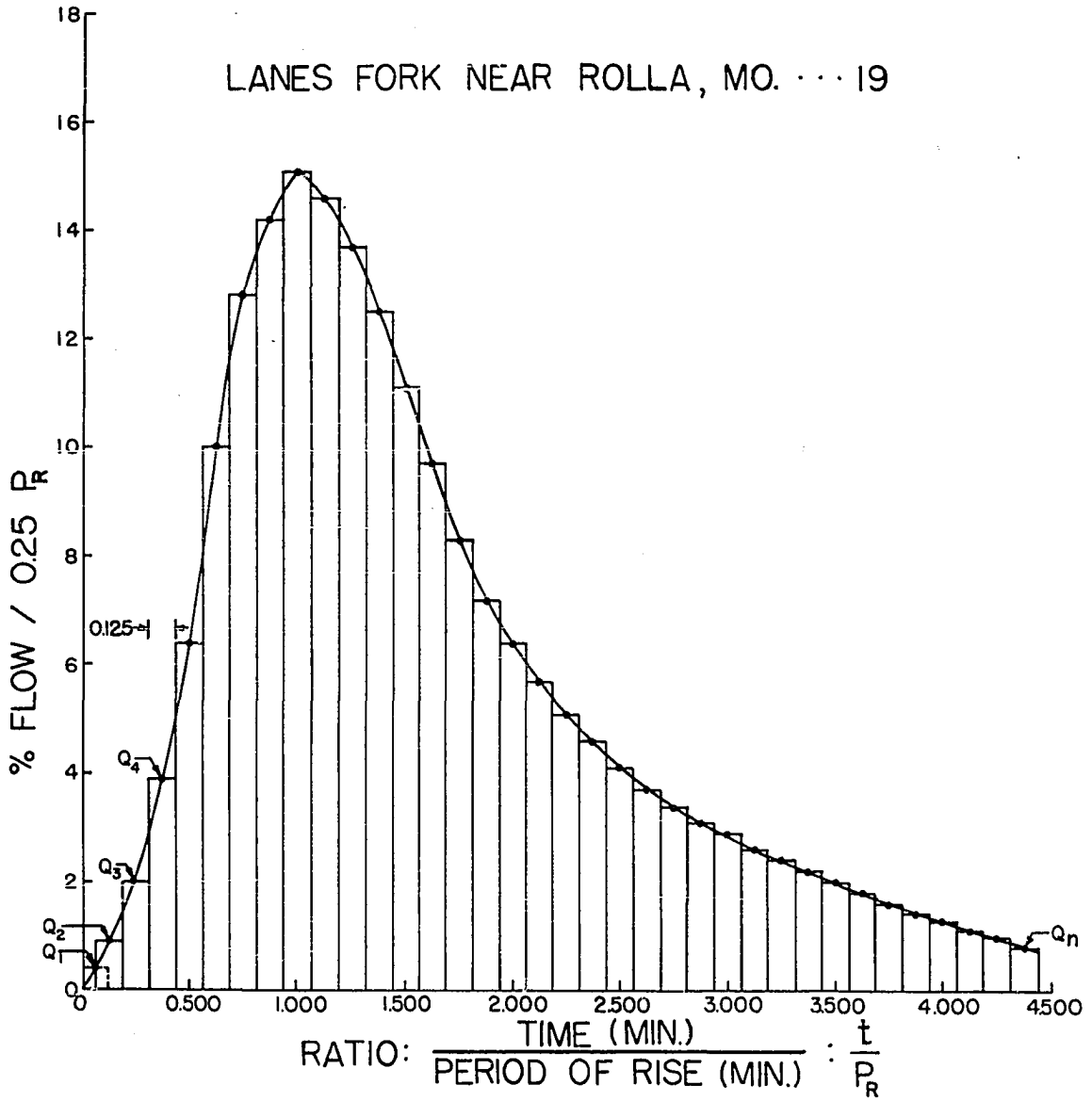
LANES FORK NEAR ROLLA, MO. · · · 19
% FLOW / 0.25 P_R
0.125
Q_1
Q_2
Q_3
Q_4
Q_n
0
2
4
6
8
10
12
14
16
18
0.500
1.000
1.500
2.000
2.500
3.000
3.500
4.000
4.500
RATIO: $\frac{\text{TIME (MIN.)}}{\text{PERIOD OF RISE (MIN.)}} : \frac{t}{P_R}$

4. The punched cards were then introduced to the IBM 650 and the estimators of the parameters, γ', q and $\bar{t}/P_R$ obtained.

Before finalizing the results, an additional factor must be considered. A basic hypothesis in fitting the data required that the areas enclosed by the dimensionless graph and the theoretical distribution be equivalent. Since the area enclosed by the gamma distribution is unity, it is necessary to include the appropriate value of N in Equation 14c to obtain the desired result. The evaluation of the constant was accomplished in the following manner

1. Approximate area, A_D, bounded by a dimensionless graph.

$$A_D = (Q_1/2)(0.083) + (Q_2)(0.125) + (Q_3)(0.125) + (Q_4)(0.125) \cdots$$

$$\cdots\cdots\cdots + (Q_n)(0.125)$$

$$A_D = (Q_1/2)(0.083) + 0.125 \sum_{n=2}^{n} Q_n \,. \qquad (32a)$$

For practical work, only small error will be introduced if it is assumed,

$$(Q_1/2)(0.083) \cong 0.125\ Q_1$$

therefore, Equation 32a reduces to

$$A_D \cong 0.125 \sum_{n=1}^{n} Q_n \,. \qquad (32b)$$

But,

$$\sum_{n=1}^{n} Q_n = 200 \text{ percent.} \qquad (32c)$$

Substituting Equation 32c into Equation 32b, it follows

$A_D \cong 25.0$ percent.

2. Area bounded by the two-parameter gamma distribution of the dimensionless graph, A_G (see Equation 14c).

$$A_G = N \int_{t/P_R=0}^{\infty} \frac{(\gamma')^q}{\Gamma(q)} e^{-\gamma' t/P_R} \left(t/P_R\right)^{q-1} d(t/P_R)$$

But

$$\int_{t/P_R=0}^{\infty} \frac{(\gamma')^q}{\Gamma(q)} e^{-\gamma' t/P_R} \left(t/P_R\right)^{q-1} d(t/P_R) = 1 .$$

It follows that for A_D to be equal to A_G, the constant, N, of the two-parameter gamma distribution must have a numerical value of 25.0 percent.

On the plotted figures (see Figures 35-45), the theoretical curves have been given a finite maximum value of t/P_R. Obviously, this is not theoretically correct because the distribution is defined by the integral from $t/P_R = 0$ to $t/P_R = \infty$. The volume of flow occurring beyond these maximum values is usually very small, however, and in part has been compensated for by the increased value of the constant.

Figure 35. Dimensionless graphs and fitted two-parameter gamma distributions for watersheds 1, 2, 3, and 4

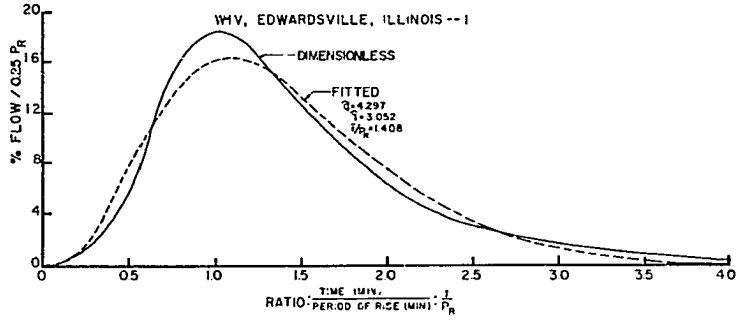
WHV, EDWARDSVILLE, ILLINOIS--1
DIMENSIONLESS
FITTED
q̄=4.297
t̄=3.052
t̄/tR=1.408
% FLOW / 0.25 PR
RATIO: TIME (MIN.) / PERIOD OF RISE (MIN) : 1/PR

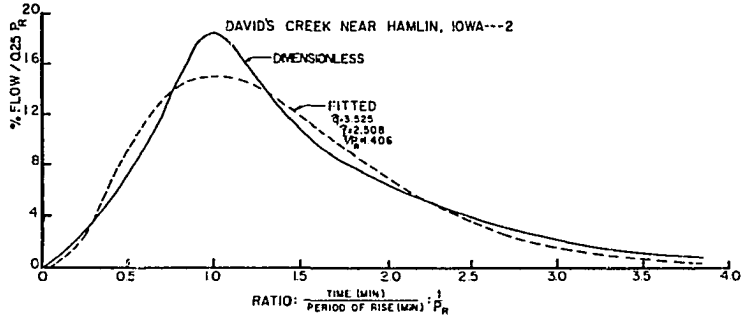
DAVID'S CREEK NEAR HAMLIN, IOWA---2
DIMENSIONLESS
FITTED
q̄=3.525
t̄=2.508
t̄/tR=1.406
% FLOW / 0.25 PR
RATIO: TIME (MIN) / PERIOD OF RISE (MIN) : 1/PR

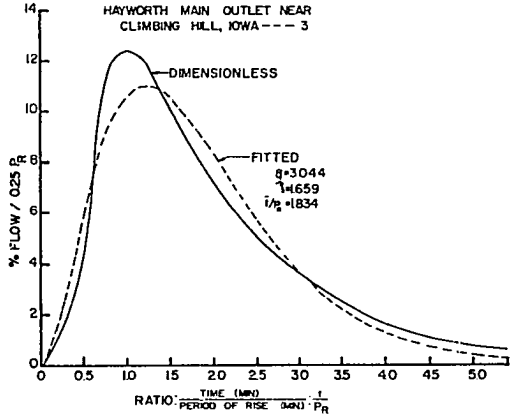
HAYWORTH MAIN OUTLET NEAR
CLIMBING HILL, IOWA--- 3
DIMENSIONLESS
FITTED
q̄=3044
t̄=1659
t̄/tR=1834
% FLOW / 0.25 PR
RATIO: TIME (MIN) / PERIOD OF RISE (MIN) : 1/PR

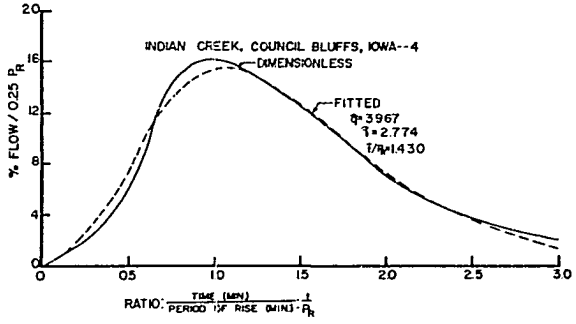
INDIAN CREEK, COUNCIL BLUFFS, IOWA--4
DIMENSIONLESS
FITTED
q̄=3967
t̄=2.774
t̄/tR=1.430
% FLOW / 0.25 PR
RATIO: TIME (MIN) / PERIOD OF RISE (MIN) : 1/PR

Figure 36. Dimensionless graphs and fitted two-parameter gamma distributions for watersheds 5, 6, 7, and 8

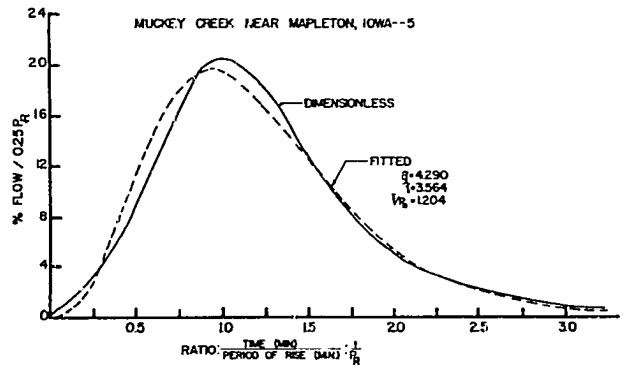
MUCKEY CREEK NEAR MAPLETON, IOWA--5
DIMENSIONLESS
FITTED
q=4.290
τ=3.564
1/β=1.204
% FLOW / 0.25 P_R
RATIO: TIME (MIN) / PERIOD OF RISE (MIN) · 1/P_R

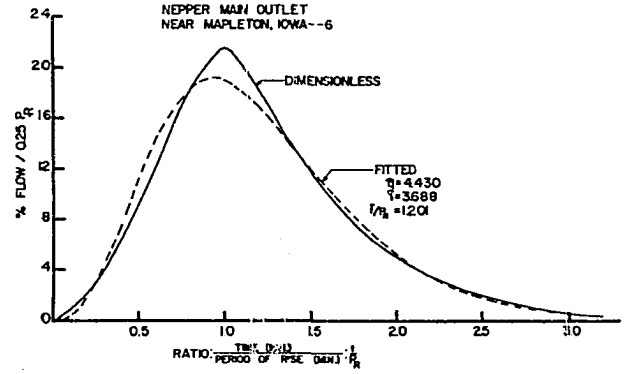
NEPPER MAIN OUTLET
NEAR MAPLETON, IOWA--6
DIMENSIONLESS
FITTED
q=4.430
τ=3.688
1/β=1.201
% FLOW / 0.25 P_R
RATIO: TIME (MIN) / PERIOD OF RISE (MIN) · 1/P_R

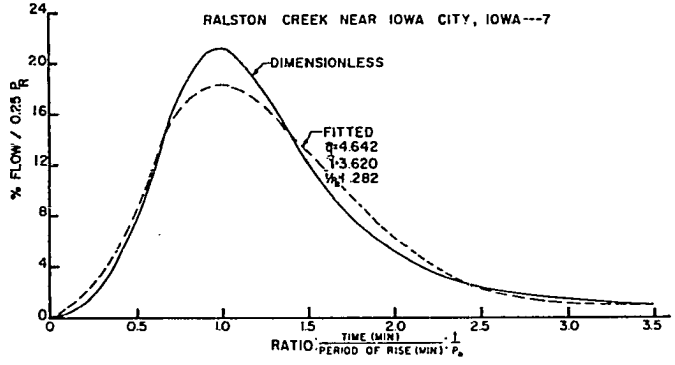
RALSTON CREEK NEAR IOWA CITY, IOWA---7
DIMENSIONLESS
FITTED
q=4.642
τ=3.620
1/β=1.282
% FLOW / 0.25 P_R
RATIO: TIME (MIN) / PERIOD OF RISE (MIN) · 1/P_R

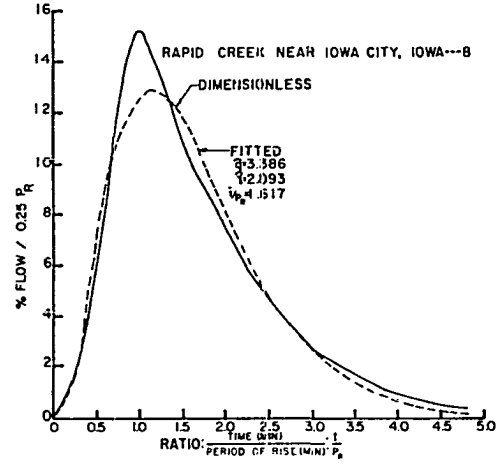
RAPID CREEK NEAR IOWA CITY, IOWA---8
DIMENSIONLESS
FITTED
q=3.386
τ=2.093
1/β=1.517
% FLOW / 0.25 P_R
RATIO: TIME (MIN) / PERIOD OF RISE (MIN) · 1/P_R

Figure 37. Dimensionless graphs and fitted two-parameter gamma distributions for watersheds 9, 10, 11, and 12

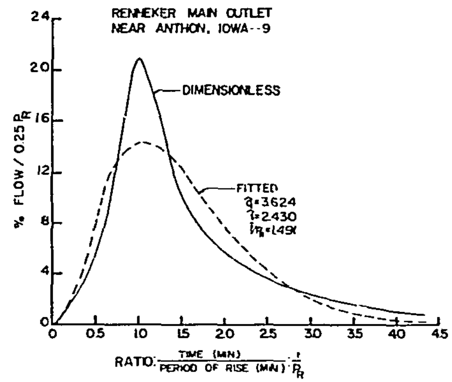
RENNEKER MAIN OUTLET
NEAR ANTHON, IOWA--9
DIMENSIONLESS
FITTED
% FLOW / 0.25 P_R
RATIO: TIME (MIN) / PERIOD OF RISE (MIN) : t / P_R

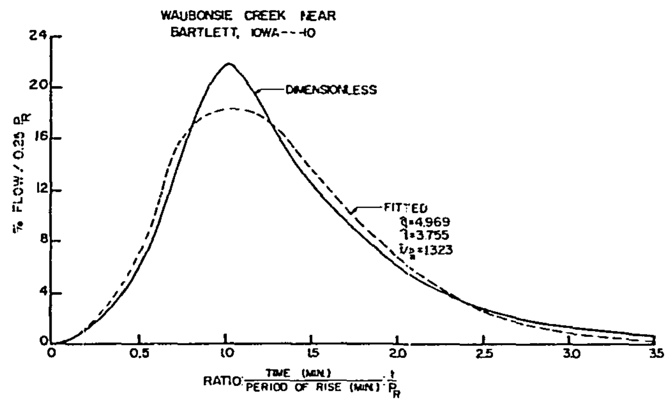
WAUBONSIE CREEK NEAR
BARTLETT, IOWA--40
DIMENSIONLESS
FITTED
% FLOW / 0.25 P_R
RATIO: TIME (MIN) / PERIOD OF RISE (MIN) : t / P_R

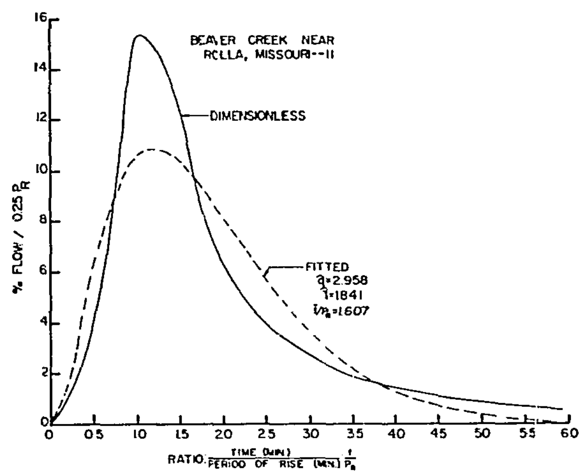
BEAVER CREEK NEAR
ROLLA, MISSOURI--11
DIMENSIONLESS
FITTED
% FLOW / 0.25 P_R
RATIO: TIME (MIN) / PERIOD OF RISE (MIN) : t / P_R

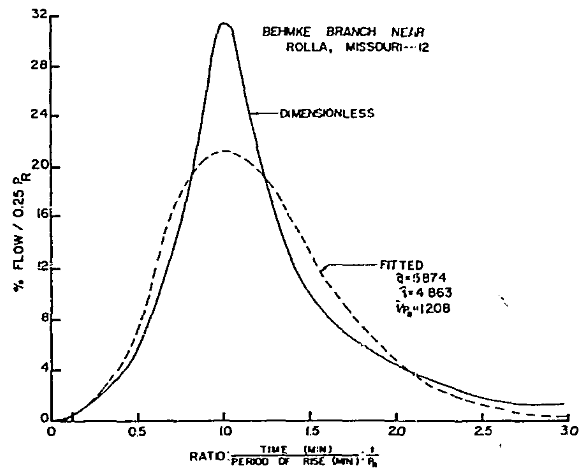
BEHMKE BRANCH NEAR
ROLLA, MISSOURI--12
DIMENSIONLESS
FITTED
% FLOW / 0.25 P_R
RATIO: TIME (MIN) / PERIOD OF RISE (MIN) : t / P_R

Figure 38. Dimensionless graphs and fitted two-parameter gamma distributions for watersheds 13,14, 15 and 16

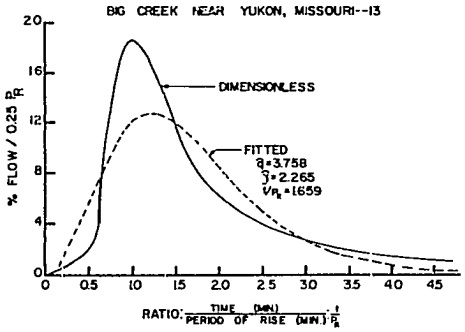
BIG CREEK NEAR YUKON, MISSOURI--13
DIMENSIONLESS
FITTED
% FLOW / 0.25 P_R
RATIO: $\frac{\text{TIME (MIN)}}{\text{PERIOD OF RISE (MIN.)}} \cdot \frac{1}{P_R}$

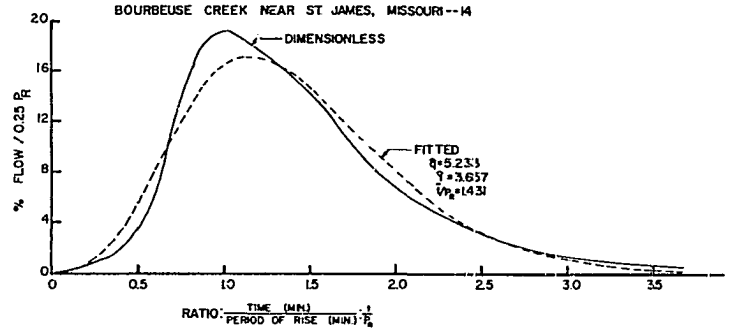
BOURBEUSE CREEK NEAR ST JAMES, MISSOURI--14
DIMENSIONLESS
FITTED
% FLOW / 0.25 P_R
RATIO: $\frac{\text{TIME (MIN)}}{\text{PERIOD OF RISE (MIN.)}} \cdot \frac{1}{P_R}$

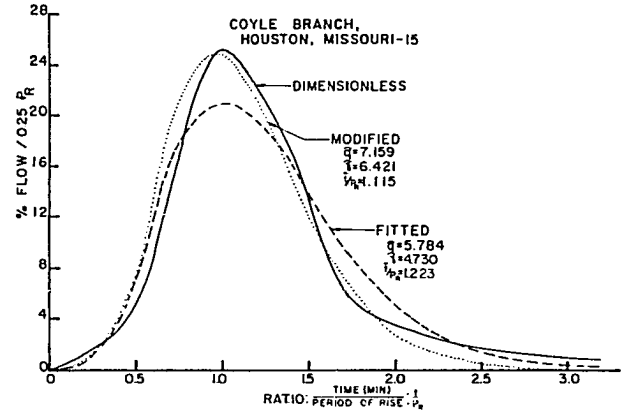
COYLE BRANCH,
HOUSTON, MISSOURI-15
DIMENSIONLESS
MODIFIED
FITTED
% FLOW / 0.25 P_R
RATIO: $\frac{\text{TIME (MIN)}}{\text{PERIOD OF RISE}} \cdot \frac{1}{P_R}$

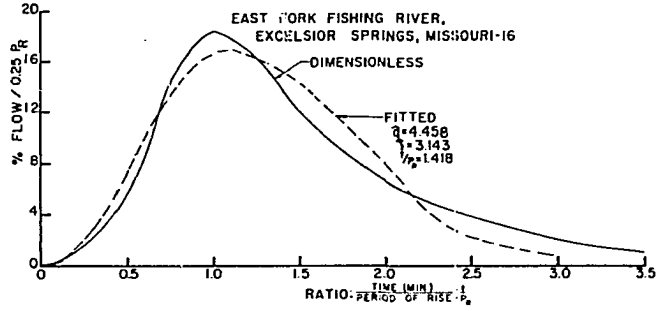
EAST FORK FISHING RIVER,
EXCELSIOR SPRINGS, MISSOURI-16
DIMENSIONLESS
FITTED
% FLOW / 0.25 P_R
RATIO: $\frac{\text{TIME (MIN)}}{\text{PERIOD OF RISE}} \cdot \frac{1}{P_R}$

Figure 39. Dimensionless graphs and fitted two-parameter gamma distributions for watersheds 17, 18, 19, and 20

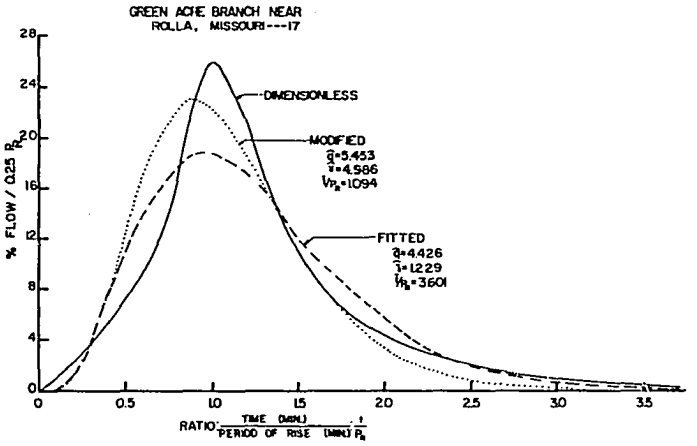
GREEN ACRE BRANCH NEAR
ROLLA, MISSOURI---17
DIMENSIONLESS
MODIFIED
FITTED
% FLOW / 0.25 R_R
RATIO: TIME (MIN) / PERIOD OF RISE (MIN) R_R

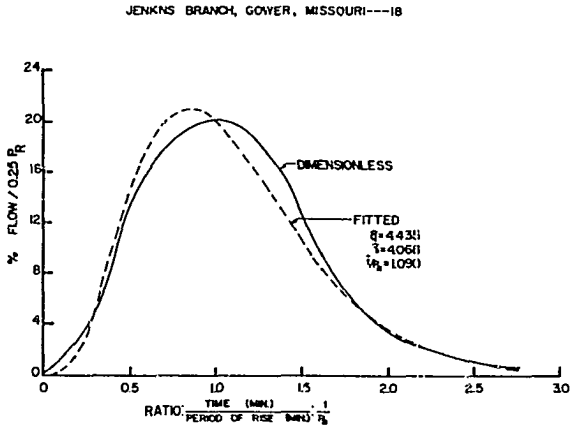
JENKNS BRANCH, GOWER, MISSOURI---18
DIMENSIONLESS
FITTED
% FLOW / 0.25 R_R
RATIO: TIME (MIN) / PERIOD OF RISE (MIN) R_R

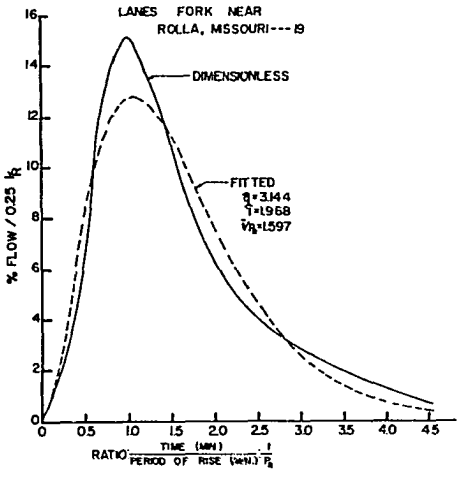
LANES FORK NEAR
ROLLA, MISSOURI---19
DIMENSIONLESS
FITTED
% FLOW / 0.25 R_R
RATIO: TIME (MIN) / PERIOD OF RISE (MIN) R_R

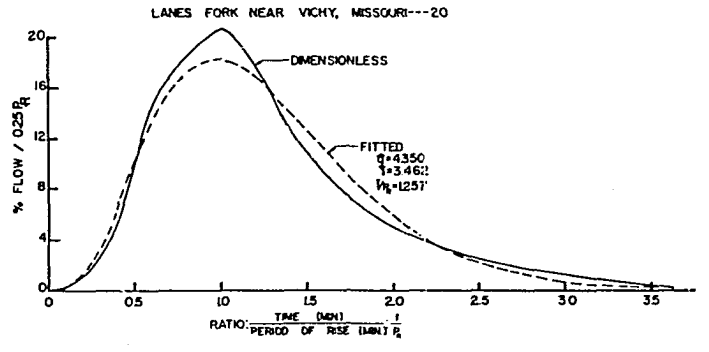
LANES FORK NEAR VICHY, MISSOURI---20
DIMENSIONLESS
FITTED
% FLOW / 0.25 R_R
RATIO: TIME (MIN) / PERIOD OF RISE (MIN) R_R

Figure 40. Dimensionless graphs and fitted two-parameter gamma distributions for watersheds 21, 22, 23, and 24

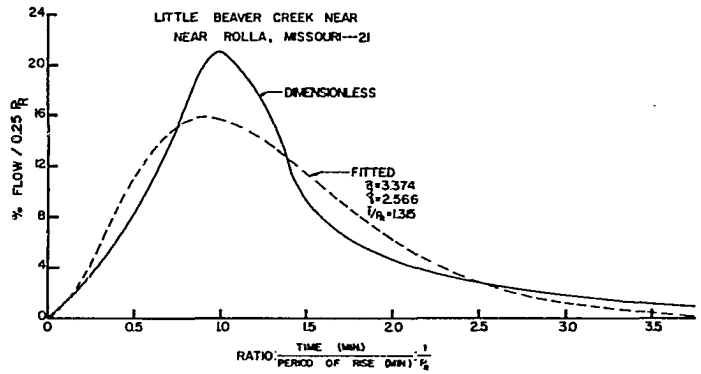
LITTLE BEAVER CREEK NEAR
NEAR ROLLA, MISSOURI---21
DIMENSIONLESS
FITTED
β=3.374
γ=2.566
t/t_R=1.36
% FLOW / 0.25 R_t
RATIO: TIME (MIN) / PERIOD OF RISE (MIN) · 1/t_R

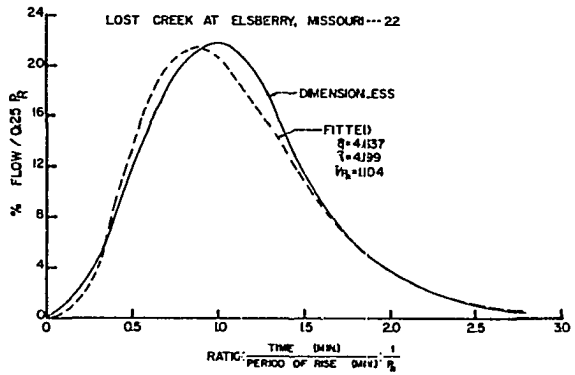
LOST CREEK AT ELSBERRY, MISSOURI--- 22
DIMENSIONLESS
FITTED
β=4.137
γ=4.199
t/t_R=1.104
% FLOW / 0.25 R_t
RATIO: TIME (MIN) / PERIOD OF RISE (MIN) · 1/t_R

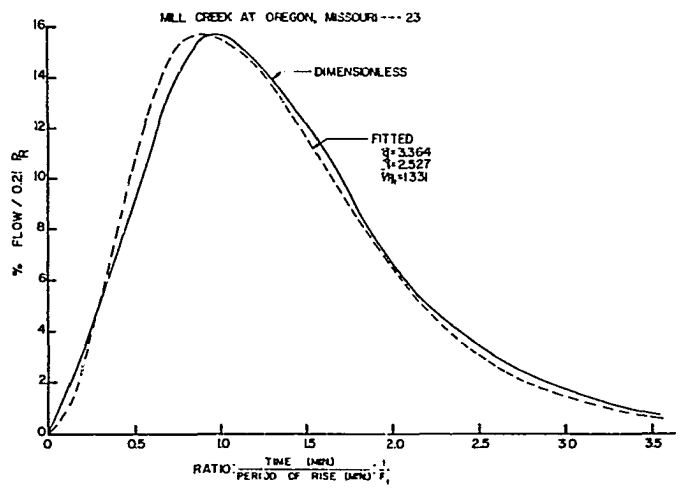
MILL CREEK AT OREGON, MISSOURI --- 23
DIMENSIONLESS
FITTED
β=3.364
γ=2.327
t/t_R=1.331
% FLOW / 0.21 R_t
RATIO: TIME (MIN) / PERIOD OF RISE (MIN) · 1/t_R

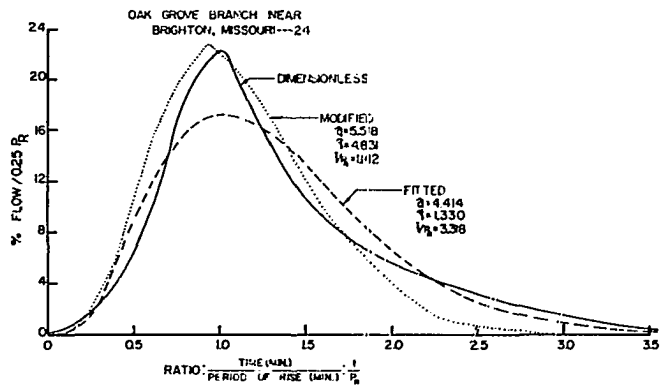
OAK GROVE BRANCH NEAR
BRIGHTON, MISSOURI---24
DIMENSIONLESS
MODIFIED
β=5.518
γ=4.831
t/t_R=1.112
FITTED
β=4.414
γ=1.330
t/t_R=3.38
% FLOW / 0.25 R_t
RATIO: TIME (MIN) / PERIOD OF RISE (MIN) · 1/t_R

Figure 41. Dimensionless graphs and fitted two-parameter gamma distributions for watersheds 25, 26, 27, and 28

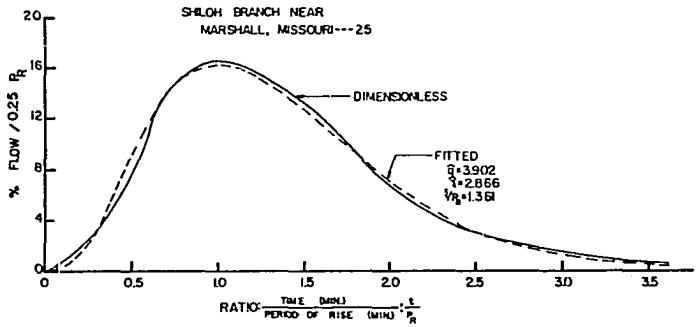
SHILOH BRANCH NEAR
MARSHALL, MISSOURI---25
DIMENSIONLESS
FITTED
a=3.902
λ=2.866
½=1.361
% FLOW / 0.25 QR
RATIO: TIME (MIN) / PERIOD OF RISE (MIN) : t/tR

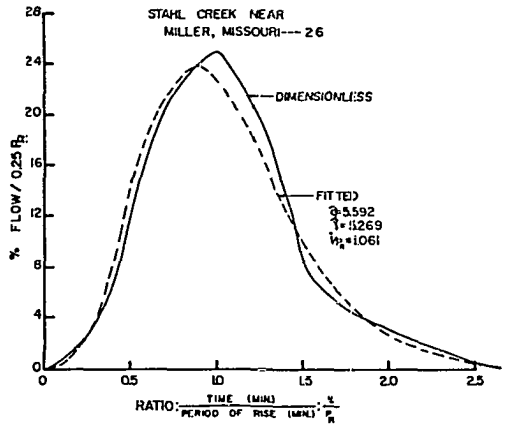
STAHL CREEK NEAR
MILLER, MISSOURI---26
DIMENSIONLESS
FITTED
a=5.592
λ=1.269
½=1.061
% FLOW / 0.25 QR
RATIO: TIME (MIN) / PERIOD OF RISE (MIN) : t/tR

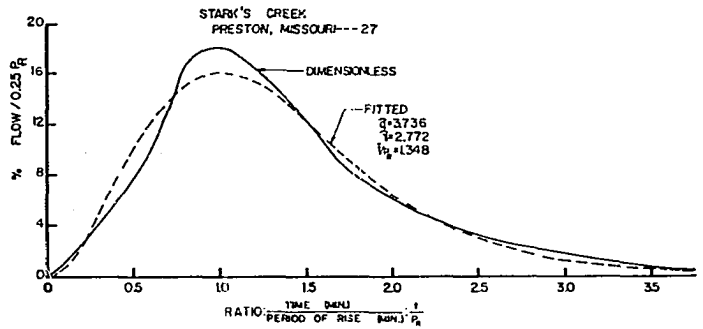
STARK'S CREEK
PRESTON, MISSOURI---27
DIMENSIONLESS
FITTED
a=3.736
λ=2.772
½=1.348
% FLOW / 0.25 QR
RATIO: TIME (MIN) / PERIOD OF RISE (MIN) : t/tR

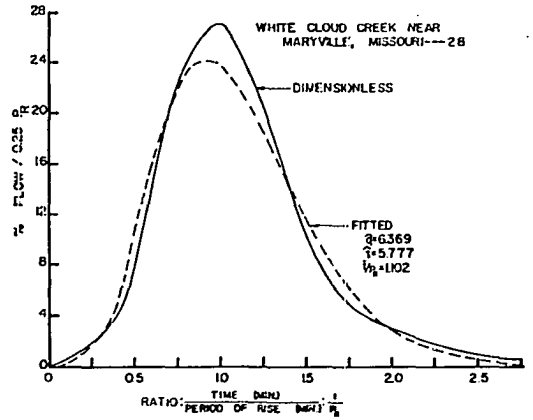
WHITE CLOUD CREEK NEAR
MARYVILLE, MISSOURI---28
DIMENSIONLESS
FITTED
a=6.369
λ=5.777
½=1.102
% FLOW / 0.25 QR
RATIO: TIME (MIN) / PERIOD OF RISE (MIN) : t/tR

Figure 42. Dimensionless graphs and fitted two-parameter gamma distributions for watersheds 29, 30, 31, and 32

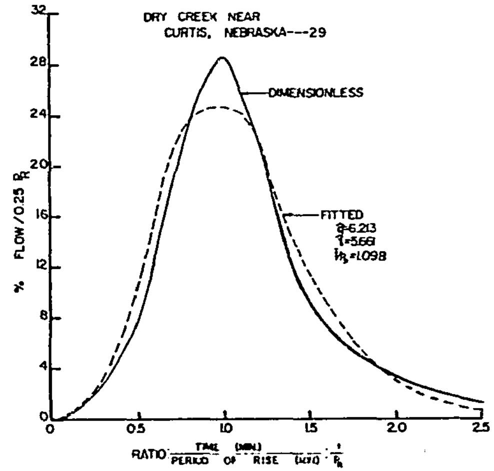
DRY CREEK NEAR
CURTIS, NEBRASKA---29
DIMENSIONLESS
FITTED
β=6.213
γ=5.661
t/t_R=1.098
% FLOW / 0.25 P_R
RATIO: TIME (MIN.) / PERIOD OF RISE (MIN.) : t/P_R

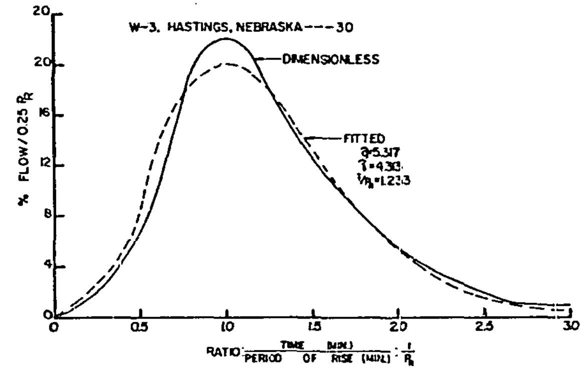
W-3, HASTINGS, NEBRASKA---30
DIMENSIONLESS
FITTED
β=5.317
γ=4.33
t/t_R=1.233
% FLOW / 0.25 P_R
RATIO: TIME (MIN.) / PERIOD OF RISE (MIN.) : t/P_R

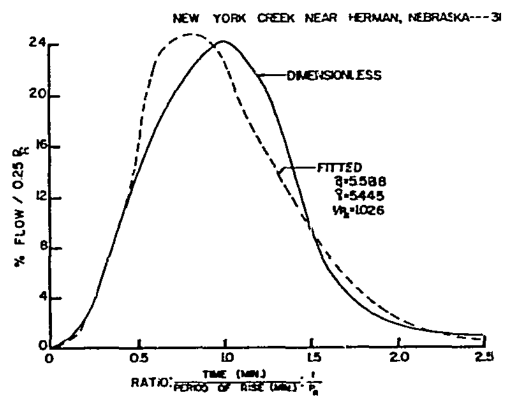
NEW YORK CREEK NEAR HERMAN, NEBRASKA---31
DIMENSIONLESS
FITTED
β=5.588
γ=5.445
t/t_R=1.026
% FLOW / 0.25 P_R
RATIO: TIME (MIN.) / PERIOD OF RISE (MIN.) : t/P_R

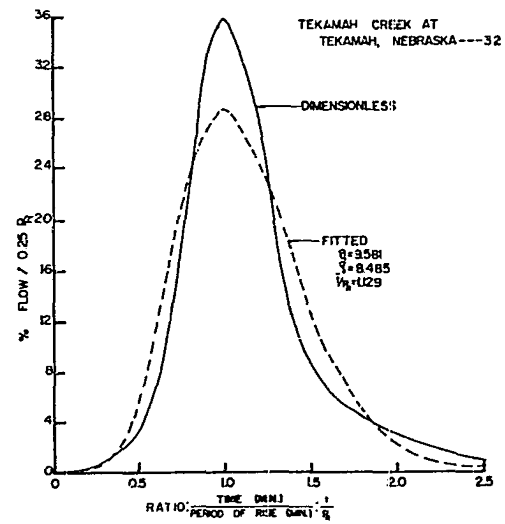
TEKAMAH CREEK AT
TEKAMAH, NEBRASKA---32
DIMENSIONLESS
FITTED
β=9.581
γ=8.485
t/t_R=1.129
% FLOW / 0.25 P_R
RATIO: TIME (MIN.) / PERIOD OF RISE (MIN.) : t/P_R

Figure 43. Dimensionless graphs and fitted two-parameter gamma distributions for watersheds 33, 34, 35, and 36

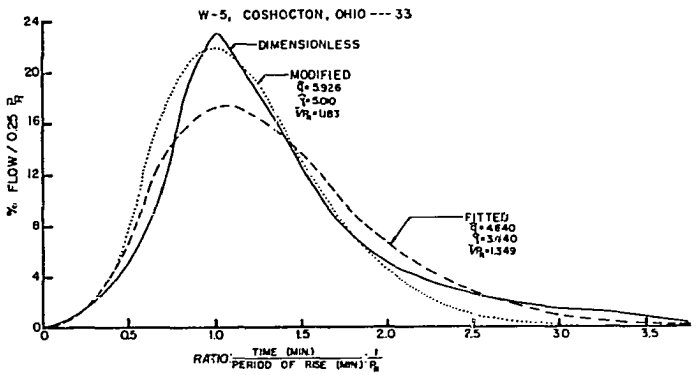
W-5, COSHOCTON, OHIO --- 33
DIMENSIONLESS
MODIFIED
FITTED
% FLOW / 0.25 R_R
RATIO: TIME (MIN) / PERIOD OF RISE (MIN) : $\frac{t}{P_R}$

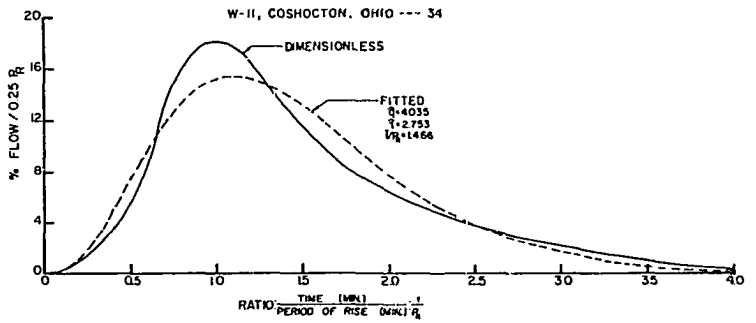
W-11, COSHOCTON, OHIO --- 34
DIMENSIONLESS
FITTED
% FLOW / 0.25 R_R
RATIO: TIME (MIN) / PERIOD OF RISE (MIN) : $\frac{t}{P_R}$

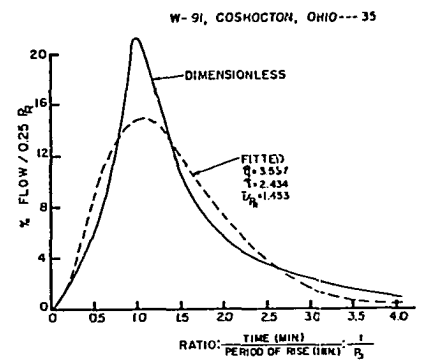
W-91, COSHOCTON, OHIO--- 35
DIMENSIONLESS
FITTED
% FLOW / 0.25 R_R
RATIO: TIME (MIN) / PERIOD OF RISE (MIN) : $\frac{t}{P_R}$

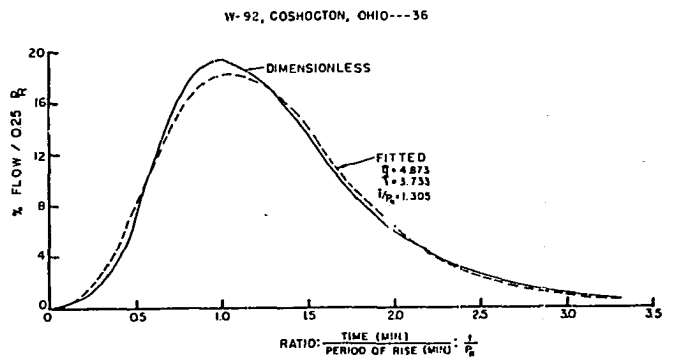
W-92, COSHOCTON, OHIO---36
DIMENSIONLESS
FITTED
% FLOW / 0.25 R_R
RATIO: TIME (MIN) / PERIOD OF RISE (MIN) : $\frac{t}{P_R}$

Figure 44. Dimensionless graphs and fitted two-parameter gamma distributions for watersheds 37, 38, 39, and 40

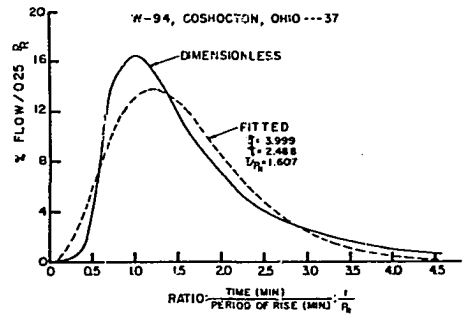
W-94, COSHOCTON, OHIO ---37
DIMENSIONLESS
FITTED
% FLOW / 025 R_t
RATIO: TIME (MIN) / PERIOD OF RISE (MIN) : $\frac{t}{P_R}$

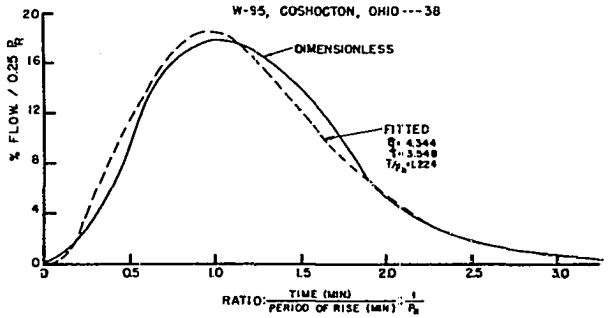
W-95, COSHOCTON, OHIO ---38
DIMENSIONLESS
FITTED
% FLOW / 0.25 R_t
RATIO: TIME (MIN) / PERIOD OF RISE (MIN) : $\frac{t}{P_R}$

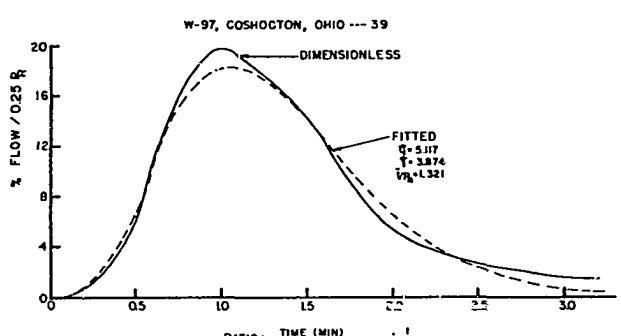
W-97, COSHOCTON, OHIO --- 39
DIMENSIONLESS
FITTED
% FLOW / 0.25 R_t
RATIO: TIME (MIN) / PERIOD OF RISE (MIN) : $\frac{t}{P_R}$

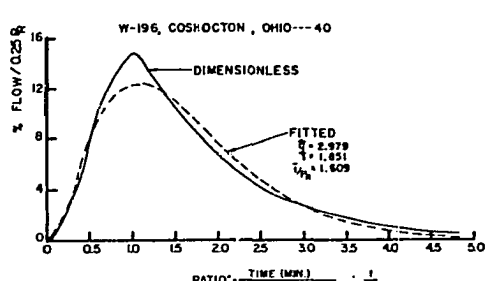
W-196, COSHOCTON , OHIO---40
DIMENSIONLESS
FITTED
% FLOW / 0.25 R_t
RATIO: TIME (MIN) / PERIOD OF RISE (MIN) : $\frac{t}{P_R}$

Figure 45. Dimensionless graphs and fitted two-parameter gamma distributions for watersheds 41 and 42

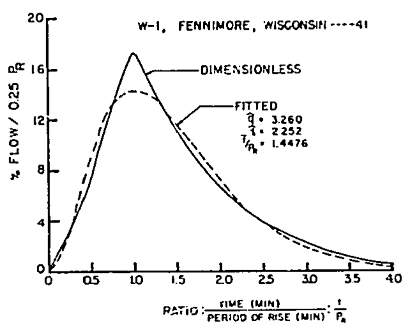
W-1, FENNIMORE, WISCONSIN ----41
DIMENSIONLESS
FITTED
% FLOW / 0.25 PR
RATIO : TIME (MIN) / PERIOD OF RISE (MIN) : t / PR

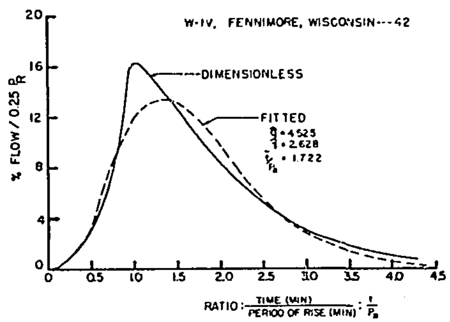
W-IV, FENNIMORE, WISCONSIN---42
DIMENSIONLESS
FITTED
% FLOW / 0.25 PR
RATIO : TIME (MIN) / PERIOD OF RISE (MIN) : t / PR

APPENDIX F: APPLICATION OF RESULTS

Step Procedure in Development of a Unit Hydrograph for a Given Area

Problem

Define the unit hydrograph for a watershed, 5 square miles in area, which falls within a region of comparable geologic, physiographic, and climatic conditions as those of Western Iowa. The following information was obtained from an available topographic map: $L = 3.80$ miles and $S_c = 0.57$ percent.[1]

Procedures

Step 1. Determine parameters; P_R, γ' and q.

A. With $L/\sqrt{S_c} = 3.80/\sqrt{0.57} = 5.03$ miles, enter Figure 15a and select; $P_R/\hat{\gamma} = 16.6$ minutes.

B. With $P_R/\hat{\gamma} = 16.6$ minutes, enter Figure 17 and obtain; $P_R = 57$ minutes.

Therefore: $\hat{\gamma} = 57/16.6 = 3.434$.

C. Set the peak to fall at $t/P_R = 1$, by substituting $\hat{\gamma} = 3.434$ into Equation 19 and solve for; $q = 4.434$. These are the best estimators of γ' and q.

[1] If topographic maps are not available and the characteristics of the area under study are closely related to those of the Nebraska-Western Iowa region, estimates of L and S_c can be obtained from Figures 3 and 14, respectively.

Step 2. Compute the ordinates of the dimensionless graph.

A. Using Equation 16, compute the % flow/$0.25P_R$ at the respective values of t/P_R = 0.125, 0.375, 0.625 ..... and every succeeding increment of t/P_R = 0.250, until the sum of the ordinates approximates 100 percent (see Table 13). Also calculate the peak percentage. At the peak,

$$Q_{(1)} = \frac{25.0\ (3.434)^{4.343}}{\Gamma(4.434)}\ e^{-3.434}\ (1)^{4.434} = 18.0 \text{ percent.}$$

Step 3. Develop the unit hydrograph.

A. Compute the necessary conversion factor.

Volume of unit hydrograph, V

$$V = 1 \text{ in.} \times 5 \text{ mile}^2 \times 640 \frac{\text{acre}}{\text{mile}^2} \times \frac{1}{12 \text{ in/ft}} \times 43560 \frac{\text{ft}^2}{\text{acre}}$$

$$= 11{,}616{,}000 \text{ ft}^3 .$$

Volume of dimensionless graph, V_D

$$V_D = \Sigma\text{cfs} \times 0.25 \times 57 \text{ min.} \times 60 \frac{\text{sec.}}{\text{min.}} = 855\ \Sigma\text{cfs - sec.}$$

Since the two volumes; V, V_D, must be equal, it follows that

Σcfs = 11,616,000/855 = 13,590 cfs.

B. Convert the dimensionless graph ordinates to cfs.

$$Q_t = \frac{\%\ \text{flow}/0.25P_R}{100} \times \Sigma\text{cfs}$$

Table 13. Coordinates of the synthesized unit hydrograph

t/P_R	Accumulated time min.	% flow / $0.25P_R$	Cumulative % flow / $0.25P_R$	Unit graph cfs
0.000	0.0	0.0	0.0	0
0.125	7.1	0.3	0.3	41
0.375	21.4	5.3	5.6	720
0.625	35.6	13.0	18.6	1,767
0.875	49.9	17.6	36.2	2,392
1.000	57.0	-	-	2,446[a]
1.125	64.1	17.6	53.8	2,392
1.375	78.4	14.9	68.7	2,025
1.625	92.6	11.2	79.9	1,522
1.875	106.9	7.7	87.6	1,046
2.125	121.1	5.0	92.6	680
2.375	135.4	3.1	95.7	421
2.625	149.6	1.9	97.6	258
2.875	163.9	1.1	98.7	150
3.125	178.1	0.6	99.3	81
3.375	192.4	0.3	99.6	41
3.625	206.6	0.2	99.8	27
3.875	220.9	0.1	99.9	14
4.125	235.1	0.1[b]	100.0	13
		Total	100.0	13,590

[a]Peak discharge rate; not included in total.

[b]Taken as 0.1 to terminate hydrograph.

Therefore, at the peak,

Q_p = 18.0/100 x 13,590 = 2,446 cfs.

C. Convert the time base of the dimensionless graph to absolute time units.

At the peak, t/P_R = 1; therefore, t = 57 minutes.

Step 4. Plot the unit hydrograph (see Figure 46).

According to Figure 8, the time of beginning of surface runoff should be placed coincident with the centroid of precipitation. For best results, the unit hydrograph should be associated with unit-storm periods of approximately, $0.40P_R$ - $0.50P_R$-duration.

Figure 46. Synthetic unit hydrograph for five-square-mile watershed used in illustrative problem

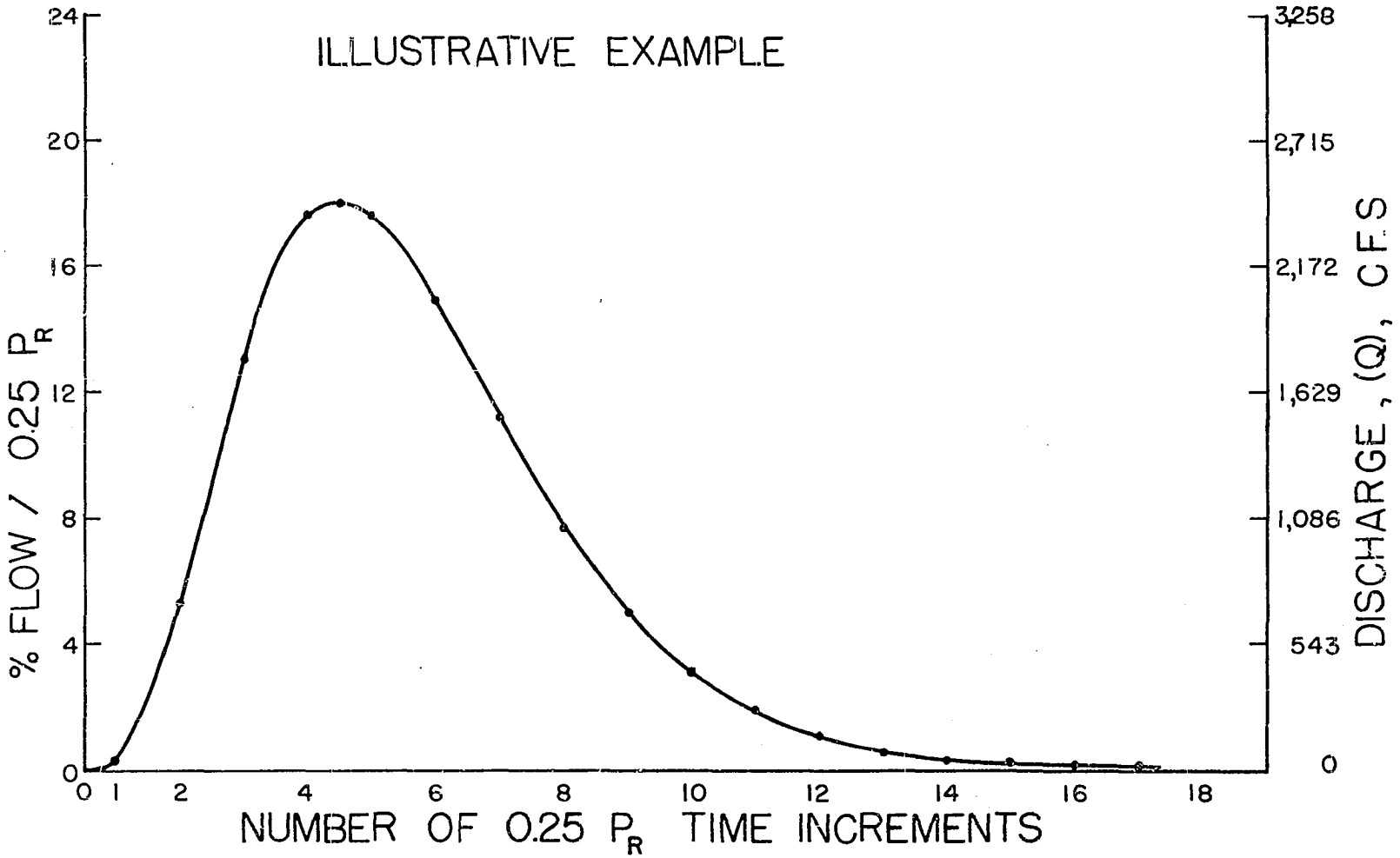
ILLUSTRATIVE EXAMPLE
% FLOW / 0.25 P_R
DISCHARGE, (Q), CFS
NUMBER OF 0.25 P_R TIME INCREMENTS
0
4
8
12
16
20
24
543
1,086
1,629
2,172
2,715
3,258
0 1 2 4 6 8 10 12 14 16 18